GL

OPERATING 24/7

PROJECT #153J

REMAINING STRENGTH OF CORRODED PIPE UNDER SECONDARY (BIAXIAL) LOADING

GL Industrial Services Restricted

Restricted to: US Dept of Transportation, PRCI & GL Industrial Services

Prepared for:

R Smith

US Dept of Transportation

Pipeline and Hazardous Materials
Safety Administration
1200 New Jersey Avenue
SE Building, Second Floor
Washington DC 20590
USA

Prepared by:

J Liu, V Chauhan, P Ng, S Wheat, and C Hughes

GL Industrial Services UK Ltd

Holywell Park
Ashby Road
Loughborough Leicestershire
LE11 3GR
United Kingdom

Tel: +44 (0)1509 282363
Fax: +44 (0)1509 283119

E-mail: Jianhui.Liu@gl-group.com

Website: www.gl-group.com

Customer Reference: DTPH56-05-T0003 - Project 153

Report Issue / Amendment Record

Report Title: PROJECT #153J	
REMAINING STRENGTH OF CORRODED PIPE UNDER SECONDARY (BIAXIAL) LOADING	
Report Number: R9068	Project Title: Project #153J Remaining Strength of Corroded Pipe Under Secondary (Biaxial) Loading
	Project SAP Code: 1/07620

Amendment details

Issue	Description of Amendment	Originator/Author
1.0	Draft for Comment by PRCI Project Team	V Chauhan, P Ng, S Wheat and C Hughes
2.0	Review Comments by PRCI Project Team Addressed	J Liu
3.0	Review Comments by PHMSA Addressed	J Liu

Report approval

Issue	Checked by	Approved by	Date
1.0	P Ingham	C Ward	September 2006
2.0	V Chauhan	P Ingham	June 2008
3.0	V Chauhan	P Ingham	August 2009

Previous issues of this document shall be destroyed or marked SUPERSEDED

Project Code: 1/07620

Distribution

Name	Company
R Smith A Mayberry S Nanney J Merritt	US Dept of Transportation Pipeline and Hazardous Materials Safety Administration 1200 New Jersey Avenue SE Building, Second Floor Washington DC 20590 USA
M Piazza D Johnson R Owen R Espiner	PRCI
I Wood	Electricore, Inc.

DISCLAIMER

Executive Summary

Corrosion metal-loss is one of the major damage mechanisms to transmission pipelines worldwide. Several methods have been developed for assessment of corrosion defects, such as ASME B31G, RSTRENG and LPC. These methods were derived based on experimental tests and theoretical/numerical studies of the failure behavior of corroded pipelines subjected only to internal pressure loading. In the vast majority of cases, internal pressure loading will be the main loading mechanism on the pipeline. However, there may be instances when pipelines could also be subjected to significant loading from the environment. For onshore pipelines, these additional loads could be as a result of ground movement due to landslides, mining subsidence, or even seismic activity. In the case of offshore pipelines the formation of free spans may impose significant bending loads. For instance, seabed scour can lead to the development and growth of free spans of pipelines resting on the seabed, particularly if they are not trenched. Whilst, the guidance detailed in standard assessment methods will be sufficient in the majority of cases, it may be inappropriate or non-conservative to use it in cases when the pipeline may also be subjected to significant external loading. The objective of this project is to extend existing methods to allow assessment of corroded pipelines that are subject to both internal pressure and external loading. Development of this new guidance will remove an important area of uncertainty in the assessment methods currently used by the pipeline industry.

Conclusions

1. The remaining strength of corroded pipelines subject to internal pressure and external loading cannot be explicitly assessed using the ASME B31G, RSTRENG and LPC assessment methods. However, these assessment methods have been validated using pipe with real corrosion and simulated (machined) defects welded to dome ends to form a pressure vessel and subsequently failed under internal pressure loading. Consequently, existing methods include some inherent biaxial loading and the remaining strength of corroded pipelines can be assessed with a limited amount of external loading.

2. Ground movement due to landslides can impose significant external loading to transmission pipelines. Stresses in pipelines due to landslides can be greater than the stresses due to internal pressure loading.

3. Methods developed by the nuclear industry for assessing corroded pipework are given in ASME Code Case N-597-2 and based on ASME B31G when the axial extent of wall thinning is limited. For more extensive corrosion, the assessment methods are based on branch reinforcement and local membrane stress limits. Strictly the methods given in ASME Code Case N-597-2 are only applicable to the assessment of piping systems designed to the ASME Boiler and Pressure Vessel Code, Section III.

4. Failure loci of pipelines with isolated corrosion defects and subjected to combined loads have been derived for common pipeline geometries and materials. The failure loci have been validated using tests performed on 457.2mm (18-inch) and 1219.2mm (48-inch) diameter pipe under combined bending/pressure loading. These failure loci can be used to assess the limit of acceptability of existing assessment methods such as ASME B31G and RSTRENG under combined loading conditions.

Recommendations

1. The methods developed in this report should be extended to cover the assessment of higher strength pipelines up to grade X100 pipelines.

Contents

1 Introduction

Corrosion metal-loss is one of the major damage mechanisms to transmission pipelines worldwide. Several methods have been developed for assessment of corrosion defects, such as ASME B31G [1], RSTRENG [2], [3] and LPC [4]. These methods were derived based on experimental tests and theoretical/numerical studies of the failure behavior of corroded pipelines subjected only to internal pressure loading. In the vast majority of cases, internal pressure loading will be the main loading mechanism on the pipeline. However, there may be instances when pipelines could also be subjected to significant external loading from the environment[1]. For onshore pipelines, these additional loads could be as a result of ground movement due to landslides, mining subsidence, frost heave, thaw settlement, or even seismic activity. In the case of offshore pipelines the formation of free spans may impose significant bending loads. For instance, seabed scour can lead to the development and growth of free spans of pipelines resting on the seabed, particularly if they are not trenched. Whilst, the guidance given in [1], [2] and [3] will be sufficient in the majority of cases, it may be inappropriate in cases when the pipeline is subjected to internal pressure and external loading. The objective of this project is to develop a method to allow assessment of corroded pipelines that are subject to both internal pressure and external loading. Development of this new guidance will remove an important area of uncertainty in the assessment methods currently used by the pipeline industry.

A brief review of the background to existing assessment methods is given in section 2. The overall approach taken to determine the new guidance is given in section 3.

2 Assessment Methods Used by the Pipeline Industry

Existing assessment methods regularly used by the pipeline industry are ASME B31G [1], RSTRENG [2], [3], LPC [4], BS 7910 [5] and DNV RP-F101 [6]. The refinery and petrochemical industry also use AP 579-1/ASME FFS-1 [7]. These methods have been developed from the results of a large number of full-scale burst tests on ring expansion and vessel specimens. Some researchers have supplemented their database of full-scale test results with finite element (FE) analyses (see section 2.7 below). A wide range of material properties and pipeline geometries has been investigated. Most of the experimental work considered volumetric corrosion defects, predominantly longitudinally orientated, subject only to internal pressure. Some investigations have been undertaken to study the effect of in-plane bending and axial loading on pipelines. Some tests have also been undertaken on pipes with circumferentially or helically orientated corrosion defects. In the US, the Federal Regulations, CFR 192 [78] and 195 [79] recommend using only ASME B31G or RSTRENG.

A brief background to the development of the main assessment methods used by the pipeline industry is described below. Further discussion and a review of the test database used to develop these assessment methods is discussed in [82].

2.1 The ASME B31G Method

Much of the original work to develop assessment methods for damaged pipelines was conducted at the Battelle Memorial Institute located in the United States of America (USA) under the NG-18 research program sponsored by Pipeline Research Council International, Inc. (PRCI). The research was initially concentrated on the behavior of sharp defects (machined V-shaped notches and slits), but subsequently the work was extended to consider real corrosion defects in pipelines. This research formed the background to a method for assessing corrosion defects, which was subsequently incorporated into a supplement to ASME

---

[1] Environmental loading is hereafter referred to as external loading.

B31 code for pressure piping for determining the remaining strength of corroded pipelines. The guidance is codified as ASME B31G [1] for assessing axially orientated part-wall defects in a cylindrical pipe subject to internal pressure loading. The failure criterion is based on an empirical fit to 47 full-scale burst tests on pipes containing real corrosion defects. The tests generally involved severely corroded lengths of pipe removed from service after a number of years of operation, supplied by several US gas pipeline companies.

The ASME B31G method idealizes the irregular shape of the corrosion with a parabolic profile and the area of the metal loss is assumed to equal (2/3)dL. As the length of the defect increases, the parabolic representation of the metal loss area becomes less and less accurate. For long defects, ASME B31G approximates the area of metal loss to be rectangular. Briefly the assessment is undertaken using the equations below.

$$P_f = P_o R_s \tag{1}$$

$$P_o = \frac{2\bar{\sigma}}{\left(\dfrac{D}{t}\right)} \tag{2}$$

$$\bar{\sigma} = 1.1\sigma_{SMYS} \tag{3}$$

$$R_s = \frac{1 - \dfrac{2}{3}\left(\dfrac{d}{t}\right)}{1 - \dfrac{2}{3}\left(\dfrac{d}{t}\right)\dfrac{1}{\sqrt{1 + 0.8\left(\dfrac{L}{\sqrt{Dt}}\right)^2}}} \quad \text{for} \quad \left(\frac{d}{t}\right) \le 0.8\,; \frac{L}{\sqrt{Dt}} \le 4.479 \tag{4}$$

$$R_s = 1 - \left(\frac{d}{t}\right) \quad \text{for} \quad \left(\frac{d}{t}\right) \le 0.8\,; \frac{L}{\sqrt{Dt}} > 4.479 \tag{5}$$

The flow stress, $\bar{\sigma}$, is taken to be equal to 1.1 times the specified minimum yield strength, σ_{SMYS}, and the Folias factor, M, is represented by Equation (6).

$$M = \sqrt{1 + 0.8\left(\frac{L}{\sqrt{Dt}}\right)^2} \tag{6}$$

2.2   The Modified ASME B31G Method

The rationale for developing the RSTRENG method was that there was excessive conservatism embodied in the ASME B31G method. The sources of conservatism in ASME B31G were identified to be;

- The expression for the flow stress

- The Folias (bulging) correction factor

- The parabolic representation of the metal loss defect

- The inability to consider the strengthening effect of islands of full thickness or near full thickness pipe at the ends of or in-between corroded sections of the pipe

Battelle was contracted by the American Gas Association to modify the ASME B31G method in order to reduce the conservatisms and inherent limitations of the method. The method was initially validated using a

GL

more extensive database of 86 tests. The first 47 test results were the same as those used to develop ASME B31G. A more extensive validation of the RSTRENG method was undertaken using the results of 168 test results. These test results are all incorporated into the database developed by PRCI/AGA. The results from the tests on isolated defects are included into the integrated database described in this report.

Briefly, the RSTRENG method can be used in one of two ways. The first approach is often referred to as the Modified ASME B31G Method. The main changes introduced are a modified flow stress and Folias factor. The latter was modified to provide a more exact and less conservative approximation of the failure pressure. The assessment is undertaken using the equations below:

$$P_f = P_o R_s \tag{7}$$

$$P_o = \frac{2\overline{\sigma}}{\left(\dfrac{D}{t}\right)} \tag{8}$$

$$\overline{\sigma} = \sigma_{SMYS} + 10,000 \ \text{(psi)} \tag{9}$$

$$R_s = \frac{1 - 0.85\left(\dfrac{d}{t}\right)}{1 - 0.85\left(\dfrac{d}{t}\right)\dfrac{1}{\sqrt{1 + 0.6275\left(\dfrac{L}{\sqrt{Dt}}\right)^2 - 0.003375\left(\dfrac{L}{\sqrt{Dt}}\right)^4}}}$$

$$\text{for} \ \left(\dfrac{d}{t}\right) \le 0.8 \ ; \dfrac{L}{\sqrt{Dt}} \le 7.071 \tag{10}$$

$$R_s = \frac{1 - 0.85\left(\dfrac{d}{t}\right)}{1 - 0.85\left(\dfrac{d}{t}\right)\dfrac{1}{\left[3.3 + 0.032\left(\dfrac{L}{\sqrt{Dt}}\right)^2\right]}}$$

$$\text{for} \quad \left(\dfrac{d}{t}\right) \le 0.8 \ ; \dfrac{L}{\sqrt{Dt}} > 7.071 \tag{11}$$

The second method is described below.

2.3 The RSTRENG Method

A method for assessing the actual shape of the corroded area was developed as part of the RSTRENG approach. The method is based on determining an effective area and effective length of the corroded area. Briefly, the method requires a 'river bottom' profile of the corroded area. This is obtained by gathering a number of profiles of the corroded area parallel to the axis of the pipe and then combined to give the most onerous profile for assessment. Calculations of the predicted failure pressure of various subsections of the total defect profile are undertaken. The length of a subsection is taken as L and the area of metal loss, A, is

calculated. This process is repeated for all possible combinations of the various subsections and the minimum failure pressure predicted according to equations (12) to (16) below.

$$P_f = P_o \min\{R_{s,i}\} \qquad\qquad i = 1,2,3,...n \qquad\qquad (12)$$

$$P_o = \frac{2\bar{\sigma}}{\left(\dfrac{D}{t}\right)} \qquad\qquad\qquad (13)$$

$$\bar{\sigma} = \sigma_{SMYS} + 10,000 \ \ (\text{psi}) \qquad\qquad\qquad (14)$$

$$R_s = \frac{1 - \left(\dfrac{A_i}{A_{o,i}}\right)}{1 - \left(\dfrac{A_i}{A_{o,i}}\right)\dfrac{1}{\sqrt{1 + 0.6275\left(\dfrac{L_i}{\sqrt{Dt}}\right)^2 - 0.003375\left(\dfrac{L_i}{\sqrt{Dt}}\right)^4}}}$$

$$\text{for} \qquad \left(\dfrac{d}{t}\right) \le 0.8 \ ; \quad \dfrac{L_i}{\sqrt{Dt}} \le 7.071 \qquad\qquad (15)$$

$$R_s = \frac{1 - \left(\dfrac{A_i}{A_{o,i}}\right)}{1 - \left(\dfrac{A_i}{A_{o,i}}\right)\dfrac{1}{\left[3.3 + 0.032\left(\dfrac{L_i}{\sqrt{Dt}}\right)^2\right]}}$$

$$\text{for} \qquad \left(\dfrac{d}{t}\right) \le 0.8 \ ; \quad \dfrac{L_i}{\sqrt{Dt}} > 7.071 \qquad\qquad (16)$$

The effective area method is based on an iterative method. This iterative method has been incorporated into a software program, RSTRENG for Windows. In most cases, although not all, the RSTRENG effective area method will predict a failure pressure that is higher than the value predicted using the Modified ASME B31G method.

2.4 The LPC-1/BS 7910 Method

The Linepipe Corrosion (LPC) Group Sponsored Project which was led by Germanischer Lloyd (hereafter GL, then part of British Gas) undertook a program of 81 full scale vessel burst tests and 52 ring expansion tests on simulated corrosion defects in linepipe subject to internal pressure. The tests included isolated, interacting and complex shaped corrosion defects that were machined either as pits, grooves or patches on

the surface of the pipe. The pipe geometries tested included diameters from 219mm (8⅝-inch)[2] to 914.4 mm (36 inch); pipe (D/t) ratios from 8.6 to 47.9, and materials from grade X52 to X65. The test data has not been fully published in the public domain; a general summary of the limited results is presented in [8]. Full details are contained in a BG Technology (now GL) report prepared for sponsors of the project [8]. All of the tests of blunt machined defects failed in a manner consistent with failure controlled by plastic collapse, i.e. necking of the remaining ligament leading to geometric instability and failure. On the completion of the group sponsored project, the method was released to BSi for inclusion in BS 7910 [5].

Extensive three-dimensional, non-linear, elastic-plastic finite element (FE) analyses of the failure of blunt metal loss defects in closed-ended cylinders subject to internal pressure were also undertaken using ABAQUS/Standard [9]. Detailed guidance for the assessment of corrosion in line pipe was subsequently developed, based on the results of the FE and experimental studies. These studies led to the development of the assessment method that is now incorporated into Annex G of BS 7910   Guidance is given for the assessment of isolated corrosion defects; for the assessment of closely spaced corrosion defects that may interact and for the assessment of a corrosion defect using a river-bottom profile. The assessment of an isolated corrosion defect is based on the same underlying methodology developed as part of the original NG-18 research program, but the Folias factor, M, is modified based on the results of parametric finite element study. The flow stress, $\overline{\sigma}$, is taken as being equal to the ultimate tensile strength, based on the observation that the tensile strength better describes failure controlled by plastic collapse.

The failure pressure, P_f, of an isolated rectangular shaped corrosion defect of maximum depth, d and length L, in a pipe according to Annex G of BS 7910 can be determined using Equations (17) to (20) below:

$$P_f = P_o R_s \tag{17}$$

$$P_o = \frac{2\overline{\sigma}}{\left(\dfrac{D}{t} - 1\right)} \tag{18}$$

$$\overline{\sigma} = \sigma_{SMTS} \tag{19}$$

$$R_s = \frac{1 - \left(\dfrac{d}{t}\right)}{1 - \left(\dfrac{d}{t}\right)\dfrac{1}{\sqrt{1 + 0.31\left(\dfrac{L}{\sqrt{Dt}}\right)^2}}}$$

for $\quad \left(\dfrac{d}{t}\right) \le 0.85$; all lengths $\tag{20}$

Note that in contrast to ASME B31G and RSTRENG methods, this approach defines the flow stress using the specified minimum *tensile* strength rather than yield strength, as this was found to give more accurate predictions.

---

[2] 7 tests were undertaken on Grade X52 pipe with wall thicknesses ranging from 24.5mm to 25.4mm. All vessels contained external groove defects with a (d/t) ratio range 0.2 to 0.94. Deeper defects resulted in failure of the vessel as a leak. Failure of the vessel by rupture was obtained for defect (d/t) ratios in the range 0.5 to 0.72. Failure pressures ranged from 685 bar to 1241 bar.

The intent of the guidance given in BS 7910 is to provide simplified, conservative procedures for the assessment of corroded pipelines or pressure vessels. If the corrosion defects are found to be unacceptable using the procedures given, then the user has the option of considering an alternative course of action. This could include, but is not limited to, detailed finite element (FE) analysis and/or full scale testing. Recommendations for conducting non-linear FE analysis to determine safe operating pressures of corroded pipelines and pressure vessels are described in Annex G of BS 7910 and the PRCI Guidance Document[3] [10].

2.5 The DNV RP-F101 Method

The results of the Linepipe Corrosion Project were merged with those of a similar project conducted by Det Norske Veritas (DNV). This resulted in the development of a Recommended Practice, DNV RP-F101 [6]. The DNV project generated a database of 12 burst tests on pipes containing machined corrosion grooves, primarily to develop guidance for assessing combined internal pressure and environmental loading [11]. All the tests were conducted on 323.9mm (12¾-inch) diameter (D/t = 31.5) grade X52 pipe.

The recommended practice contains guidance for the assessment of isolated corrosion defects; for the assessment of adjacent corrosion defects that may interact and for the assessment of a corrosion defect using a river-bottom profile, all considering internal pressure loading only, and guidance for the assessment of isolated corrosion defects subject to internal pressure and environmental loads. Guidance for assessing isolated and interacting defects is based on the same approach as that developed for BS 7910. The recommended practice consists of two parts; Part A is based on the Load and Resistance Factor Design format and makes use of the concept of partial safety factors, Part B is based on the Allowable Stress Design format and makes use of a single safety factor.

2.6 The API 579-1/ASME FFS-1 Method

API 579-1/ASME FFS-1 [7] provides guidelines for performing fitness for service (FFS) assessments that can be used for assessing damage mechanisms of the type found in the refining and petrochemical industries. The assessment methods in API 579-1/ASME FFS-1 were originally developed to assess pressure equipment designed and constructed to US codes used in the petrochemical industry, in particular, the ASME Boiler and Pressure Vessel Code, Section VIII, Division 1 and 2 [12], the power and chemical piping codes ASME B31.1 [13] and ASME B31.3 [14], and the tank codes API 650 [15] and API 620 [16]. It is not, at present, specifically intended for application to pipelines.

API 579-1/ASME FFS-1 describes methods for the assessment of general metal loss, local metal loss and pitting corrosion. However, it is noted that API 579-1/ASME FFS-1 gives procedures for assessing the fitness-for-purpose of a variety of different types of defects in pressurized components such as pressure vessels, piping and storage tanks. It does not specifically address pipelines. The underlying approach is, however, based on the ASME B31G and RSTRENG methods. The API 579-1/ASME FFS-1 criterion has been modified and interpreted in terms of a remaining strength factor (RSF). The authors of the recommended practice have also modified the Folias factor, M. The API 579-1/ASME FFS-1 criterion was compared with a database of test results compiled from the public domain. This database was primarily obtained from PRCI [17] and the resulting assessment method is claimed to reduce the level of conservatism when compared to ASME B31G and RSTRENG.

Three assessment levels are described in the document. A simple Level 1 criterion is given based on the maximum defect length and depth dimensions and a more complex Level 2 criterion that can be used on the

---

[3] Note that the Guidance Document will be re-issued when the work on Project #153 has been completed.

basis that a detailed cross-sectional profile of the defect is available, i.e. the approach is based on the RSTRENG method described in section 2.3 above. A Level 3 assessment using finite element stress analysis is also described.

2.7   The Non-Linear Finite Element Analysis (Level 3) Method

The failure pressure of internally pressurized ductile steel pipe with either local or general metal loss defects, such as corrosion, can be predicted by numerical analysis using the non-linear finite element (FE) method with a validated failure criterion. Complex flaw shapes and combined loading conditions can be considered in the analysis. This procedure is now well documented, see for example BS 7910 Annex G [5], the PRCI Corrosion Assessment Guidance Document [10] and API 579-1/ASME FFS-1 [7]. Briefly, the method consists of four major steps as follows;

- Create a finite element model of the corroded pipe or vessel, using information on the flaws detected, the measured material properties and the structural constraints and loads applied.
- Perform a non-linear large deformation stress analysis using a verified finite element analysis software package and a validated analysis procedure.
- Examine analysis results obtained from the stress analysis.
- Determine the failure or critical pressure value based on the variation of local stress or strain states with reference to a validated criterion.

The method is well tried and can reliably predict the failure pressure of pipelines with smooth metal loss features. The method has, however, only been validated for pipelines subjected only to internal pressure loading. Consequently, full-scale burst tests would be required to validate the method for pipelines subjected to combined internal pressure and environmental loading. The authors are aware that some research work has been done is this area [23], [24], [25], [26] and [27].

2.8   PRCI Review

The Line Pipe Research Supervisory Committee of PRCI commissioned a project in 2000 with GL (then BG Technology), Battelle Memorial Institute and Shell Global Solutions to critically review a number of existing and newly emerging methods for assessing corroded pipelines [19]. As part of this review, an integrated database of 256 tests on corroded pipe was produced. Test results from four major sources were reviewed and collated in the database. The first source is the PRCI database of 124 tests, compiled in 1994 [18], the second source is a database of 20 tests published by University of Waterloo [20], the third source is a database of 33 tests produced by GL in 1992 [21], [22] and the fourth source is a database of 79 tests produced by GL for the group sponsored project on line pipe corrosion during 1994-1997 [9].

Figures 1 and 2 show the distribution of pipe grade and (D/t) ratio contained in the overall database. There are almost 50 tests undertaken on grade X65 pipe. It is noted the database did not include tests conducted on pipes under both internal pressure and external loading.

2.9   Alyeska Pipeline Service Company Tests by Southwest Research Institute

Alyeska Pipeline Service Company (Alyeska) had recognized the potential for premature failure in corroded pipelines sections subjected to significant external loading. They initiated a program of work with Southwest Research Institute (SWRI) aimed at developing guidelines for predicting rupture of pipelines subject to combined internal pressure and external loading.

The results of the work were published in References [23], [24] and [25]. A total of seventeen tests were conducted on 1219.2mm (48-inch) diameter and wall thickness 11.73mm (0.462-inch) grade X65 pipe. Simulated corrosion defects were machined on the external surface of the test specimens that were approximately 18.3m (60 feet) length. The defects were machined at the mid-span of the test specimen

were designed to simulate the maximum size of defects found in-service. All the defects were rectangular patches of axial length (L_A) and circumferential width (L_H) and uniform depth as summarized in Table 22. The tests included the study of defects on the tension and compression sides of the pipe wall. The loading was applied in a controlled sequence. In general, loading on the pipe was initiated with internal pressure to a pre-defined pressure, followed by bending of the pipe (using a custom made four point bending rig) to a given strain or displacement and final pressurization of the pipe to failure. Compressive axial loading was also included in the loading sequence to counteract the effects of pressure end loads on the pipe.

The load path and failure point of each test is summarized in Table 22.

2.10   Buckling

When a structure (subjected usually to compression) undergoes visibly large displacements transverse to the applied load then it is said to buckle. For small loads the process is elastic because the displacements disappear when the load is removed.

Buckling proceeds in a manner which may be either stable or unstable. In the former case the displacements increase in a controlled fashion as the load is increased and the structure's ability to sustain loads is maintained. In the latter case deformations increase instantaneously, the load carrying capacity decreases rapidly and the structure collapses catastrophically due to one of the following reasons:

1. Including the presence of the corrosion defect itself, there are imperfections in the pipeline; these could be due to out of straightness or ovality in the pipe, misalignment at the welds and residual stresses.

2. The structure is loaded asymmetrically.

3. Non-uniformity in material properties.

Local buckling of plates or shells is indicated by the growth of bulges, waves or wrinkles, and is commonly encountered in the component plates of thin structural members. Buckling has become more of a problem in recent years since the use of high strength material requires less material for load support - structures and components have become generally more slender and buckle - prone.

In the case of pipelines, the above factors coupled with the presence of corrosion defects may result in failure at pressures lower than those derived using the standard assessment methods described in section 2. For example, large compressive stresses may cause the pipe to buckle and the presence of metal loss may further increase the susceptibility to buckling. The assessment of a pipeline's susceptibility to buckling under external loading is not covered in existing guidance available to the pipeline industry.

2.11   Discussion

Only DNV RP-F101 [6] provides publicly available guidance available in the public domain for assessing corroded pipelines subjected to combined internal pressure and bending/axial loads. This is because the standard was primarily developed for the assessment of offshore pipelines where it was recognized that bending and axial loading could be significant. However, it is to be noted that the guidance is based on the results of only ten full-scale burst tests on one pipe (D/t) ratio.

Some work has also been undertaken by SWRI on 1219.2mm (48-inch) diameter grade API 5L X65 pipeline for the Alyeska Pipeline Service Company [23], [24], [25], [26]. PRCI have also funded work with Battelle Memorial Institute in the mid 1990's to develop guidance for assessing corroded pipelines subject to combined pressure and axial loads [27]. Guidance was developed using shell models, generated using a special purpose finite element (FE) software package, PCORR. Non-linear material behavior was modeled using a Ramberg Osgood formulation and the analysis was limited to small deformation theory. The defects were modeled as rectangular patches by reducing the thickness of the elements which represented the

corroded area. It was recognized by the authors that PCORR was not as rigorous as fully non-linear FE analysis using three dimensional brick elements and that only limited experimental validation work had been undertaken. It was, therefore, recommended that further work be undertaken before the guidance could be used by industry.

Based on the above discussion, a need was identified to develop robust guidance for assessing the remaining strength of corroded pipe subject to internal pressure combined with external loading, including susceptibility to buckling due to compressive axial loading. It was also noted that the existing assessment methods such as ASME B31G and RSTRENG were validated using damaged pipe sections welded to form pressure vessels and subsequently burst to failure. Consequently, these methods include an inherent level of biaxial stress in pipe and depending on the level of external loading can still be used to assess the remaining strength of corroded pipe subjected to external loading.

Section 3 below describes the approach taken to develop new guidance to assess the remaining strength of corroded transmission pipelines subjected to significant external loading.

3   Approach

The approach taken to develop a new method for assessing volumetric corrosion defects in pipelines subject to internal pressure and external loading was as follows:

1. Review case histories of ground movement incidences on transmission pipelines and determine the relative magnitude of external loading that could be imposed on pipelines due to ground movement (section 4).

2. Review standards developed by the nuclear industry to assess corrosion/erosion damage in pipework and assess their applicability to assessing the remaining strength of corroded pipe (section 5).

3. Undertake a series of finite element simulations to determine failure loci[4] of corroded line pipe subject to internal pressure combined with external (bending or axial) loading (section 6).

4. Validate the results of the simulations using full-scale testing and data available in the public domain (section 7 and section 8).

5. Recommend failure loci for common pipeline (D/t) ratios and materials (Appendix A, Appendix C, Appendix D).

4   External Loading on Pipelines – Case Histories

Transmission pipelines can be subjected to significant external loading caused by natural or human activities. Relatively large permanent ground movements are usually due to landslides, mining subsidence, frost heave, thaw settlement and earthquake induced movements (fault movements, liquefaction of soil, etc). Some of the design codes have provisions that apply to pipelines that may be subjected to these loads. A detailed discussion and guidance related to strain based design of pipelines is given in [83]. It is noted that external loading on the pipeline can be either displacement controlled or load controlled. In the former

---

[4] A locus (plural loci) is defined as is a line traced by a point which varies its position according to some determinate law. In this report a failure loci are for pipelines subject to combined internal pressure and external loading. Any combination of internal pressure and external loading above the failure locus is deemed to be unsafe and any combination below is deemed safe.

case the structural response of the pipeline is governed by imposed geometric displacements, for example a pipeline subjected to ground movement; in the latter case the structural response of the pipeline is governed by the imposed loads, for example a free spanning subsea pipeline. There are a variety of intermediate cases where both types of loading may be applied to the pipeline, see [83].

A review of different kinds of permanent ground movement affecting high-pressure transmission pipelines has been undertaken and it was concluded that ground movement loading due to landslides is considered the most onerous type of loading on transmission pipelines. Note that wave propagation due to earthquake loading is transient and difficult to predict. In the case where loads due to earthquakes have been imposed on a pipeline, then detailed analysis and assessment on a case-by-case basis would be required.

Figure 3 [28] and Figure 4 [29] shows examples of how ground movement can impose significant external loading on onshore pipelines. Section 4.1 briefly discusses ground movement due to landslides and section 4.2 describes the results of an assessment to determine the magnitude of external loading that could be imposed on transmission pipelines due to a landslide.

4.1 Ground Movement due to Landslides

There are many different types and sizes of landslides. They can range from small slides involving only a few cubic feet of soil with movement of a few feet, to massive slides of several square miles and millions of cubic feet of materials with movement of up to one mile. Similarly, the rate of movement is highly variable; mud flows may move several feet per second, while some large landslides may move intermittently at rates of only a few inches per year [30].

Where landslides occur, there may be a group of slips that will occur at the same time, due to the surrounding geology. One example of this is the Northridge, California earthquake in the San Fernando Valley that triggered more than 11,000 landslides over an area of nearly 2590 square kilometers (1000 square miles) [31].

Skempton and Hutchinson [32] classified different types of landslides as illustrated in Figure 5. A survey was carried out in the UK on nearly 9000 recorded landslides [33]. It revealed that, of all the landslides that can be classified, the largest groups are rotational slides (slides that occur as a rotational movement on a circular or spoon-shaped slip surface) and translational slides (non-circular failure which involves translational motion on a near-planar slip surface), which accounted for 27.5% and 24.5% respectively (the other 48% are falls, flows and complex slides). Ground movements of these two types of landslides can be defined more precisely. Therefore, only the movements due to rotational and translational slides are considered.

Table 4 summarizes the details and relevant soil properties of landslide case histories that were considered. A review of published papers did not produce any transmission pipeline failures due to landslides.

Based on the available information on landslides, idealized rotational and translational slides have been derived as shown in Figure 6. Rotational slide was assumed to have a circular slip surface while translational slide have a planar slip surface parallel to the slope. Both slides were assumed to have block movement in the longitudinal direction, and spatially distributed ground movement in the transverse direction. Two pipe configurations have been considered: perpendicular and parallel crossings relative to the landslide. Only longitudinal soil movement is considered relevant to the parallel crossing and only transverse soil movement is considered relevant to the perpendicular crossing.

Table 5 shows the chosen dimensions of 'small', 'medium' and 'large' landslides that have been studied.

4.2 Estimation of External Loading on Pipelines due to Landslides

One of the methods for modeling a soil/pipe system subjected to ground movement is to use the theory of an elastic beam on an elastic foundation. The theory assumes the pipe as an elastic beam in contact with

elastic springs along the pipe, representing the soil. The springs are mounted perpendicular to the pipe axis in the vertical and horizontal directions to restrain the pipe from longitudinal bending. Springs are also mounted parallel to the pipe axis to restrain the pipe from axial extension and compression. Typical load-displacement behavior of the soil springs is non-linear.

One of the major uncertainties in a soil/pipe interaction problem is the determination of the appropriate soil restraints. This is influenced by the pipe size and cover depth, the trench geometry, the pipe coating, the soil properties, and the restraint direction. Non-linear hyperbolic soil restraints were determined in all four directions (upward, downward, lateral and axial). This method is superior to the common assumptions of linear and bi-linear elastic soil restraints. Sensitivity studies assuming four bounding soil types and conditions (soft and stiff clay; loose and dense sand) on three pipe geometries 457.2mm (18-inch), 914.4mm (36-inch) and 1219.2mm (48-inch) were investigated. The three pipe geometries and material grades, as shown in Table 6, were agreed with the PRCI project team.

4.2.1 Soil Properties

The following summarizes the assumptions used to select the soil properties and other parameters for calculating soil restraints:

Density –   The density is based on information obtained from case histories (Tables 4 and 7) and from previous measurements undertaken by GL of cohesive (clay) and granular (sand) backfill materials in the UK (over 800 samples).

Strength –   The strength range is based on information obtained from case histories (Tables 4 and 7) and on published data of the strength of loose and dense granular materials.

                The strength range for the granular (sand) backfill is based on the sand being in a loose condition for the lower bound, and the upper bound assumes the backfill matches the natural ground condition.

                The strength range for the cohesive (clay) natural ground is based on information from case histories (Tables 4 and 7) and on previous measurements of the strength of cohesive materials in the UK (over 200 samples).

                The strength range for the cohesive backfill is based on previous measurements of the undrained shear strength of cohesive backfill materials in the UK (over 800 samples).

Sliding friction –   Values for adhesion and angle of sliding friction for the soil/pipe interface are based on previous direct shear testing of cohesive and granular backfill materials on simulated coal tar enamel and fusion boned epoxy surfaces. No imported granular fill (i.e. no sand annulus) was assumed surrounding the pipeline.

Trench width –   Lower bound based on no influence from the natural ground.
                Upper bound based on construction guidance and field data.

Water table –   Lower bound based on water table at ground surface level.
                Upper bound based on no influence from water table.

Tables 8 and 9 summarize the input soil parameters. Note that the lower and upper bound cohesive materials represent soft and stiff clay respectively; while lower and upper bound granular materials represent loose and dense sand respectively.

4.2.2   Soil Restraints

The calculation methods for soil restraints were taken from international design standards and established research, such as NEN 3650 [34], ASCE Guideline [35], Vesic [36] Hansen [37], and Ovesen [38]. These methods have been validated using full-scale pipe loading tests [39] and other available data.

Tables 10 to 12 show the calculated bi-linear soil restraints for the 457.2mm (18-inch), 914.4mm (36-inch) and 1219.2mm (48-inch) diameter pipes respectively (see Table 3 for pipe properties). The values of the two soil types (cohesive and granular) have been rationalized by averaging to produce a single data set of lower and upper bound restraint values. The values were then converted to hyperbolic soil restraints (Tables 13 to 15) for use in the subsequent analyses.

4.2.3   Stress Analysis

The calculated soil restraints, together with the assumed ground movement, were input into a stress analysis program PIPELINE [40] developed by GL. PIPELINE is a WINDOWS™ based stress analysis program for linear buried pipe systems subjected to internal and external loadings. It is based on the well-known finite difference theory for elastic beam on elastic foundation problems. The pipe properties are assumed to be linear elastic and the supporting springs are hyperbolic elastic. The software has been fully validated against analytical solutions and commercial software [41].

In PIPELINE, tensile stress is positive and compressive stress is negative. However, equivalent stress is always positive.

Sensitivity studies, based on the 94.4mm (36-inch pipe) (Table 6), were undertaken on a number of parameters, including soil restraints, width or length of landslide, magnitude of landslide movement and internal pressure. Table 16 lists the parameters tested in the sensitivity studies. Note that only combinations that provide upper or lower bound loads, and some 'in-between' combinations were investigated (for details see section 4.2.4). The findings were also applied to the 457.2mm (18-inch) and 1219.2mm (48-inch) diameter pipes. Based on the sensitivity study results, a number of bounding load cases were derived for the three pipes. Bounding axial forces and bending moments were then calculated from the load cases, and subsequently used in conjunction with the results obtained from the finite element analyses described in section 6.

4.2.4   Sensitivity Studies

The sensitivity of several parameters was considered, including the effect of varying soil restraints, width of landslide, magnitude of landslide movement, and internal pressure loading on a perpendicular crossing (Figure 3b).

Using the 914.4mm (36-inch) diameter pipe and a small landslide with movement of 1m (39.4-inch) (Table 5), the effects of using different soil restraints have been studied. Figure 7 shows the analysis model in PIPELINE, which illustrates a 200m (656 ft) pipeline subjected to a 20m (65.6 ft) wide translational slide. The soil restraints were assumed identical along the length of the pipeline. It was found that the higher the soil restraint, the larger the pipe displacement (Figure 8) and higher the stresses (Figure 9). This is because more loading was transferred from the ground displacement to the pipe at higher soil restraints. It should be noted that the bending stress profiles above the specified minimum yield strength (SMYS) are unrealistic because PIPELINE uses linear elastic material properties for the pipe. They were only shown to illustrate that the pipe would yield under the particular combination of landslide dimensions and soil restraints.

The effect of varying the width of a landslide was also studied. Using the 914.4mm (36-inch) diameter pipe, a landslide movement of 1m (39.4-inch) and upper bound rationalized soil restraints, Figure 10 shows that beyond a critical width (i.e. the width associated with the peak stress in the figure) the wider the landslide, the lower the stress on the pipe. This is because the wider spatially distributed transverse ground movement imposes a more gradual pipe displacement, and hence generates lower stress. However, when a landslide

is very narrow, smaller than the critical width, the force it can impose onto the pipeline is much reduced and hence stresses generated are lower. Figure 10 shows that a peak stress is generated when the width of landslide is approximately 22m (72.2 ft). This critical width is dependent on the pipe and soil properties. Under the particular combination of landslide dimensions and soil restraints, the pipe would yield if the landslide is wider than 3m (118.1-inch) and narrower than 70m (229.7 ft).

The effect of varying the movement of the landslide was studied based on the 914.4mm (36-inch) diameter pipe, a small landslide and lower bound rationalized soil restraints. Figure 11 shows the non-linear increase in maximum bending stress and maximum pipe movement, with increasing soil movement. This is due to the use of non-linear hyperbolic soil restraints, which represents a more realistic behavior. This study also shows that when the soil strength is very low (lower bound soil restraints), the pipe may not yield even when subjected to relatively large soil movement.

The above study (Figure 11) was based on zero internal pressure in the pipe. Figure 12 shows the maximum equivalent stresses for the pipe under different internal pressures and soil movements. At the same soil movement, the increase of internal pressure causes an approximately linear increase in stresses. Under the particular combination of landslide dimensions and soil restraints, the pipe would yield if the internal pressure were higher than 60bar (870.2 psi) at a soil movement of 5m (16.4 ft). Figure 12 also shows that the stresses due to the landslide could be greater than the stresses due to internal pressure. Therefore, external loading due to ground movement is the dominant load under some circumstances, and must be taken into account when designing/analyzing a pipeline system. This agrees with the recommendation given in the UK transmission pipeline design standard, IGE/TD/1 Edition 4 [42], that environmental loads arising from, for example slope instability, should be accounted for in the design of pipelines.

Similar sensitivity studies have been carried out on parallel crossings (see Figure 3d). Using the 914.4mm (36-inch) pipe and a small translational landslide with movement of 0.2m (7.9-inch), the effects of upper and lower bounds rationalized soil restraints have been studied. It was found that the higher the soil restraint, the higher the axial stress, as shown in Figure 13. Under the particular combination of landslide dimensions, the pipe would not yield even if the soil restraints are very high. However, rotational landslides generate an additional bending stress component. Figures 14 to 17 show the vertical bending stress, axial stress and total equivalent stress distributions along the pipe respectively. Under the particular combination of landslide dimensions (a small rotational landslide with movement of 1m (39.4-inch), the pipe would yield when the soil restraints are very high.

The effect of varying the magnitude of landslide movement has also been studied based on the 914.4mm (36-inch) pipe, a landslide length of 50m (164.0 ft) and upper bound rationalized soil restraints. For a translational landslide, Figure 18 shows that the greater the landslide movement, the higher the stress on the pipe, and the relationship is approximately linear. Under the particular combination of landslide dimensions and soil restraints, the pipe would yield if the movement is larger than 0.9m (35.4-inch). For a rotational landslide, Figure 18 shows that the greater the landslide movement, the higher the stress on the pipe, and the relationships is approximately linear. Under the particular combination of landslide dimensions and soil restraints, the pipe would yield if the movement is larger than 0.45m (17.7-inch). Comparing Figures 17 and 18, under similar conditions, the axial stresses generated by translational and rotational slides are similar. However, the additional bending stress component from the rotational slide produced a much higher total equivalent stress.

The effect of varying the length of a translational landslide has been studied based on the 914.4mm (36-inch pipe), a landslide movement of 0.2m (7.9-inch) and upper bound rationalized soil restraints. Figure 19 shows that the longer the landslide, the higher the stress on the pipe, and the relationship is approximately linear. Under the particular combination of landslide dimensions and soil restraints, the pipe would yield if the landslide is longer than 180m (590.5 ft).

4.2.5   Load Cases

From the results of the sensitivity studies presented above, the combinations of landslide dimensions and soil restraints that would produce lower and upper bound loadings have been summarized in Table 17. Based on the combinations, eight load cases were derived for calculating the lower and upper bound loadings for the three selected pipe geometries (see Table 18).

It should be reiterated that, under certain combinations of landslide dimensions and soil restraints, the ground movements from a landslide could impose external loading that causes the pipeline to yield. Under these cases, the upper bound load was manually reduced to the load that would cause the pipe material to just yield (i.e. the load to just yield the pipe is reported).

Tables 19 to 21 show the summary of maximum stresses of the 457.2mm (18-inch), 914.4mm (36-inch) and 1219.2mm (48-inch) pipes resulted from the load cases. Because of the linear elastic material behavior for the pipeline in the software, some of the stresses calculated are higher than the SMYS of the pipe material. Values in the tables presented in italics have been manually reduced to the stresses that cause the pipe material to just yield. In cases where axial or bending stresses alone had caused yielding, they were assumed to be equal during the adjustment. Because of the adjustments made, most of the axial force results are equal in tension and compression, while the bending moment results are all with equal tension and compression.

4.2.6   Conclusions

The following was concluded from the study of ground movement loading on transmission pipelines:

1.   The higher the soil restraint (i.e. the stronger the soil), the higher the loading onto the pipeline.

2.   The larger the ground movement, the higher the loading onto the pipeline.

3.   For perpendicular crossings, a narrow slide generates higher stresses than a very wide slide, until a critical width is reached. This critical width is dependent on the pipe and soil properties.

4.   For parallel crossings, the longer the slide, the higher the pipe stresses.

5.   For the lower bound load cases (1, 2, 5 and 6), the pipe stresses are predicted to be below the yield stress. For the upper bound load cases (3, 4, 7 and 8), however, the pipe is predicted to yield.

6.   The stresses due to landslide could be greater than the stresses due to internal pressure. Therefore, external loading due to ground movement must be taken into account when designing/analysing a pipeline system.

5   Nuclear Standards Review

Wall thinning caused by the flow of water in power piping systems became a major concern to the nuclear power industry in 1986 when a 609.6mm (24-inch) feedwater line ruptured at a nuclear power station in the US (Surry-2 power station). The failure initiated from thinned piping and blew out a section of pipe and several contractors working in the area subsequently died of severe burns. Following this incident the nuclear industry developed methods to assess wall thinning in nuclear piping components and new criteria have been developed for inclusion in Section XI of the ASME Boiler and Pressure Vessel Code 43 for inspecting and evaluating locally thinned areas in carbon steel piping. Initial efforts resulted in the development of ASME Code Case N-480 [44, 45]. Further work led to a revision in 1998 with the issue of Code Case N-597; the latest version is now published as Code Case N-597-2 [46].

5.1   Brief Overview of ASME Code Case N-597-2

Code Case N-597-2 provides evaluation procedures for corroded piping and fittings; these procedures were originally proposed by the Electric Power Research Institute (EPRI). The method given in Code Case N-597-2 is strictly only applicable to the assessment of piping systems designed to the ASME Boiler and Pressure Vessel Code, Section III [47].

The evaluation process begins with a measurement and prediction of the remaining wall thickness. The flow diagram shown in Figure 20 describes the evaluation procedure. A three step procedure is given which includes:

1. A screening comparison against the nominal wall thickness.

2. Determination of, and comparison to, the actual minimum pipe wall requirements.

3. An evaluation of the extent and depth of local thinning.

The evaluation begins with a measurement and prediction of the remaining wall thickness. This thickness is shown in Figure 21 as t_p and is the minimum predicted wall thickness of the component at the end of the period for which it is being evaluated.

The predicted wall thickness is first compared with the nominal wall thickness (t_{nom}). If the predicted wall thickness is within the specified wall thickness tolerance ($t_p > 0.875 t_{nom}$), the component is acceptable with no further evaluation needed. At the other extreme, if the predicted wall thickness is only a small fraction of the nominal wall thickness, repair or replacement is required without further evaluation. A predicted wall thickness of less than 30% of the nominal wall thickness ($t_p < 0.3 t_{nom}$) was chosen as a reasonable lower bound of acceptability.

For intermediate cases, where the predicted wall thickness is less than the nominal wall thickness minus the manufacturing tolerance (12.5%), but greater than 30% of the nominal wall thickness, a more detailed evaluation is permitted.

A key parameter for the second step of the evaluation is the component minimum wall thickness (t_{min}), which depends on the construction code, material properties, internal pressure and external loading on the pipe. The governing equation for t_{min} is generally the equation for hoop stress due to internal pressure. For straight pipes, bends and elbows, t_{min} is determined by:

$$t_{min} = \frac{PD_o}{2(S + yP)}$$

(19)

where y is a design factor required by the appropriate construction code.

Design codes also put restrictions on axial stress due to pressure and primary bending loads. The need to confirm that t_{min} satisfies the design code axial stress requirements poses a problem if the bending loads or stresses are not available. Either bounding values must be determined or it must be conservatively assumed that t_{min} equals $0.875 t_{nom}$.

If the predicted wall thickness is greater than the design minimum thickness ($t_p > t_{min}$), then the component is acceptable for continued operation.

If the minimum wall thickness requirements cannot be met, the following three local thinning options are given in the Code Case.

Axial Corrosion

Guidance is taken directly from the ASME B31G method described in section 2.1. It has been recognized that the guidance given in ASME B31G was derived using a series of burst tests on pipes under only

internal pressure loading. For nuclear plant piping, where bending loads in particular may be significant, the extent of circumferential wall thinning is limited to $\sqrt{Rt_{min}}$. The allowable thinning is shown in Figure 22 (the red curve) where the local allowable wall thickness, t_{aloc}, is shown as a function of the axial extent of local thinning below t_{min}.

Branch Reinforcement

Codes used to design nuclear piping provide guidelines for the design of branch connections. These guidelines include requirements for the amount of material that must be added, its location and distribution relative to the opening. The rules for branch reinforcement and the requirement that sufficient material must remain over the thinned area were used to derive the following requirements:

$$L_m \leq 2.65\sqrt{Rt_{min}} \text{ and } t_{nom} > 1.13 t_{min} \tag{20}$$

$$t_{aloc}/t_{min} \geq \frac{1.15\sqrt{Rt_{min}}}{L}\left[1 - \frac{t_{nom}}{t_{min}}\right] + 1 \tag{21}$$

$$t_{aloc}/t_{min} \geq 0.353 L_m\sqrt{Rt_{min}} \tag{22}$$

As an alternative, the reinforcement adjacent to opening is based on the following equation:

$$t_{aloc}/t_{min} \geq 1 - \left(\frac{0.935 A_{rein}}{L_m t_{min}}\right) \tag{23}$$

Local Membrane Stress

The requirements of the minimum wall thickness, t_{min}, in the design codes depend on general membrane stress limits assuming t_{min} is the same over the entire pipe cross- section. For cases where the thickness is reduced over a localized region of the pipe, a less conservative approach is more appropriate. Local thickness effects are not covered in the design code but alternative design by analysis rules are given in ASME Section III. These rules allow a local primary membrane stress limit of $1.5 S_m$[5] over a distance $\sqrt{Rt_{min}}$. It is recognized that these alternative rules are applicable only to ASME Section III Class 1 components but it is judged that application of the rule to piping systems designed to other codes is justified as long as the allowable stress limit is taken from the original construction code. With the conservative assumption that wall thinning extends fully around the circumference of the pipe, a curve to define the acceptable depth and axial extent of local thinning has been developed and is shown by the blue curve in Figure 22. It is to be noted that this curve incorporates axial stresses generated in the pipe due to applied bending loads.

Choice of Evaluation Procedure

The choice of evaluation procedure to determine the acceptability of the local wall thinning below t_{min} is shown in Figure 23 and may be based on axial corrosion, branch reinforcing, or the local membrane stress approach. Figure 23 shows the logic used to select the appropriate local wall thickness evaluation procedure according to Code Case N-597-2.

---

[5] S_m is the allowable stress based on the design code

It is to be noted that range of validity (i.e. material properties, pipe (D/t) ratio, etc) of the methods given in the Code Case is not clearly stated and therefore caution needs to be exercised if the method is to be used to assess corrosion damage in pipework not designed to the ASME Boiler and Pressure Vessel Code, Section III.

5.2 Technical Basis for Allowable Local Wall Thickness for Limited and Unlimited Transverse Extent in N-597-2

The technical basis for the allowable local wall thickness given by the red curve in Figure 22 is from ASME B31G [1] as discussed in section 2.1. However, it has been recognized that the ASME B31G criteria only allows the amount of wall thickness required to sustain internal pressure loading. To take into account significant bending loads in nuclear piping, the ASME B31G acceptance criteria in code case N-597-2 is limited to a transverse extent not exceeding $(R_{min}t_{min})^{1/2}$, where the parameter R_{min} is the pipe mean radius and t_{min} is the pipe wall thickness. Discussion in Reference [48] indicates that for a transverse extent of wall thinning not exceeding $(R_{min}t_{min})^{1/2}$, an adequate margin would still be maintained for the pipe subjected to external bending moments.

The technical basis for the allowable local wall thickness given by the local membrane stress curve (the blue curve) in Figure 22 is based on evaluations of local membrane stress for a fully circumferential, uniformly thinned section in a cylinder with thickness beyond the thinned area equal to t_{min}. The geometry was modelled as an infinitely long cylinder of mean nominal outside radius R and wall thickness t_{min}, which contains a locally thinned area of length L and wall thickness t_{aloc}.

5.3 Technical Basis for Allowable Local Wall Thickness for Limited Axial and Transverse Extent in N-597-2

The technical basis for evaluating allowable local wall thickness for limited axial and transverse extent of wall thinning is described in Reference [48].

Protection Against Pressure Blowout

To protect against pressure blow out, the local thinned area is idealized as a circular plate with diameter, L_m, and uniform thickness, t, as shown in Figure 24. The dimension L_m is the maximum extent of a local thinned area of predicted wall thickness, exclusive of the corrosion allowance, t_{min}. Assuming the plate is subjected to pressure loading on one side equal to the design pressure, P, a relation between the minimum allowable local wall thickness, t_{aloc} and the axial extent L_m is derived using the limit on primary membrane plus bending stress from ASME [47] as follows:

$$\frac{t_{aloc}}{t_{min}} = \frac{0.353 L_m}{(R_{min} t_{min})^{1/2}} \qquad (24)$$

Area Reinforcement

Briefly, the requirements of openings in Class 1 piping of Section III of the ASME Boiler and Pressure Vessel Code [47] were adapted to develop an equation to limit the allowable local wall thickness to satisfy the area reinforcement requirements. With reference to Figure 25, equation (25) was derived for Class 1 piping:

$$\frac{t_{aloc}}{t_{min}} = 1 - 1.5 \frac{(R_{min} t_{min})^{1/2}}{L} \left(\frac{t_{nom}}{t_{min}} - 1 \right) \qquad (25)$$

where

$$L_A = \frac{L}{2} + 0.5(R_{min} t_{min})^{1/2} \tag{26}$$

6 Non Linear Finite Element Analysis

Non-linear finite element (FE) analyses of pipe with simulated corrosion defects were undertaken using the procedures described in BS 7910 [5] and the PRCI Guidance Document [10], see section 2.7 above. The method described in section 2.7 has only been validated for internal pressure loading. In the analyses described below both internal pressure and external loading was applied to the pipe, and, therefore, to validate the results of the FE analyses a focused program of full-scale tests was undertaken. The test program is described in section 7.

6.1 Pipeline Material Grades and Geometries

Four pipeline geometries and materials were agreed with the PRCI project team for analysis and assessment. These are summarized below and were chosen on the basis that they are the most common material grade and geometry. A selected number of analyses were undertaken for 1219.2mm (48-inch) diameter grade X65 pipe. This choice was made because full-scale tests under combined loading had been undertaken for Alyeska (see section 2.9). The results of these tests were available in the public domain and were considered a good method of providing an independent validation of the FE analyses.

- Pipe Diameter, D, 914.4mm (36-inch) and wall thickness, t, 12.7mm (0.5-inch)

  [D/t=72], API 5L Grade X65

- Pipe Diameter, D, 457.2mm (18-inch) and wall thickness, t, 5.6mm (0.219-inch)

  [D/t=82], API 5L Grade B/X42

- Pipe Diameter, D, 219.1mm (8-inch) and wall thickness, t, 8.2mm (0.322-inch)

  [D/t=27], API 5L Grade B/X42

- Pipe Diameter, D, 1219.2mm (48-inch) and wall thickness, t, 11.73mm (0.462-inch)

  [D/t=104], API 5L Grade X65

A selected number of analyses were undertaken for this latter pipe diameter and material. These analyses are described in section 8.

6.2 Defect Geometries

For the 914.4mm (36-inch), 457.2mm (18-inch) and 219.1mm (8-inch) diameter pipes, single pit, groove and patch defects on the external surface of the pipe were investigated. In the case of groove defects, both axial and circumferential orientations were investigated. Defect depths ranging from 20%, 50% and 80% of the wall thickness, t, were considered.

For the 1219.2mm (48-inch) diameter pipe, a selected number of groove and patch defects of depth equal to 50% of the wall thickness were modeled to compare with actual failures reported in the public domain by SWRI (see section 2.9).

6.3   FE Models

Three-dimensional FE models of the corroded pipes were constructed using the PATRAN 2001 r3 [49] mesh generating software and analyzed using the general-purpose FE code ABAQUS/Standard version 6.41 [50].

All the models were constructed using 20-noded reduced integration brick elements of ABAQUS type 'C3D20R'. At least four layers of elements were used through the remaining ligament of each corrosion defect; this was to ensure that the high stress gradients at the minimum ligament could be modeled with sufficient accuracy. Mesh convergence studies concluded that this level of model refinement was sufficient in order to capture stress gradients with adequate accuracy. The meshes were transitioned to one or two elements through the thickness in the main body of the pipe away from the defect location. Figures 26 to 29 show typical FE meshes of each of the four pipe geometries that were selected.

The total lengths of the pipes were modeled sufficiently long to ensure that the boundary conditions applied to the FE models had no effect on the stresses in the regions of interest.

Due to the highly non-linear characteristics of the problem, the analyses allowed for both material non-linearity and large localized non-linear deformation to be considered (NLGEOM).

6.4   Material Properties

6.4.1   Grade X65

The true stress versus true plastic strain curve that was used for the analyses for the 914.4mm (36-inch) diameter models is shown in Figure 30. This data was obtained from a modern API 5L Grade X65 linepipe steel and was generated by GL (then part of the former British Gas) in support of the Line Pipe Corrosion Group Sponsored Project (GSP). Grade X65 steel was chosen because a large proportion of transmission pipelines, both in North America and Western Europe, are constructed from this material grade. Tensile tests were undertaken using both longitudinal and circumferential round bar and flattened strip specimens. Because the FE study considered a variety of defects orientated both axially and circumferentially to the pipe axis it was decided that a lower bound fit of the tensile test results would be most appropriate. When defining plasticity data in finite element codes such as ABAQUS, true stress versus true strain data must be used. A rate-independent plasticity model using the von Mises yield criterion and isotropic hardening rule was adopted. The true stress versus true strain average curve shown in Figure 30 was input into ABAQUS as a piece-wise linear approximation using the *PLASTIC option.

The true ultimate tensile strength (UTS) of the material, derived by the test house was equal to 675 MPa (97942.5 psi); this value was confirmed using a graphical method using the true stress versus true strain curve, often referred to as Considèré's construction, see for example [51].

Stress versus strain data for the 1219.2mm (48-inch) diameter grade X65 pipe used for the Alyeska tests undertaken by South West Research Institute (SWRI) was available in Reference [23]. The true stress versus true plastic strain curve is shown in Figure 31 and was input into ABAQUS in a consistent manner to that described above.

A comparison of Figures 30 and 31 shows that there is good agreement between the stress versus strain curves for 914.4mm (36-inch) and 1219.2mm (48-inch) diameter grade X65 pipe.

Young's Modulus and Poisson's ratio of 210000 MPa (30471ksi) and 0.3 were used for steel.

6.4.2   Grade B/X42

The true stress versus true strain curve for Grade B/X42 material that was used for the 457.2mm (18-inch) and 203.2mm (8-inch) diameter models is shown in Figure 32. The curve was obtained from round bar

tensile tests using material obtained from pipe used in the validation tests described in section 7. The mill certificate for the pipe is given in Appendix A. The stress versus strain data was input into ABAQUS in a consistent manner to that described in section 6.4.1 for X65 grade material.

6.5 Boundary Conditions

Symmetry boundary conditions were used as appropriate for the models in order to reduce their size and thereby reduce computer run times. Full models were used where required, for example, to ensure non-symmetric buckling modes were accounted for in the buckling assessment (see section 6.7).

6.6 Loading

Internal pressure loading was applied to inner faces of each model using the ABAQUS *DLOAD option. In order to apply external loading, a single reference node at the end of the model, coincident with the pipe centerline was introduced. External loading (either a bending moment or compressive axial load) was applied to the model via this reference node using the ABAQUS 'kinematic coupling' constraint option. This option allows loads to be applied with respect to a local coordinate system and can be used in geometrically non-linear analysis. The definition of a local coordinate system at the reference node enables free radial expansion of the pipe end throughout arbitrary motion of the structure.

The following external loads were included in the analyses:

- Negative bending moment; compression of the corroded ligament

- Positive bending moment; tension of the corroded ligament

- Negative axial force; compression of the corroded ligament (excluding the 1219.2mm (48-inch) diameter pipe, where only bending loads were analyzed)

Positive axial force (i.e. tension of the corroded ligament) has not been presented, as this was shown at an early stage of the study to result in higher limit loads than the applicable negative axial force loading.

The pressure loading was applied to all internal surfaces. In order to represent the pipes being 'capped off', as in the full scale tests simulated, a pressure end load, F, force was applied to the ends of the pipes at the reference nodes according to the following equation:

$$F = P \, \pi \, R_{int}^{2} \qquad\qquad (27)$$

where:

R_{int} = internal pipe radius

Bending moment or axial force loadings (as appropriate) were also applied at the reference nodes. The analyses apply the pressure load in the first step, followed by an increasing external load in the second step. Investigation was undertaken to ensure that the results were not different if the external loading was applied in the first step, followed by increasing internal pressure.

6.7 Buckling

The buckling behavior of pipelines was assessed using the ABAQUS/Standard [9]. Non- linear geometrical behavior and material non-linearity was considered. The analysis was conducted in two steps. In the first step, a modal analysis is undertaken to predict the eigenmodes of the pipe containing the corrosion defect. This part of the analysis is used to determine the most critical imperfect shape that would lead to the lowest collapse load. The second stage is to introduce an imperfection into the pipe. The magnitude of the imperfection 'seeded' into the model was based on the manufacturing tolerances of pipe given in API 5L [52]. For example, for the 203.2mm (8-inch) diameter pipe, API 5L gives a tolerance of ±0.75% with respect

to the outside diameter and an out out-of-straightness tolerance 0.2% of the length. It is, however, noted that this procedure is required to initiate a buckle in a geometrically perfect structure. In the case of the models analyzed, an imperfection in the form of the corrosion defect was already present. The presence of a deep corrosion defect should be sufficient to induce buckling of the pipe. However, for a shallow corrosion defects (e.g. <20% deep), in the pipe with a high D/t ratio it is possible that the manufacturing tolerances and geometry may dominate the buckling behavior of the pipe. Therefore, the buckling analyses were undertaken by 'seeding' in manufacturing tolerances stipulated in API 5L as appropriate.

To ensure that both symmetric and antisymmetric buckling modes were accounted for, full three dimensional brick models of the pipe were constructed. Care was taken to ensure that the mesh density chosen was sufficient. This was done by conducting a convergence study to ensure that the relative change in eigenvalues was not significant with increasing refinement of the FE mesh. Figure 33 shows an example of the first eigenmode for an 203.2mm (8-inch) diameter pipe with an 80% deep axially orientated groove, subjected to a compressive force. It is to be noted that the first eigenmode may not give the lowest buckling load. Therefore the first twenty eigenmodes were investigated to determine the lowest buckling load.

To assess the onset of buckling, the stress at the ligament and at a point 180º, diametrically opposite the defect was monitored as the internal pressure/external loading was increased. In addition, the change in displacement and rotation of the pipe ends was also monitored to measure the onset of global instability (or buckling) of the pipe.

6.8   Failure Criteria

To summarize, the criteria used to assess failure of the pipe was assessed as follows:

a) The von Mises equivalent stress in the ligament is monitored against the true ultimate tensile strength (UTS) of the pipe. This is consistent with the approach used to determine the failure pressure of the pipe under only internal pressure loading. Figure 34 summarizes how the failure pressure is predicted.

b) The von Mises equivalent stress in the pipe is monitored at a point 180° (i.e. diametrically opposite) from the corrosion defect against the yield strength of the pipe.

c) The onset of local collapse or global instability/buckling.

Failure of the pipe is deemed to occur when the lowest pressure/external loading combination from the above three criteria.

6.9   Results

Figure 35 shows a typical example of the failure locus obtained for a 457.2mm (18-inch) diameter by 5.56mm (0.219-inch) wall grade B/X42 pipe under combined internal pressure and bending loads with an 80% deep axial groove. In this case, the failure locus is obtained using the von Mises equivalent stress at the ligament criterion and the von Mises equivalent stress at a point 180º (i.e. diametrically opposite corrosion defect). A locus is subsequently derived based on the lowest pressure internal pressure and external loading criteria as shown in Figure 36. Any combination of internal pressure and external loading above the failure locus is deemed to be unsafe and any combination below is deemed safe.

As discussed in section 2 existing assessment methods such as ASME B31G, RSTRENG and LPC are based on the results from an extensive program of full-scale burst tests. These tests were conducted on sections of corroded pipe, or pipe with machined defects, which then had dome ends welded at the ends to form a pressure vessel. The internal pressure was subsequently increased up to the point that failure occurred. Therefore the existing assessment methods have effectively been calibrated with both hoop and axial load loading, i.e. there is already an inherent level of biaxial loading accounted for in the derivation of existing assessment methods. Figure 36 also shows a plot of the failure pressure obtained using RSTRENG

and LPC methods. This plot illustrates how the failure locus can be used to determine the limit of applicability of existing assessment methods such as RSTRENG or LPC under combined loading conditions. This example shows that RSTRENG remains valid even if the pipeline is subjected to an external bending moment of up to 250MNmm (184366 lbf.ft). The example also shows that if the LPC method is used (which generally predicts a less conservative failure pressure than RSTRENG or ASME B31G), then the LPC method remains valid even if the pipeline is subjected to an external bending moment of up to 50MNmm (36873 lbf.ft).

The results of the FE analyses are summarized in the form of a failure locus for each geometry/material investigated as follows:

1. Appendix A 203.2mm (8-inch) diameter pipe failure loci.

2. Appendix C 457.2mm (18-inch) diameter pipe failure loci.

3. Appendix D 914.4mm (36-inch) diameter pipe failure loci.

A comprehensive derivation of failure loci has been generated for each of these geometries. In some instances, for example for a shallow (20% deep pit), the failure of the pipe is dominated by global yielding rather than failure at the corrosion defect. In this case, the failure locus for the defect to be assessed is not given in the Appendices and it has to be assumed that failure is due to yielding of the pipe.

7 Validation Tests

7.1 Introduction

A full-scale burst test program was devised and agreed with the PRCI project team to validate the FE analyses described in section 6. Due to budget constraints, only one pipe diameter 457.2mm (18-inch) and material (grade B/X42) was chosen for the test program. Testing was limited to combination of internal pressure and external bending loads. The results of a test program conducted by SWRI for the Alyeska Pipeline Services Company were also available in the public domain (see section 2.9). Sufficient details were available to model a selection of these tests using the same the assessment methods as those described in section 6. Use of a selection of the SWRI tests was considered a cost effective method of providing an independent means of validating the results of the FE analyses described in this report.

7.2 Material and Geometry

All the tests were undertaken using modern 457.2mm (18-inch) outside diameter (OD) by 5.6mm (0.219-inch) wall thickness, welded ERW steel linepipe, material API 5L grade B/X42. Mill test certificates for the pipe tested are given in Appendix A.

7.3 Design of Test Rig

A purpose made test rig was designed and constructed to support and apply pure bending in a four-point configuration to an internally pressurized pipe.

Bending loads were applied via vertically orientated 101.6mm (4-inch) diameter hydraulic rams, each having a maximum load capacity of 352kN (79137lbf) per ram and a maximum travel of up to 305mm (12-inches). Appendix E shows a general arrangement of the test rig and an example of a fully instrumented test vessel prior to testing. For each test, the hydraulic rams were positioned 1.5m (39.4-inches) from each reaction points.

7.4 Test Matrix

A matrix of six full scale tests was devised and agreed with the PRCI Project Team as summarized in Table 23. All the defects were chosen to have a depth of 80% of the wall thickness (t). Two defects were chosen to be round-bottomed grooves orientated either axially or circumferentially. The length and width of the groove defects was chosen to be 8t by 2t respectively. The third defect was chosen to be a square patch of dimension 8t by 8t. In each case the corner radius of the defect was 1t.

Three tests were conducted with only internal pressure loading to confirm failure pressure predictions from the FE analyses. The same defects were machined in a further three vessels using pipe from the same section. Metrology on each vessel in the vicinity of the defect was undertaken for each vessel; the results are given in Appendix F.

7.5 Design of Test Vessels and Instrumentation

A dimensional survey was conducted on each test pipe. Defects were subsequently machined onto the external surface of each test pipe. Metrology in the vicinity of the machined defect was undertaken to determine the actual defect depth and length achieved by machining (see Appendix F). End caps were welded to the pipe to form a pressure vessel approximately 9.1m (30 feet) in length. Defects were machined on the external surface of the pipe at the mid-span position. The vessel was instrumented by connecting pressure and temperature transducers to monitor internal pressure and pipe metal temperature. In addition, high elongation strain gages were placed on the inner surface of the vessel, directly below the defect center. Additional strain gages were also placed on the outer surface of the pipe wall away from the defect pair in order to monitor the overall structural response to the loading. In total, eighteen strain gages were used to monitor strains for vessel numbers 2, 4 and 6. A load cell was also installed at each ram to monitor the magnitude of the load applied throughout the test. In addition a linear variable differential transformer (LVDT) was used to measure the deflection at the center of the pipe.

The defects were orientated both axially and circumferentially as summarized in Table 23.

7.6 Test Procedure

All the tests were undertaken in accordance with GL's in house hydrotesting procedures [53].

7.6.1 Internal Pressure Only Tests

Vessel numbers 1, 3 and 5 were subjected to a monotonically increasing pressure until either failure occurred at the defect or gross plasticity/buckling of the pipe was observed.

7.6.2 Combined Internal Pressure and Bending Tests

Vessel 2

Load steps were applied during the test as detailed below.

1. With the vessel depressurized, a 10 tonne (22046.2 lb) load was applied at each hydraulic ram. This level of load is sufficient to give only elastic deformation of the pipe. The axial strain and deflection at the mid-span of the vessel was recorded and confirmed that the correct bending loads applied to the pipe.

2. The ram load was removed and the vessel was pressurized to 60 bar (870.2 psi). The hoop and axial strains in the main body of the pipe were measured.

3. With the pressure held constant at 60 bar (870.2 psi), a 10 tonne (22046.2 lb) load was applied at each hydraulic ram. Axial and hoop strains were measured in the main body of the vessel; in the vicinity of the defect and at a point diametrically opposite the defect.

4. The ram load was then increased to a value to give a maximum bending moment of 218 MNmm (160767lbf.ft) at the mid-span of the pipe.

Vessel 4

Load steps were applied during the test as detailed below.

1. With the vessel depressurized, a 15 tonne (33069.3 lb) load was applied at each hydraulic ram. This level of load is sufficient to give only elastic deformation of the pipe. The axial strain and deflection at the mid-span of the vessel was recorded to confirm that the correct bending loads were applied to the pipe.

2. The ram load was removed and the vessel was pressurized to 50 bar (725psi). The hoop and axial strains in the main body of the pipe were measured.

3. With the pressure held constant at 50 bar (725 psi), a 15 tonne (33069.3 lb) load was applied at each hydraulic ram. Axial and hoop strains were measured in the main body of the vessel; in the vicinity of the defect and at a point diametrically opposite the defect.

4. The ram load was then increased to a range 18 tonne (39683.2 lb) to 20 tonne (44092.4 lb), to give a bending moment at the pipe mid-span of 260 MNmm (191740 lbf.ft).

Vessel 6

Load steps were applied during the test as detailed below.

1. With the vessel depressurized, a 10 tonne (22046.2 lb) load was applied at each hydraulic ram. This level of load is sufficient to give only elastic deformation of the pipe. The axial strain and deflection at the mid-span of the vessel was recorded to confirm that the correct bending loads were applied to the pipe.

2. The ram load was removed and the vessel was pressurized to 25 bar (362.6 psi). The hoop and axial strains in the main body of the pipe were measured.

3. With the pressure held constant at 25 bar (362.6 psi), a load of approximately 10 tonne (22046.2 lb) was applied at each hydraulic ram. Axial and hoop strains were measured in the main body of the vessel; in the vicinity of the defect and at a point diametrically opposite the defect.

4. The ram load was then increased to approximately 21.6 tonne (47619.8 lb) to give a bending moment at the pipe mid-span of 318 MNmm (234513.27 lbf.ft).

7.7   Test Results

Vessel 1

Figure 37 shows the pressure versus time plot for vessel number 1. Failure of the vessel occurred at the defect at an internal pressure of 77.4bar (1122.6psi). The failure extended along the length of the defect ligament. The defect did not extend into the main body of the pipe. This is a typical failure of a deep volumetric corrosion defects in high toughness pipe.

The actual failure pressure compares well with the FE predicted failure pressure of 74.5 bar (1080.5 psi). The predicted failure pressure was therefore conservative and to within approximately 4% of the actual failure pressure. Generally predictions using the FE method are to within ±10% of the actual failure pressure. This result provides confidence in the FE model and the underlying assumptions used.

GL

Vessel 2

Figure 38 shows the pressure versus time plot and ram load versus time plot for vessel number 2. At a ram load of 9.1 tonne (20062lb) the deflection at mid-span was measured to be approximately 22mm (0.87-inch). Hand calculations predict a mid-span deflection of just less than 20mm (0.79-inch) under four point bending. Strain gage readings on the tension side gave values of 760µs; this value is again very close to the hand calculated elastic strain in the pipe of 762µs under four point bending.

On removal of the ram load, the mid-span deflection and strain gage readings at the mid-span were reduced to zero readings thus concluding that the vessel had deformed in an elastic manner.

With the vessel pressurized to 60 bar (870.2 psi), axial and hoop strains in the main body of the vessel were measured to be 350µs and 1010µs. With the internal pressure held constant at 60bar (870.2 psi), and the ram load increased to 14.8 tonne (32628.4 lb), the mid-span deflection was measured to be 41mm (1.6-inch). The vessel did not fail at this point and therefore it was decided to raise the internal pressure whilst keeping the ram load at a target value of just less than 15 tonne (33069.3 lb). As the pressure was increased, manual adjustment of the ram loads was required. Failure of the vessel at the defect occurred when the internal pressure was increased to 66.3 bar (961.6psi). The failure was similar to that observed for vessel 1, i.e. a short crack running the along the length of the ligament which did not extend into the main body of the pipe. Figure 39 shows a view of the vessel at the end of the test.

Figure 40 shows the failure point marked on the bending-pressure failure locus for 457.2mm (18-inch) diameter pipe (see Appendix C). The failure point is above the failure locus in the unsafe part of the graph. The actual failure pressure was approximately 10% above that predicted. This result provides confidence in the FE model and the underlying assumptions made to derive the failure point under combined loading.

Vessel 3

Figure 41 shows the pressure versus time plot for vessel number 3. The internal pressure was increased up to 90 bar (1305.3 psi) and gross yielding at the center of the test vessel was observed. The FE analysis had predicted failure by gross yielding at an internal pressure of 89.3bar (1295.2 psi). The internal pressure was increased up above 90bar (1305 psi) to determine whether failure at the defect could be achieved. The test was finally terminated at an internal pressure of 96.8bar (1404 psi) and was considered to provide data that would be required for the combined loading test on vessel 4.

Vessel 4

Figure 42 shows the pressure versus time plot and ram load versus time plot for vessel number 4. At a ram load of just less than 10 tonne (22046.2 lb) the deflection at the pipe mid-span was measured to be approximately 23mm (0.91-inch). Hand calculations predict a mid-span deflection 20mm (0.79-inch) under four point bending. Axial strain gage readings on the tension side gave an average value of 750µs diametrically opposite the defect; this value is again close to the hand calculated elastic strain in the pipe of 762µs under four point bending.

On removal of the ram load, the mid-span deflection and strain gage readings at the mid-span were reduced to zero readings thus concluding that the vessel had deformed in an elastic manner.

In general, the behavior of the vessel under four-point bending was similar to that for vessel 2 when a 10 tonne (22046.2 lb) ram load was applied.

With the vessel pressurized to 50 bar (725 psi) and with zero ram load, the hoop strains in the main body of the vessel were measured to be 848µs. With the internal pressure held constant at 50 bar (725 psi), and the ram load increased to 20 tonne (44092lb), the mid-span deflection was measured to be 50mm (1.97-inch). The vessel did not fail at this point and therefore it was decided to raise the internal pressure whilst keeping the ram load at a target value in the range 15 tonne (33069lb) to 20 tonne (44092lb). The pressure was increased to 80 bar (11608 psi) but failure at the defect did not occur. At this point, the test was terminated.

A mid-span deflection of 100mm (3.94-inch) was measured for this load combination. When both the internal pressure and ram loads were reduced to zero, a permanent deflection of 66mm (2.6-inch) was measured at the pipe mid-span. It is to be noted that yielding of the pipe is also included in the derivation of the failure locus and therefore it was concluded that this was a valid test. Figure 43 shows the vessel at the end of the test with internal pressure and ram loads reduced to zero.

Figure 44 shows two test points marked on the bending-pressure failure locus for 457.2mm (18-inch) diameter pipe (see Appendix C). The test points are above the failure locus in the unsafe part of the graph and once again this result provides confidence in the FE model and the underlying assumptions made to derive the failure locus.

Vessel 5

Figure 45 show the pressure versus time plot until failure for vessel number 5. Failure of the vessel occurred at the defect at an internal pressure of 81.1bar (1176.3 psi), similar to that observed for vessel 1 and 3. The FE analysis predicted failure at a pressure of 85.9bar (1245.9 psi) i.e. a difference of nearly 6% between the predicted and actual failure pressure. This level of accuracy is within the generally accepted tolerance of ±10%. Reference to Appendix F shows that the depth of the *actual* patch defect machined in the pipe wall was nearly 83% of the wall thickness (t). The FE model used to predict the failure pressure was based on a defect depth of exactly 80% of the wall thickness. Variations such as these can explain the apparent discrepancy between the actual versus predicted failure pressures. This result was again considered to provide confidence in the FE model.

Vessel 6

Figure 46 shows the pressure versus time plot and ram load versus time plot for vessel number 6. At a ram load of just less than 10 tonne (22046.2 lb) the deflection at the pipe mid-span was measured to be approximately 20mm (0.79-inch). Hand calculations predict a mid-span deflection 20mm (0.79-inch) under four point bending. Axial strain gage readings on the tension side gave an average value of 750μs diametrically opposite the defect; this value is again very close to the hand calculated elastic strain in the pipe of 762μs under four point bending.

On removal of the ram load, the mid-span deflection and strain gage readings at the mid-span were reduced to zero readings thus concluding that the vessel had deformed in an elastic manner.

In general, the behavior of the vessel under four point bending was similar to that for both vessel 2 and 4.

With the vessel pressurized to 25 bar (362.5psi) the ram load increased to 21.6 tonne (47619.8lb), the mid-span deflection was measured to be 50mm (1.97-inch). Although there was considerable deformation at the pipe mid-span, the vessel did not fail at the defect at this point. It was decided to increase the ram load with the vessel internal pressure held constant at 25 bar (362.5 psi). Ram loads were slowly increased and reached a value of 23.5 tonne (51808.6 lb). At this point, buckling of the pipe was observed at one ram, as shown in Figure 47, and the test was terminated. A permanent deflection at the pipe mid-span deflection of 82mm (3.23-inch) was recorded. As with vessel 4, the vessel did not fail at the defect, but gross yielding at the mid-span and buckling at the loading points was obtained. As was concluded with vessel 4, the results of the test are considered valid. Figure 48 shows the test points marked on the bending-pressure failure locus for 457.2mm (18-inch) diameter pipe (see Appendix C). As with vessel 4, the test point is above the failure locus in the unsafe part of the graph. This result again provides confidence in the FE model and the underlying assumptions made to derive the failure locus.

8 Validation Using the Alyeska Test Results

Selected tests performed by SWRI for the Alyeska were modeled using the FE method and assumptions consistent with those described in section 6. With reference to Table 22, three tests identified as, II-2, II-3 and II-4 were analyzed. Figure 29 shows an example of the quarter symmetry finite element model that was

constructed. Material properties used in the analyses are discussed in section 6.4.1. Loading was applied to the FE model in the same manner as that described for each test [23]. The internal pressure was increased to the level given in Table 22, i.e. 66.5 bar (950psi) for Test II-2; 67.6 bar (980psi) for Test II-3; and 57.9 bar (840psi) for Test II-4. A pure bending moment was then applied to the model until failure was predicted using the criteria described in section 6.8.

Table 24 shows a comparison of the actual test results and those predicted using FE analysis. The following results were obtained:

Test II-2

Failure was predicted initially by global yielding in the pipe diametrically opposite the defect when the bending moment reached a value of +3980MNmm (35,250kip-in). Reference [23] states that failure of the pipe occurred by a wrinkle at the pipe when the bending moment reached the value +4150MNmm (36,757kip-in). It was concluded that the failure point could be predicted conservatively to within 4% of that reported for Test II-2 according to the criteria described in section 6.8.

Test II-3

Failure was predicted initially by global yielding in the pipe diametrically opposite the defect when the bending moment reached a value of +4470MNmm (39,591kip-in). A slightly higher bending moment of -4580MNmm (-40,565kip-in) was predicted with defect positioned on the compressive side. Failure at the defect was predicted when the bending moment was increased to -5230MNmm (-46,323kip-in). It was concluded that the failure point could be predicted conservatively to within a range 3% to 13% according to the criteria described in section 6.8.

Test II-4

Failure was predicted initially by global yielding in the pipe diametrically opposite the defect when the bending moment reached a value of +4930MNmm (+43,666kip-in). A higher bending moment of -5620MNmm (49,777kip-in) was predicted with the defect positioned on the compressive side. Failure at the defect was predicted when the bending moment was increased to -6500MNmm (-57,571kip-in). It was concluded that the failure point could be predicted conservatively to within a range 5% to 8% according to the criteria described in section 6.8.

9 Failure Predictions Using DNV RP-F101

Failure predictions were conducted for the validation tests described in this report using the procedures described in DNV RP-F101 for combined internal pressure and external bending load. The results of the assessment are summarized in Table 25. It is noted that in two cases (GL vessel 4 and SWRI test II-2), the failure pressures calculated using DNV RP-F101 are higher the test points given in Table 25. As discussed earlier, failure is based on global yielding, or buckling instability at the corrosion defect. For GL vessel 4, failure first occurred by yielding of the pipe; in the case of SWRI test II-2, failure first occurred by wrinkling. This may explain why DNV RP-F101 gives non-conservative results. For the other cases DNV RP-F101 predicts very conservative failure pressures.

10 Discussion

A method for predicting the failure behavior of pipelines with isolated corrosion defects subjected to combined loading has been developed for common transmission pipeline geometries. The method has been developed based on an extensive study using non-linear finite element analysis and validated using full-scale test results from two independent sources. The results are presented in a series of failure locus diagrams for pipe (D/t) ratios ranging from 27 to 72, and material grades Grade B to X65. Guidance is given to assess defect depths ranging from 20% to 80% of the wall thickness (t).

Case histories show that for onshore pipelines, significant external loading can be imposed on transmission pipelines. Stress analyses undertaken on 457.2mm (18-inch), 914.4mm (36-inch) and 1219.2mm (48-inch) diameter pipe conclude that bending moments in the range 7.32MNmm (64.8kip-in) to 8880MNmm (78651kip-in) and axial loads in the range 0.35MN (78687lbf) to 17.2MN (3866906lbf) can be generated due to landslides; external loading of this magnitude is large enough to cause failures in pipelines. For example, for 457.2mm (18-inch) pipe operating at 70 bar (1015 psi), a bending moment of 342MNmm (3029kip-in) could be generated (see Table 19). An 80% deep patch in grade B/X42 pipe would be unsafe (see Figure C3) for such loads. Similarly a compressive load of 1.74MN (391lbf) could be generated in the pipe, which would result in an 80% deep patch being unacceptable (see Figure C8).

Existing assessment methods used by the pipeline industry such as ASME B31G and RSTRENG were validated using corroded pipes welded with dome ends to form pressure vessels and subsequently pressurized to failure. Consequently a degree of biaxial loading is accounted for in the assessment methods. The failure loci developed can be used to assess the limit of acceptability of ASME B31G, RSTRENG and LPC when assessing corroded pipelines that are subject to external loading.

Methods have been developed by the nuclear industry to assess the integrity of corroded pipework. Different assessment methods are recommended in ASME Code Case N-597-2 depending on the extent of the corrosion damage. Strictly the assessments given in the code case are applicable to pipework that has been designed to the ASME Boiler and Pressure Vessel Code Section III, Division 1, Rules for the Construction of Nuclear Power Plant Components. For higher safety class (Class 1) pipework, the maximum depth of corrosion is limited to 70% of the wall thickness. For lower safety class pipework, the limit is relaxed to 80%; this is consistent with ASME B31G and RSTRENG.

The methods developed in this report have so far considered materials up to strength grade X65. Work has been conducted on Project #153H to extend assessment methods up to grade X100 [82] and [84]. However, the methods described are applicable only for assessing the remaining strength of pipelines subject to internal pressure loading. Additional work is currently being undertaken in Phase 2 of Project #153H to address this knowledge gap [85]. Once the work in Phase 2 has been completed, the failure locus diagrams presented in this report will be normalized allowing them to be incorporated into the PRCI Guidance Document. The normalized failure locus diagrams will be presented in Reference [85].

In addition, the methods developed so far have only considered isolated defects in the main body of the pipe and not at or near girth or seam welds. In reality, in-line inspections may report the presence of a large number of closely spaced defect clusters that may interact with each other. Remaining strength predictions of corroded pipelines will in general be sensitive to the interaction criterion used and the method by which clusters are deemed to interact. Defect interaction rules are generally agreed between the inspection company and the pipeline operator. New and improved interaction rules have been developed for defects in pipelines subjected to internal pressure loading [77], [80], [81]. It should be noted that use of these interaction rules may not be appropriate in cases when assessing defects in pipelines subjected to internal pressure and external loading. It is judged that remaining strength assessments of corroded pipelines for these cases would not be routinely required. In the event that assessments are required for such a case then it is recommended that they are conducted on a case by case basis.

11   Conclusions

1. The remaining strength of corroded pipelines subject to internal pressure and external loading cannot be explicitly assessed using the ASME B31G, RSTRENG and LPC assessment methods. However, these assessment methods have been validated using pipe with real corrosion and simulated (machined) defects welded to dome ends to form a pressure vessel and subsequently failed under internal pressure loading. Consequently, existing methods include some inherent biaxial loading and the remaining strength of corroded pipelines can be assessed with a limited amount of external loading.

2. Ground movement due to landslides can impose significant external loading to transmission pipelines. Stresses in pipelines due to landslides can be greater than the stresses due to internal pressure loading.

3. Methods developed by the nuclear industry for assessing corroded pipework are given in ASME Code Case N-597-2 and based on ASME B31G when the axial extent of wall thinning is limited. For more extensive corrosion, the assessment methods are based on branch reinforcement and local membrane stress limits. Strictly the methods given in ASME Code Case N-597-2 are only applicable to the assessment of piping systems designed to the ASME Boiler and Pressure Vessel Code, Section III.

4. Failure loci of pipelines with isolated corrosion defects and subjected to combined loads have been derived for common pipeline geometries and materials. The failure loci have been validated using tests performed on 457.2mm (18-inch) and 1219.2mm (48-inch) diameter pipe under combined bending/pressure loading. These failure loci can be used to assess the limit of acceptability of existing assessment methods such as ASME B31G and RSTRENG under combined loading conditions.

12 Recommendations

1. The methods developed in this report should be extended to cover the assessment of higher strength pipelines up to grade X100 pipelines.

13 Nomenclature and Unit Conversions

A_{rein} Reinforcement area available in pipe wall based on the predicted thickness distribution in excess of t_{min}

D   Nominal outside diameter of pipe

R   Nominal outside radius of pipe

t   Pipe wall thickness

t_{min} Minimum wall thickness required by construction code to sustain pressure exclusive of tolerances and any allowances for corrosion

t_{aloc} allowable local wall thickness

t_{nom} nominal wall thickness of pipe

L   Defect length (or maximum extent of a local thinned area)

L_m Maximum extent of a local thinned area with wall thickness less than t_{min}

d   Defect depth

P_f Predicted failure pressure of corroded pipe

P_o Predicted burst pressure of plain pipe

σ_{flow} Flow stress

M   Folias (bulging correction) Factor

R_S Remaining Strength Factor (dimensionless, less than unity)

σ_{flow} Flow stress

σ_{smys} Specified Minimum Yield Strength

σ_{smts} Specified Minimum Tensile Strength

σ_{fail} Failure stress of pipe with a part wall defect

c Shear Strength of Soil

c' Drained Shear Strength of Soil

c_u Undrained Shear Strength of Soil

N Blow Count from Standard Penetration Test

ϕ' Drained Friction Angle in Degrees

ϕ_u Undrained Friction Angle in Degrees

γ Bulk Unit Weight of Soil

P   Design pressure

P_u Transverse Limiting Stress of Soil

R_u Axial Limiting Shear Stress of Soil

δ Ground Movement

n   constant

L_L Length of the Landslide

W_L Width of the Landslide

H_L Depth of landslide

S   Code specified allowable stress

UNIT CONVERSIONS

14.5psi = 1 bar = 0.1MPa = $0.1N/mm^2$

1psi = 6.895×10^{-3} MPa

1 inch = 25.4mm

1 foot = 0.3048m

1 lbf = 4.448N

1 lbf.ft = 1356Nmm

1 tonne = 1000kg = 2204.7lb

1 kip-in = 112903Nmm

14   References

1. Anon. 'Manual for Determining the Remaining Strength of Corroded Pipelines, A Supplement to ASME B31 Code for Pressure Piping', ASME B31G-1991, The American Society of Mechanical Engineers, 1991

2. Kiefner, J. F. and Vieth, P. H. 'A modified criterion for evaluating the remaining strength of corroded pipe', Final report on PR-3-805 to Pipeline Corrosion Supervisory Committee of the Pipeline Research Committee of the American Gas Association, Battelle, Ohio

3. Vieth P. H. and Kiefner, J. F. RSTRENG2 user's manual, Final report on PR-218-9205 to Corrosion Supervisory Committee, Pipeline Research Committee, American Gas Association, Kiefner & Associates, Inc., Ohio

4. Fu, B. and Batte, A. D. 'Advanced methods for the assessment of corrosion in linepipe', Summary report OTO 97065, UK Health and Safety Executive, London, 1998.

5. Anon: 'Guide to Methods for Assessing the Acceptability of Flaws in Metallic Structures', BS 7910:2005, BSI, 27 July 2005

6. Anon. 'Corroded Pipelines', Recommended Practice DNV-RP-F101, Det Norske Veritas, October 2004

7. Anon. 'Fitness-For-Service', API 579-1/ASME FFS-1, The American Petroleum Institute and The American Society of Mechanical Engineers, June 2007

8. Fu, B. and Vu, D.Q., 'Failure of Corroded Line Pipe (1) - Experimental Testing', Technical report GRTC R.1803, BG Technology, Loughborough, 1997. (GL Confidential)

9. Anon. 'ABAQUS/Standard', ABAQUS, Inc.

10. Fu, B., Jones, C.L. and Chauhan, V., 'Guidance for Assessing the Remaining Strength of Corroded Pipeline', Pipeline Research Council International, Inc., Catalog No. L51958, Advantica Technologies, Inc., August 2002

11. Bjørnøy, O.H., Sigurdsson, G. and Cramer, E., 'Reliability of Corroded Pipes – Laboratory Burst Tests', Det Norske Veritas Technical Report No. 96-3393, Rev. 2. Private Report for Joint Industry Partners, December 1997

12. Anon. 'ASME Boiler and Pressure Vessel Code, Rules for Construction of Pressure Vessels', American Society of Mechanical Engineers, 2004

13. Anon: 'Power Piping', ASME B31.1, American Society of Mechanical Engineers, 2004

14. Anon. 'Process Piping', ASME B31.3, American Society of Mechanical Engineers, 2004

15. Anon. 'Welded Steel Tanks for Oil Storage', API 650, American petroleum Institute, 2003

16. Anon. ' Design and Construction of Large, Welded, Low-Pressure Storage Tanks, API 620, Tenth Edition (with Addenda June 2004 Addenda)', American Petroleum Institute, 2002

17. Vieth P.H. and Kiefner J.F., 'Database of Corroded Pipe Tests, Final report on PR-218-9206 to Line Pipe Research Supervisory Committee, Pipeline Research Committee, American Gas Association, Kiefner & Associates, Inc., Ohio, 1994

18. Shannon, R.W.E., 'The Failure Behaviour of Line Pipe Defects', International Journal of Pressure Vessels and Piping, Vol.2, pp.243-255, 1974

19. Fu B., Stephens D., Ritchie D and Jones CL: 'Methods for Assessing Corroded Pipeline – Review, Validation and Recommendations', Prepared for Pipeline Research Council International, Inc., Catalog. No. L51878, Advantica Technologies, Inc., October 2000

20. Kiefner JF, Vieth PH and Roytman I: 'Continued Validation of RSTRENG', Final report on PR-218-9304 to Line Pipe Research Supervisory Committee, Pipeline Research Committee of PRC International, Kiefner & Associates, Inc., Ohio, 1996

21. Hopkins P and Jones DG: 'A Study of the Behaviour of Long and Complex-Shaped Corrosion in Transmission Pipelines', Proceedings of the 11th International Conference on Offshore Mechanics and Arctic Engineering (OMAE'91), Vol.5 (Pipeline Technology). New York, American Society of Mechanical Engineers, pp.211-218. 1991

22. Craig G and Sisterson G: 'Simulated Corrosion Full-Scale tests', British Gas Technical Report ERS R.4648, Engineering Research Station, Newcastle-upon-Tyne, 1991. (Advantica Confidential)

23. Smith, M.Q. and Waldhart, C.J., 'Combined Loading Tests of Large Diameter Corroded Pipelines', 3rd ASME International Pipeline Conference, ASME 2000

24. Grigory, S.C. and Smith, M.Q., 'Residual Strength of 48-Inch Diameter Corroded Pipe Determined by Full-Scale Combined Loading Experiments', 1st ASME International Pipeline Conference, Volume 1, ASME 1996

25. Smith, M.Q. and Grigory, S.C., 'New Procedures for the Residual Strength Assessment of Corroded Pipe Subjected to Combined Loads', 1st ASME International Pipeline Conference, Volume 1, ASME 1996

26. Kanninen, M.F., Roy, S., Grigory, S.C., Couque, H.R., Smith, M.Q. Simmons, G.C., Kim, H., Maple, J.A., 'Assessing the Reliability of Corroded Oil Transmission Pipelines under the Combined Loading Arising In Service', 12th ASME Offshore Mechanics and Arctic Engineering Conference, ASME 1993

27. Stephens, D.R., Bubenik, T.A., Francini, R.B., 'Residual Strength of Pipeline Corrosion Defects Under Combined Pressure and Axial Loads', NG-18, Report 216, Prepared for Pipeline Research Council International, Inc., Catalog No. L51722, Battelle Memorial Institute, February 1995

28. O'Rourke, T.D., Stewart, H.E & Jeon, S.-S., Geotechnical aspects of lifeline engineering, 'Geotechnical Engineering', Vol 149, Issue 1, pp 13–26, 2001

29. Ng, P.C.F., 'Behaviour of Buried Pipelines Subjected to External Loading', Ph.D. thesis, University of Sheffield, UK, 1994

30. Miller, J.A. and Koloski, J.W., Landslides Present Risks to Buried Steel Pipelines, 'Pipeline and Gas Journal', January 1999, pp 53-54

31. Miles, S.B. and Keefer D.K., 'Seismic Landslide Hazard for the City of Berkele, California', US Department of the interior, US Geological Survey, 2003, http://geopubs.wr.usgs.gov/map-mf/mf2378/berkpamph.pdf

32. Skempton, A.W. and Hutchinson, J.N., Stability of natural slopes and embankment foundations, 'Proc. 7th ICSMFE', Mexico City, State-of-the-Art volume, pp 291–340, 1969

33. Jones, D.K.C. & Lee, E.M., 'Landsliding in Great Britain', Department of the Environment, London, HMSO, 1994

34. NEN, Nederlandse Norm NEN 3650, 'Eisen voor stalen transportleiding systemen (Requirements for Steel Pipeline Transportation Systems)', Publikatie uitsluitend ter kritiek, 1991

35. ASCE, 'Guidelines for the Seismic Design of Oil and Gas Pipeline Systems', Committee on Gas and Liquid Fuel Lifelines, ASCE, 1984

36. Vesic, A.S., Breakout Resistance of Objects Embedded in Ocean Bottom, 'ASCE Ocean Engineering Conference', Miami Beach, 1969

37. Hansen J.B., 'The Ultimate Resistance of Rigid Piles to Transversal Forces', The Danish Geotechnical Institute, Bulletin No. 12. Copenhagen, 1961

38. Ovesen, N.K., 'Anchor Slabs, Calculation Methods and Model Tests', The Danish Geotechnical Institute, Bulletin No. 16, Copenhagen, 1964

39. Ng, P.C.F., Leach, G. & Harrold, S., International collaborative research on soil/pipe interaction, 'Proceedings of the 2001 International Gas Research Conference', IGRC 2001, Amsterdam, Netherlands. 5–8 November 2001

40. Ng, P.C.F., Pyrah, I.C. and Anderson, W.F., Modelling of laterally loaded pipelines using elastic beam on elastic foundation approach, Developments in Computational Techniques for Structural Engineering, 'Proceedings of the Sixth International Conference on Civil and Structural Engineering Computing', Cambridge, UK, 28–30 August 1995, pp. 71–76

41. Ng, P.C.F., 'Benchmark Tests for WOMODNT Version 3', Advantica Technologies Ltd., June 1999

42. IGE, 'Steel Pipelines for High Pressure Gas Transmission, Recommendations on Transmission and Distribution Practice', IGE/TD/1 Edition 4, Communication 1670, The Institution of Gas Engineers, 2001 (UK)

43. Anon. 'Rules for In Service Inspection of Nuclear Power Plant Components', Section XI, Division 1, ASME Boiler and Pressure Vessel Code, 2004 Edition with Addenda

44. Anon. 'Examination Requirements for Pipe Wall Thinning due to Single Phase Erosion and Corrosion', ASME Boiler and Pressure Vessel Code, Code Case N-80, Section XI, Division 1, May 1990, Annulled September 2001

45. Deardroff, A.F. and Bush, S.H., 'Development of ASME XI Criteria for Erosion-Corrosion Thinning of Carbon Steel Piping', ASME PVP, Vol. 186, 1990, pp. 71-75

46. Anon. 'Requirements for Analytical Evaluation of Pipe Wall Thinning', ASME Boiler and Pressure Vessel Code, Code Case N-597-2, Section XI, Division 1, November 2003

47. Anon. 'Rules for the Construction of Nuclear Power Plant Components', ASME Boiler and Pressure Vessel Code, Section III, Division 1, 2004 Edition with Addenda

48. Scarth, D.A., Hasegawa, K., Goyette, L.F. and Rush, P., 'Supplementary Technical Basis for ASME Section XI Code Case N-597-2', Proceeding of the 2006 ASME Pressure Vessels and Piping Division Conference, PVP2006-ICPVT-11, July 23-27, Vancouver, BC, Canada

49. MSC/PATRAN 2001 r3, MacNeal-Schwendler Corporation.

50. ABAQUS/Standard Version 6.4, Hibbitt, Karlsson & Sorensen Inc., 2004.

51. Pascoe, K.J. 'An Introduction to the Properties of Engineering Materials', Third Edition, Van Nostrand Reinhold (UK) Co. Ltd., 1982

52. American Petroleum Institute: 'Specification for Linepipe.' API Specification 5L, Forty Second Edition, January 2000 (Effective Date: July 1, 2000).

53. Anon. 'Recommended Practice for Conducting Mechanical Tests on Ferrous Materials used for Gas Transmission, Distribution and Storage Systems', NGT document TM1, November 1979

54. Lawson, A.C. et al, 'The California Earthquake of April 18 1906', Report of the California State Earthquake Investigation Commission: Carnegie Inst., Washington, pub. 87, v.1 and Atlas, 1908

55. Henkel, D.J. & Skempton, A.W., A landslide at Jackfield, Shropshire in an overconsolidated clay, 'Géotechnique', Vol 5, No 2, pp 131–137, 1955

56. Skempton, A.W., Long-term stability of slopes, 'Géotechnique', Vol 14, No 2, pp 77–101, 1964

57. Fell, R, MacGregor, J.P., Williams, J. & Searle, P., Hue Hue Road landslide, Wyong, 'Soil Slope Instability and Stabilisation', Walker & Fell (eds), pp 315–324, 1987

58. Fell, R, Sullivan, T.D. & Parker, C., The Speers Point landslides, 'Soil Slope Instability and Stabilisation', Walker & Fell (eds), pp 325–331, 1987

59. Rigby, R.J. & Carr, R.J., Monitored failure of an excavation in an ancient landslide within the Newcastle coal measures, 'Soil Slope Instability and Stabilisation', Walker & Fell (eds), pp 397–402, 1987

60. Hamada, M., Damage to Piles by Liquefaction-induced ground displacements, 'Lifeline Earthquake Engineering: Proceedings of third US Conference', ASCE, Cassaro (ed), pp 1172–1181, 1991

61. Hutchinson, J.N., Bromhead, E.N. & Chandler, M.P., Investigations of the landslides at St Catherine's Point, Isle of Wight 'Slope Stability Engineering', Developments and Applications, Chandler (ed), ICE, pp 169–180, 1991

62. Yue, Z.Q. & Lee, C.F., A plane slide that occurred during construction of a national expressway in Chongqing, SW China, 'Quarterly Journal of Engineering Geology and Hydrogeology', Vol 35, pp 309–316, 2002

63. Dixon, N & Bromhead, E.N., Landsliding in London Clay coastal cliffs, 'Quarterly Journal of Engineering Geology and Hydrogeology', Vol 35, pp 327–343, 2002

64. Orense, R. Vargas-Monge, W. & Cepeda, J., Geotechnical aspects of the January 13, 2001 El Salvador earthquake, 'Soil and Foundations', Vol 42, No 4, pp 57–68, 2001

65. Bentley, S.P. & Smally, I.J., Landslips in sensitive clay, in 'Slop Instability', Brunsden & Prior (Eds), Wiley, 1984

66. Sevaldson, R.A., The slide at Lodalen, October 6, 1954, 'Géotechnique', Vol 6, pp 167–182, 1956

67. Edward, D.C., 'A Theoretical Prediction of the Pipeline Strains Resulting from the Landslip at Shelford Farm', British Gas ERS internal report R5365, 1994

68. Brown, S., 'Analysis of Soils Samples from a Geotechnical Site Investigation on the 600mm Keighley to Burley Bank Pipeline at Ben Rhydding near Ilkley', BG Technology internal report R3571, 2000

69. Martel, S, 'Case Histories: Translational Landslides', University of Hawaii, 2002, http://ww.soest.hawaii.edu/martel/courses/gg454/gg454_lec_22.pdf

70. GEO, 'Landslide information from GEO (Hong Kong) internal reports', 2003, http://hku.hk/earthsci/tools/landslide/landslidedata.pdf

71. McCormick, M.V., 'Urban landslide hazards, Millbrae, CA landslide: case history', The Geological Society of America 98th Annual Meeting, 2002, http://gsa.confex.com/gsa/2002CD/finalprogram/abstract_34955.htm

72. Crabb, G.I. & Atkinson, J.H., Determination of soil strength parameters for the analysis of highway slope failures, 'Slope Stability Engineering, Developments and Applications', Chandler (ed), ICE, pp 13–18, 1991

73. Bjerrum, L. & Eide, O., 'Anvendelse av Kompensert Fundamentering I Norge', NGI Publication No 70, 1956

74. Nakano, R. & Shimizu, H., Comparison of strength parameters obtained from back analyses of a landslide with laboratory tests and with special reference to artesian pressure, 'Landslides in Research, Theory and Practice', Thomas Telford, London, Vol 3, pp 1081–1086, 2000

75. Wilson, A.J., Murphy, W. & Petley, D.N., Some observations on the Geotechnics and movement of large volume earth flows in Alpine regions, 'Landslides in Research, Theory and Practice', Thomas Telford, London, Vol 3, pp 1581–1586, 2000

76. Dikau, R., 'Landslide Recognition: Identification, Movement and Courses', Dikau, Brunsden, Schrott & Ibsen (Eds), Wiley, 1996

77. Chauhan, V. and Sloterdijk, W., 'Advances in Interaction Rules for Corrosion Defects in Pipelines', Proceedings of the 2004 International Gas Research Conference, 1-4 November 2004, Vancouver, British Columbia, Canada

78. Anon. 'Title 49 - Transportation. Part 192 - Transportation of Natural and other Gas by Pipeline: Minimum Federal Safety Standards', Research and Special Programs Administration, US Department of Transportation

79. Anon. 'Title 49 – Transportation. Part 195 - Transportation of Hazardous Liquids by Pipeline: Minimum Federal Safety Standards', Research and Special Programs Administration, US Department of Transportation

80. Chauhan, V., Grant, R., 'Improved Methods for the Assessment of the Remaining Strength of Corroded Pipelines', Final Report for the PRCI Materials Technical Committee, Project Number PR-273-9803, Phase 4, Catalog No. L51968, Advantica Technologies, Inc., October 2002

81. Chauhan, V. and Wood, A., 'Experimental Validation of Methods for Assessing the Interaction of Closely Spaced Corrosion Defects', Final Report for the PRCI Materials Technical Committee/GRI, Contract No. GRI-8549, Advantica, Inc., February 2005

82. Chauhan, V. and Brister, J., 'A Review of Methods for Assessing the Remaining Strength of Corroded Pipelines', Advantica Report Number 6781, Issue 4.0, June 2008

83. Mohr, W., 'Strain Based Design of Pipelines', EWI Report Submitted to The US Department of Interior, Minerals and Management Service and The US Department of Transportation, Research and Special Programs Administration, Report Project No. 45892GTH, October 2003

84. Chauhan, V. and Crossley, J., 'Project #153H Corrosion Assessment Guidance for Higher Strength Steels Phase 1', Advantica Report R9017 Issue 2.0, June 2008

85. Liu, J., Mortimer, L. and Wood, A., Project #153H Corrosion Assessment Guidance for Higher Strength Steels Phase 2', Advantica Number 7930 Issue 1.0, Draft in Preparation

15 Tables

Pipe Diameter, D (mm)	406.4	to	762.0
Wall Thickness, t (mm)	7.87	to	9.65
D/t ratio	51.3	to	81.1
Material Grade (API 5L)	A25	to	X52
d/t ratio	0.31	to	1.0
Defect Length (2c), mm	0.7	to	7.8
Defect Width, w (mm)	Not Available		
Burst Pressure, Pf (bar)	56.5	to	147.5

Table 1. Range of Experimental Parameters Used to Validate the ASME B31G Method

Pipe Diameter, D (mm)	273.0	to	1219.2
Wall Thickness, t (mm)	5.00	to	12.7
D/t ratio	40.6	to	130.3
Material Grade (API 5L)	A	to	X65
d/t ratio	0.28	to	1.0
Defect Length (2c), mm	19.4	to	3048
Defect Width, w (mm)	0.15	to	762
Burst Pressure, Pf (bar)	41.3	to	209

Table 2. Range of Experimental Parameters Used to Validate the RSTRENG Method

Pipe Diameter, D (mm)	219.1	to	914.4
Wall Thickness, t (mm)	3.4	to	25.4
(D/t) ratio	8.6[6]	to	149.4
Material Grade (API 5L)	X42	to	X65
d/t ratio	0.2	to	0.97
Defect Length (2c), mm	40.8	to	2000
Defect Width, w (mm)	0.15	to	334
Burst Pressure, Pf (bar)	46	to	1241

Table 3. Range of Experimental Parameters Used to Validate the BS 7910 and DNV RP-F101 Methods

---

[6] 7 tests were undertaken on Grade X52 pipe with wall thicknesses ranging from 24.5mm to 25.4mm. All vessels contained external groove defects with a (d/t) ratio range 0.2 to 0.94. Deeper defects resulted in failure of the vessel as a leak. Failure of the vessel by rupture was obtained for defect (d/t) ratios in the range 0.5 to 0.72. Failure pressures ranged from 685 bar to 1241 bar.

Landslide	Failure type[*]	Dimensions in metres $(W_L / L_L / H_L)$[#]	Ground movement along slip surface (m)	Soil type	Soil Properties	Ref	Remarks
1906 San Francisco, US	T	400/2000/5 300/2000/5	1 – 2 3	Various Fill	c = 29 - 201 N = 8 - 88 γ = 17.9 - 22.8	[54]	Two slides (slide and spreading) triggered by earthquake
1952 Jackfield, Shropshire, UK	T	140/170/5.5	10 – 20	Clay	c' = 7 - 10.5 ϕ = 21 - 25	[55]	Total of two successive slides
1954 Lodalen, Oslo, Norway	R	50/40/8	5 – 10	Clay	c' = 10 ϕ = 27 γ = 20.4	[56]	
1983 Wyong, Sydney, Australia	R	150/40/10 100/40/10	6 – 7 1.5	Clay	c' = 10 - 30 ϕ = 15 - 23	[57]	Two slides at South and North
1950 Speers Point, NSW, Australia	T	150/150/10	250	Clay & Sand	c' = 0 ϕ = 9 - 12	[58]	Failure was debris flow
1985, Wallsend, NSW, Australia	R	100/50/10	5.5	Clay	c' = 2 - 20 ϕ = 5 - 36	[59]	
1964 Niigata, Japan	T	600/1200/10	10	Sand	N = 2 - 10	[60]	Failure was earth flow
St Catherine's Pt, Isle of Wight, UK	R+T	12000/800/100	100	Chalk	ϕ = 8 - 10 γ = 22	[61]	
1999 Chongqing, China	T	7/53/8	13	Clay	c = 19 - 46 ϕ = 10 - 22 γ = 19.5 - 20.5	[62]	
1971 Isle of Sheppey, UK	T	30/200/20	18	Clay	c = 3.1 ϕ = 10	[63]	
1991 Las Colinas, El Salvador	T	100/600/40	700	Sand	N = 1.2 - 3.3	[64]	
1971 St Jean Vianney, Quebec, Canada	T	365/550/22.5	2900	Clay	c' = 127 - 172 ϕ' = 5 - 18 c_u = 62 - 172 ϕ_u = 24	[65]	
1954 Lodalen	R	50/50/10	10	Clay	c' = 10 ϕ = 27 c_u = 40 - 60	[66]	
1994 Shelford farm, UK	R	150/150/10	20	Clay	P_u = 0.09 R_u = 0.014	[67]	130m high pressure pipeline affected, max disp 10m
2000 Ben Rhydding, UK	R	15/40/5	2	Clay	c_u = 26 - 88 γ = 19.9 - 21.6	[68]	780m of the pipeline re-routed
1903 Frank, Alberta, Canada	T	1000/425/14	NA	NA	NA	[69]	
1982 Love Creek, CA, US	T	600/250/10	NA	NA	NA		
1970 Fat Kwong Street, Hong Kong	NA	92/118/24	NA	NA	NA	[70]	
2000 Millbrae, CA, US	NA	122/61/17	NA	NA	NA	[71]	

Table 4. Summary of World Wide Case Histories of Major Landslides

- R = Rotational slide, T = Translational slide [#] Approximation or average values

Landslide	Width (m)	Length (m)	Depth (m)	Maximum Ground Movement (m)
Small	20	50	5	2
Medium	100	200	10	5
Large	500	1000	40	50

Table 5. Dimensions of Landslides to be Studied in this Project

Nominal Size	External Diameter (mm)	Wall Thickness (mm)	Coating Type	Cover Depth (m)	Depth to Pipe Centre (m)	Grade	SMYS (MPa)
18-inch	457	5.6	Fusion bonded epoxy or coal tar enamel	1.8	2.0	X56	386
36-inch	914	12.7	Fusion bonded epoxy or coal tar enamel	1.5	2.0	X60	414
48-inch	1219	14.3	Fusion bonded epoxy or coal tar enamel	1.4	2.0	X80	551

Table 6. Pipe Property Matrix

Landslide	Soil type	Soil Properties	Reference	Remarks
Various highway slope failures	Clay	$c' = 0$ $\phi = 19 - 25$	Crabb & Atkinson [72]	Total of 8 sites
Various excavations	Clay	$c_u = 7.5 - 35$ $\gamma = 15.4 - 19.0$	Bierrum & Eide [73]	Total of 7 sites
Various landslides in Japan	Clay	$c = 0 - 45$ $\phi = 8.9 - 29.2$	Nakano & Shimizu [74]	Total of 3 sites
Various landslides in Alpine Regions	Clay	$c' = 0 - 32$ $\phi = 15.6 - 22.6$ $\gamma = 17.9 - 21.9$	Wilson, Murray & Petley [75]	Total of 3 sites
Typical material properties of a block slide	Clay and sand	$c' = 25.3 - 78.6$ $\phi = 4.5 - 12.3$ $\gamma = 20 - 21$	Dikau et al [76]	Values from 4 different authors
Typical mudslide material properties	Clay and sand	$\phi = 11 - 16.5$ $\gamma = 16.7 - 20.9$		Values from 8 different authors

Table 7. Summary of Soil Parameters of Some Landslides

Bound	Watertable	Finefill	Trench Width (metres)	Backfill Bulk Density (kg/m3)	Soil Cohesion (kN/m2)		Angle of Internal Friction (degrees)		Adhesion (kN/m2)	Angle of Sliding friction (deg)
					Natural Ground	Backfill	Natural Ground	Backfill		
Lower (Soft clay)	Existing ground level	No	>4 × pipe diameter	1680	20	6	2	0	0	20
Upper (Stiff clay)	None	No	Variable with diameter and depth	2380	160	78	20	20	17	30.5

Table 8. Input Parameter Values for Cohesive Ground Conditions

Bound	Watertable	Finefill	Trench Width (metres)	Backfill Bulk Density (kg/m³)	Soil Cohesion (kN/m²)		Angle of Internal Friction (degrees)		Adhesion (kN/m²)	Angle of Sliding friction (degrees)
					Natural Ground	Backfill	Natural Ground	Backfill		
Lower (Loose sand)	Existing ground level	No	>4 × pipe diameter	1605	0	0	28	28	0	28
Upper (Dense sand)	None	No	Variable with diameter and depth	2370	0	0	48	41	0	47

Table 9. Input Parameter Values for Granular Ground Conditions

Soil Type	Bound	Upward Restraint		Lateral Restraint		Downward Restraint		Axial Restraint	
		Stiffness (MPa/mm)	Limit Pressure (MPa)	Stiffness (MPa/mm)	Limit Pressure (MPa)	Stiffness (MPa /mm)	Limit Pressure (MPa)	Displacement to Slip (mm)	Shear Stress for Slip (MPa)
Cohesive	lower	0.0007	0.034	0.0011	0.040	0.0013	0.12	6	0.003
	upper	0.1501	0.692	0.1562	2.231	0.0302	2.66	2	0.039
Granular	lower	0.0018	0.036	0.0002	0.059	0.0040	∞	4	0.004
	upper	0.1071	0.217	0.0301	0.678	0.0361	∞	1	0.039
Rationalised	lower	0.0012	0.0346	0.0007	0.0498	0.0026	∞	5	0.0033
	upper	0.1286	0.4546	0.0932	1.4549	0.0332	∞	1.5	0.0390

Table 10. Calculated Bi-linear Restraint Values for 457.2mm (18-inch) Diameter Pipe

Soil Type	Bound	Upward Restraint		Lateral Restraint		Downward Restraint		Axial Restraint	
		Stiffness (MPa /mm)	Limit Pressure (MPa)	Stiffness (MPa/mm)	Limit Pressure (MPa)	Stiffness (MPa/mm)	Limit Pressure (MPa)	Displacement to Slip (mm)	Shear Stress for Slip (MPa)
Cohesive	lower	0.0006	0.027	0.0005	0.035	0.0007	0.12	6	0.002
	upper	0.0792	0.352	0.0642	1.834	0.0152	2.68	2	0.039
Granular	lower	0.0009	0.018	0.0002	0.040	0.0032	∞	4	0.002
	upper	0.0616	0.121	0.0200	0.434	0.0294	∞	1	0.040
Rationalised	lower	0.00075	0.0225	0.00035	0.0375	0.00195	∞	5	0.002
	upper	0.0704	0.2365	0.0421	1.134	0.0223	∞	1.5	0.0395

Table 11. Calculated Bi-linear Restraint Values for 914.4 mm (36-inch) Diameter Pipe

Soil Type	Bound	Upward Restraint		Lateral Restraint		Downward Restraint		Axial Restraint	
		Stiffness (MPa/mm)	Limit Pressure (MPa)	Stiffness (MPa /mm)	Limit Pressure (MPa)	Stiffness (MPa mm)	Limit Pressure (MPa)	Displacement to Slip (mm)	Shear Stress for Slip (MPa)
Cohesive	lower	0.0004	0.020	0.0003	0.033	0.0005	0.12	6	0.001
	upper	0.0613	0.280	0.0445	1.695	0.0115	2.70	2	0.040
Granular	lower	0.0006	0.013	0.0001	0.035	0.0030	∞	4	0.002
	upper	0.0511	0.103	0.0177	0.396	0.0269	∞	1	0.041
Rationalised	lower	0.0005	0.0165	0.0002	0.034	0.00175	∞	5	0.0015
	upper	0.0562	0.1915	0.0311	1.0455	0.0192	∞	1.5	0.0405

Table 12. Calculated Bi-linear Restraint Values for 1219.2 mm (48-inch) Diameter Pipe

Pipe	Bound	Upward Restraint		Lateral Restraint		Downward Restraint		Axial Restraint	
		Ultimate displacement (mm)	Limit pressure (MPa)	Ultimate displacement (mm)	Limit pressure (MPa)	Ultimate displacement (mm)	Limit pressure (MPa)	Displacement to slip (mm)	Shear stress for slip (MPa)
Cohesive	lower	100	0.034	114.3	0.040	228.5	0.12	6	0.003
	upper	10	0.692	45.7	2.231	228.5	2.66	2	0.039
Granular	lower	100	0.036	300	0.059	3630.0	100	4	0.004
	upper	10	0.217	60	0.678	3630.0	1000	1	0.039
Rationalised	lower	100	0.035	207.1	0.050	1929.2	50.06	5	0.003
	upper	10	0.455	52.9	1.455	1929.2	501.33	1.5	0.039

Table 13. Hyperbolic Restraint Values for 457.2 mm (18-inch) Diameter Pipe

Pipe	Bound	Upward Restraint		Lateral Restraint		Downward Restraint		Axial Restraint	
		Ultimate displacement (mm)	Limit pressure (MPa)	Ultimate displacement (mm)	Limit pressure (MPa)	Ultimate displacement (mm)	Limit pressure (MPa)	Displacement to slip (mm)	Shear stress for slip (MPa)
Cohesive	lower	100	0.027	228.5	0.035	457	0.12	6	0.002
	upper	10	0.352	91.4	1.834	457	2.68	2	0.039
Granular	lower	100	0.018	300	0.040	7259.9	100	4	0.002
	upper	10	0.121	60	0.434	7259.9	1000	1	0.040
Rationalised	lower	100	0.023	264.3	0.038	3858.5	50.06	5	0.002
	upper	10	0.237	75.7	1.134	3858.5	501.34	1.5	0.040

Table 14. Hyperbolic Restraint Values for 914.4 mm (36-inch) Diameter Pipe

Pipe	Bound	Upward Restraint		Lateral Restraint		Downward Restraint		Axial Restraint	
		Ultimate displacement (mm)	Limit pressure (MPa)	Ultimate displacement (mm)	Limit pressure (MPa)	Ultimate displacement (mm)	Limit pressure (MPa)	Displacement to slip (mm)	Shear stress for slip (MPa)
Cohesive	lower	100	0.020	304.8	0.033	609.5	0.12	6	0.001
	upper	10	0.280	121.9	1.695	609.5	2.70	2	0.040
Granular	lower	100	0.013	300	0.035	9682.5	100	4	0.002
	upper	10	0.103	60	0.396	9682.5	1000	1	0.041
Rationalised	lower	100	0.017	302.4	0.034	5146.0	50.06	5	0.002
	upper	10	0.192	91.0	1.046	5146.0	501.35	1.5	0.041

Table 15. Hyperbolic Restraint Values for 1219.2 mm (48-inch) Diameter Pipe

Orientation	Landslide type	Soil Restraint	Landslide size (m)	Landslide movement (m)	Internal Pressure (bar)
perpendicular crossing	translational	LB – cohesive UB – cohesive LB – granular UB – granular LB – rationalised UB – rationalised	20, 30, 40, 50, 60, 70, 100	0.2, 0.5, 1, 1.5, 2, 2.5, 3, 5	0, 20, 40, 60, 70
parallel crossing	translational	LB – rationalised UB – rationalised	20, 50, 70, 100, 150, 20	0.2, 0.3, 0.5, 0.7, 1	0
parallel crossing	rotational	LB – rationalised UB – rationalised	50	0.2, 0.3, 0.5, 0.7, 1	0

* Note that not all the possible combinations were tested.

Table 16. Combinations of Parameters Tested in the Sensitivity Studies

Orientation	Loading	Landslide type	Soil Restraint	Landslide size	Landslide movement
perpendicular crossing	lower bound	translational or rotational	lower bound	wide	small
	upper bound	translational or rotational	upper bound	narrow	large
parallel crossing	lower bound	translational	lower bound	short	small
	upper bound	rotational	upper bound	long	large

Table 17. Combinations of Landslide Dimensions and Soil Restraints for Lower and Upper Bound Loadings

Orientation	Loading	Load case	Soil Restraint	Landslide type	Landslide size (m)	Landslide movement (m)	Internal pressure (bar)
perpendicular crossing	lower bound	1	lower bound	translational	500	1	0
	lower bound	2	lower bound	translational	500	1	70/85
	upper bound	3	upper bound	translational	20	2	0
	upper bound	4	upper bound	translational	20	2	70/85
parallel crossing	lower bound	5	lower bound	translational	50	0.5	0
	lower bound	6	lower bound	translational	50	0.5	70/85
	upper bound	7	upper bound	rotational	1000	50	0
	upper bound	8	upper bound	rotational	1000	50	70/85

Table 18. Load Case Matrix

Load case	Internal pressure (bar)	Axial stress (MPa)	Hoop stress (MPa)	Bending stress (MPa)	Equivalent stress (MPa)	Axial force (N)	Bending moment (Nmm)
1	0	0	0	±8.3	8.3	0	±7.32E6
2	70	85.7	285.6	±8.3	255.9	6.80E5	±7.32E6
3	0	0	0	±386	386	0	±3.42E8
4	70	85.7	285.6	±353.4	386	6.80E5	±3.13E8
5	0	±44.3	0	0	44.3	±3.52E5	0
6	70	130.0	285.6	0	267.3	1.03E6	0
7	0	±193	0	±193	386	±1.53E6	±1.71E8
8	70	±219.6	285.6	±219.6	386	±1.74E6	±1.94E8

Note:
i.   Values presented in *italic* have been manually reduced to the stresses that cause the pipe material to yield.

ii.   Tensile stress +ve.

iii.   Values with ±, imply equal tensile/compressive stress/force.

iii.   Values with no sign (positive only), imply no compressive stress/force.

iv.   Equivalent stress is always +ve.

Table 19. Summary of Maximum Stresses for 457.2 mm (18-inch) Diameter Pipe

Load case	Internal pressure (bar)	Axial stress (MPa)	Hoop stress (MPa)	Bending stress (MPa)	Equivalent stress (MPa)	Axial force (N)	Bending moment (Nmm)
1	0	0	0	±10.3	10.3	0	±8.20E7
2	70	75.6	251.9	±10.3	226.4	2.72E6	±8.20E7
3	0	0	0	±414	414	0	±3.31E9
4	70	75.6	251.9	±402	414	2.72E6	±3.21E9
5	0	±17.6	0	0	17.6	±6.33E5	0
6	70	93.2	251.9	0	228.5	3.35E6	0
7	0	±207	0	±207	414	±7.44E6	±1.65E9
8	70	±239	251.9	±239	414	±8.59E6	±1.91E9

Table 20. Summary of Maximum Stresses for 914.4 mm (36-inch) Diameter Pipe

Load case	Internal pressure (bar)	Axial stress (MPa)	Hoop stress (MPa)	Bending stress (MPa)	Equivalent stress (MPa)	Axial force (N)	Bending moment (Nmm)
1	0	0	0	±12.1	12.1	0	±1.95E8
2	85	108.7	362.3	±12.1	325.0	5.88E6	±1.95E8
3	0	0	0	*±551*	*551*	0	*±8.88E9*
4	85	108.7	362.3	*±525.4*	*551*	*5.88E6*	*±8.46E9*
5	0	16.1	0	0	16.1	8.69E5	0
6	85	±124.7	362.3	0	326.0	6.75E6	0
7	0	*±275.5*	0	*±275.5*	*551*	*±1.49E7*	*±4.45E9*
8	85	*±317.1*	362.3	*±317.1*	*551*	*±1.72E7*	*±5.11E9*

Table 21. Summary of Maximum Stresses for 1219.2 mm (48-inch) Diameter Pipe

Test	Load Path P = PRESSURE A = AXIAL B = BENDING P/A = PRESSURE + AXIAL	Initial Pressure (psi)	Defect Dimensions			Failure Point		
			L_A (inch)	L_H (inch)	d/t (%)	P (psi)	M (kip-in)	Mode W = WRINKLE R = RUPTURE
II-1	P-B-P	950	18	12	25	1470	45180	R
II-2	P-B-P	950	6	30	50	950	36757	W then R
II-3	P-B-P	950	18	12	50	980	44709	R
II-4	P-B-P	800	30	6	50	840	45934	R
II-5	P-B-P	950	6	30	50	950	37820	W then R
III-1	B-P/A	0	30	6	50	965	29460	R
III-2	P/A-B	960	30	6	50	958	26125	R
III-3	P/A-B-P/A	950	6	30	50	1288	16407	W then R
III-4	A-P/A-B-P/A	400	30	6	50	926	22082	R
III-5	A-P/A-B-P/A	800	6	30	50	-	14271	W
III-6	A-P/A-B-P/A	1000	30	45	15	-	13967	W
III-7	P/A-B-P/A	150	6	30	50	1326	34114	W then R
III-8	A-P/A-B-P/A	400	30	6	50	1047	22313	W then R
W-1	A-P/A-B-P/A	500	15	15	15	1652	3871	W then R
W-2	A-P/A-B-P/A	900	15	15	15	1660	12966	W then R
W-3	A-P/A-B-P/A	500	15	45	15	1618	7635	W then R
W-4	A-P/A-B-P/A	500	15	15	30	1540	9246	W then R

Table 22. Summary of SWRI Tests for Alyeska Pipeline Services Company

Notes:

L_A and L_H are the axial and circumferential dimensions of the corrosion defect

Tests II-2, II-3 and II-4 were modeled using FE analysis

Test II-2 failed with a wrinkle and then rupture on the tension side

Test II-3 and II-4 failed as a rupture on the compression side

For comparison purposes, values of P and M in Tables 23, 24 and 25 are given in both SI and English units

Vessel Number	Defect Type and Geometry	Load Path P=PRESSURE B=BENDING	Failure Point	
			P (bar)	M (MNmm)
1	80% deep axial groove	P	74.5 (1080 psi)	N/A
2	80% deep axial groove	P-B	60 (870 psi)	-218 (-1931 kip-in)
3	80% deep circumferential groove	P	89.3 (1294.9 psi)	N/A
4	80% deep circumferential groove	P-B	50 (725 psi)	+260.5 (+2307 kip-in)
5	80% deep patch	P	85.9 (1245.6 psi)	N/A
6	80% deep patch	P-B	25 (362.5 psi)	+317.9 (+2816 kip-in)

Table 23. Validation Test Matrix for 457.2 mm (18-inch) Diameter Pipe

Note: see Appendix F for defect dimensions

Test	Test Failure Point		FE Predicted Failure Point	
	P (bar)	M (MNmm)	P (bar)	M (MNmm)
II-2	65.5 (949.8 psi)	+4150 (+36757 kip-in)	65.5 (949.8 psi)	+3980 (+35250 kip-in)
II-3	67.6 (980.2 psi)	-5048 (-44709 kip-in)	67.6 (980.2 psi)	-5230 (-46323 kip-in)
II-4	57.9 (839.6 psi)	-5186 (-45934 kip-in)	57.9 (839.6 psi)	-5620 (-49777 kip-in)

Table 24. Alyeska Tests - Comparison of Actual and FE Predicted Failure Points

Test	Corrosion Defect Dimensions			Test Failure Point		Failure Prediction DNV-RP-F101	
	L_A (mm)	L_H (mm)	d (%)	P (bar)	M (MNmm)	P (bar)	M (MNmm)
Vessel 2 (GL)	44.8	11.2	80	60 (870 psi)	-218 (-1931 kip-in)	46 (667 psi)	-218 (-1931 kip-in)
Vessel 4 (GL)	11.2	44.8	80	50 (725 psi)	+260.5 (+2307 kip-in)	99.5 (1442.8 psi)	+260.5 (+2307 kip-in)
Vessel 6 (GL)	44.8	44.8	80	25 (362.5 psi)	+317.9 (+2816 kip-in)	72.5 (1051.2 psi)	+317.9 (+2816 kip-in)
II-2 (SWRI)	152.4	762	50	65.5 (949.8 psi)	+4150 (+36757 kip-in)	86.9 (1260 psi)	+3980 (+35251.5 kip-in)
II-3 (SWRI)	457.2	304.8	50	67.6 (980.2 psi)	-5048 (+44709 kip-in)	39.8 (577 psi)	-4850 (-42957 kip-in)
II-4 (SWRI)	762	152.4	50	57.9 (839.6 psi)	-5186 (-45934 kip-in)	20.2 (293 psi)	-5620 (-49777 kip-in)

Table 25. Comparison of Test versus Predicted Failure Points

16   Figures
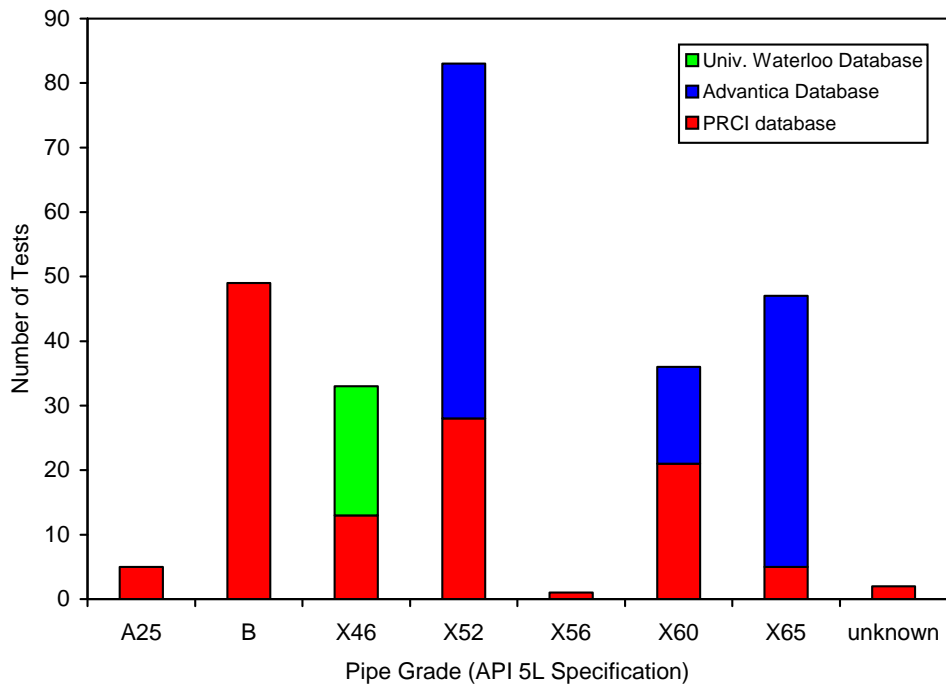
Figure 1. PRCI Review – Pipe Grade Distribution from Corrosion Defect Test Database
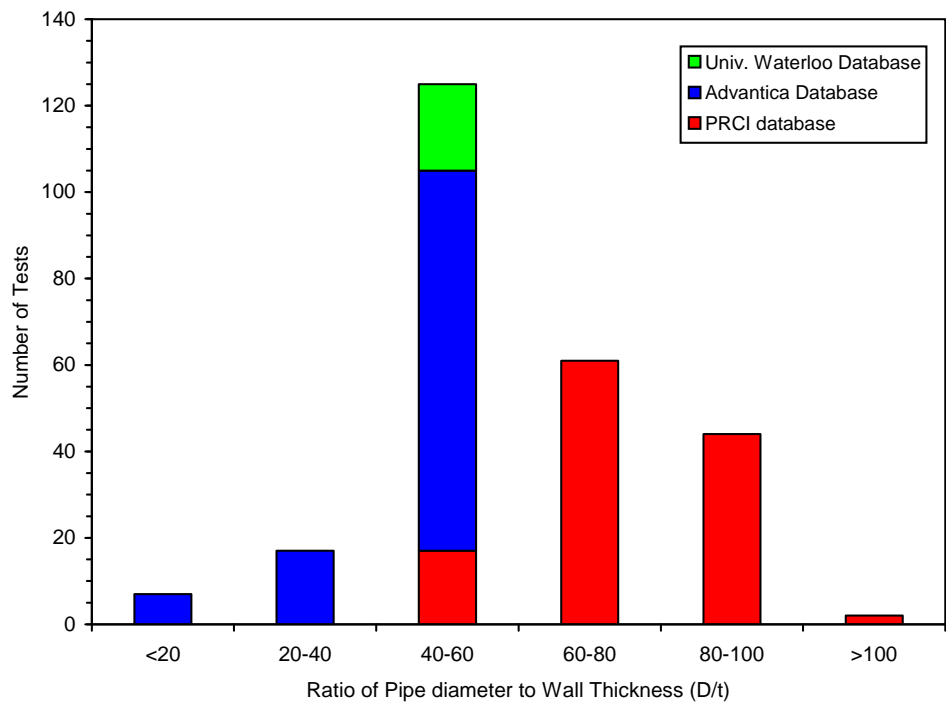
Figure 2. PRCI Review – Pipe (D/t) Ratios from Corrosion Defect Test Database
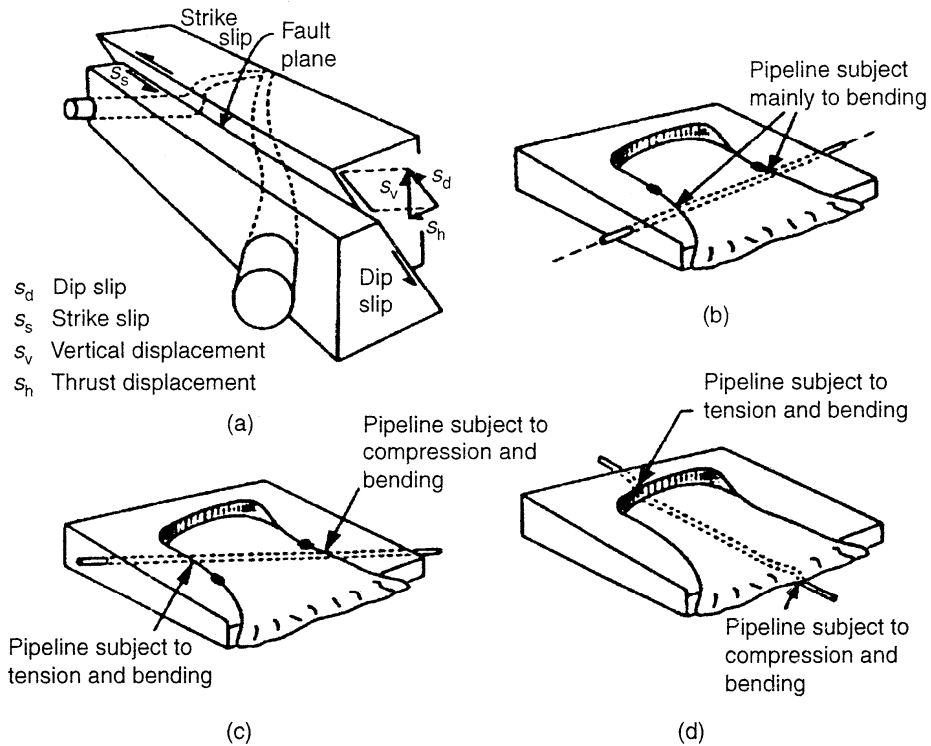
Figure 3. Principal modes of soil-pipeline interaction triggered by earthquake-induced ground movement: (a) 3-D view; (b) perpendicular crossing; (c) oblique crossing; (d) parallel crossing
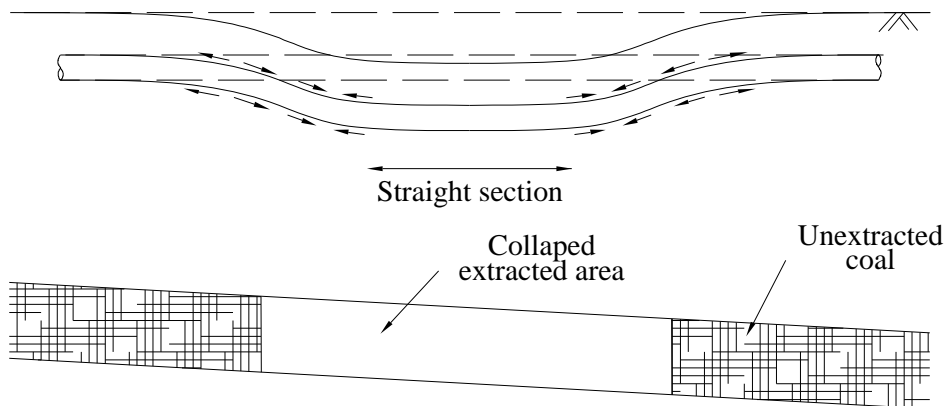
Figure 4. Ground and pipe deformation due to longwall coal mining (from Ng[2]).
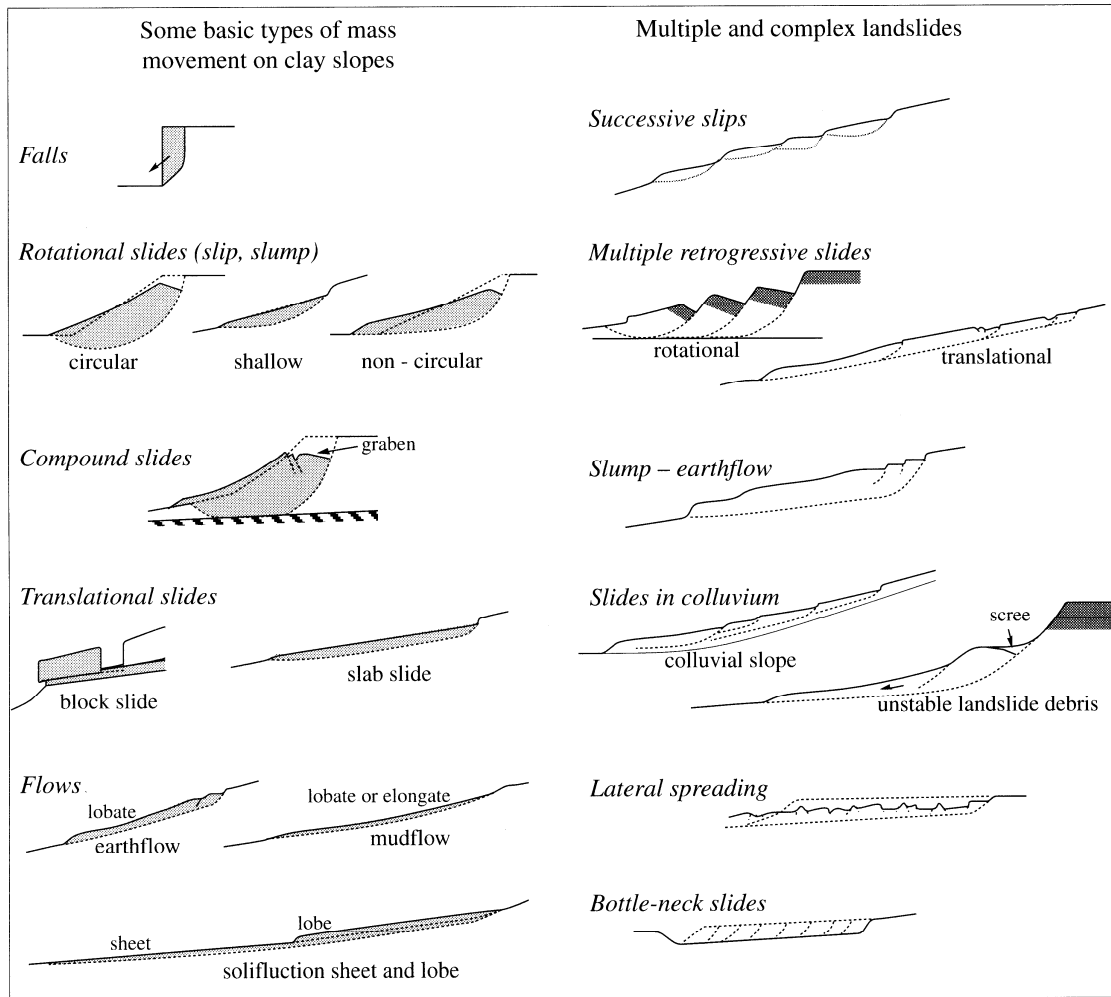
Figure 5. Classification of Landslides According to Skempton and Hutchinson
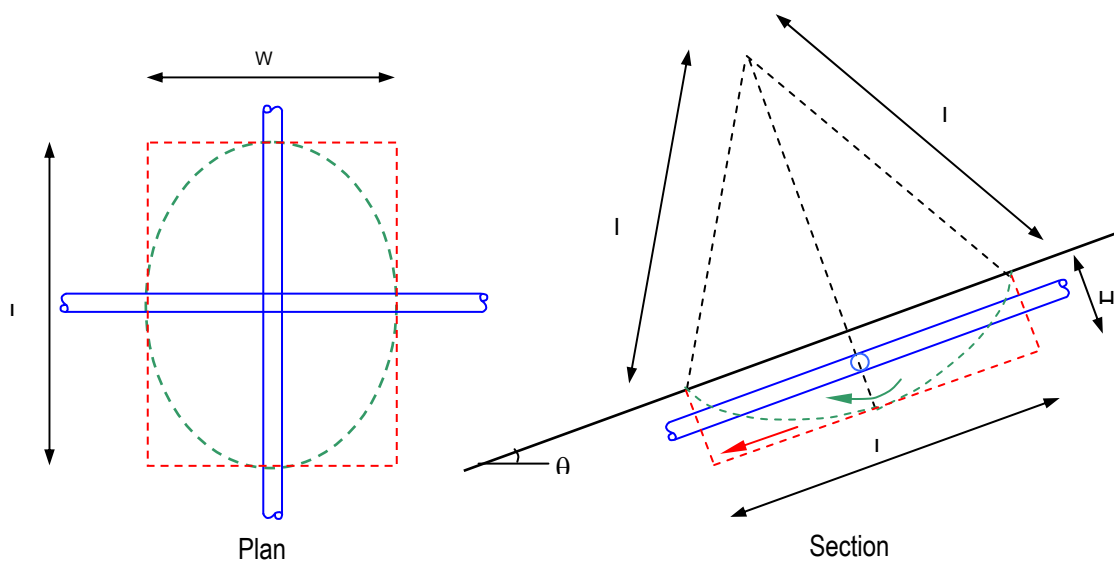
Figure 6. Geometries for Rotational (in Green) and Translational (in Red) Slides
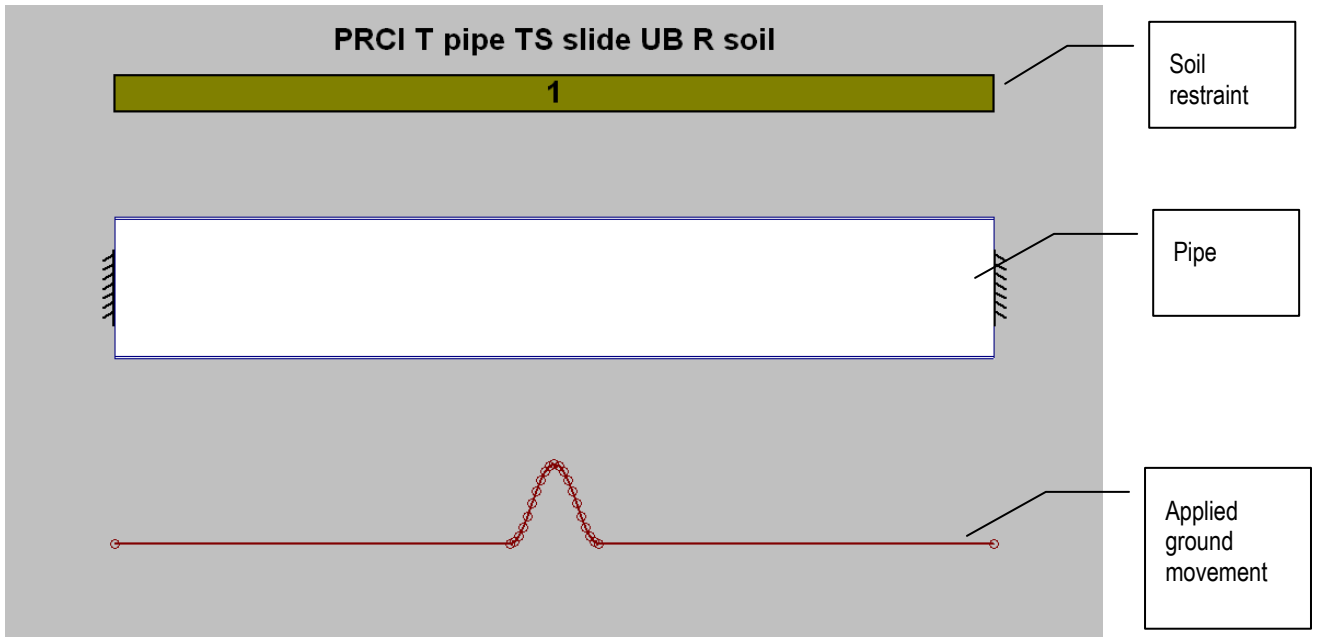
Figure 7. Analysis Model in PIPELINE
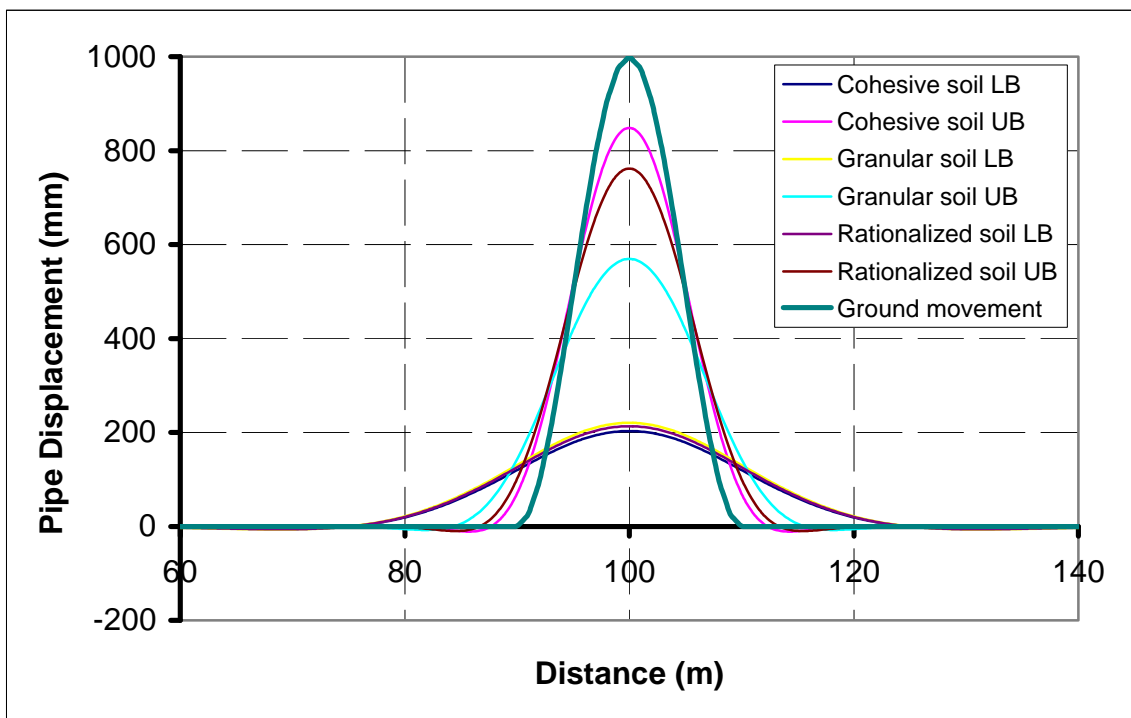
Figure 8. Applied Soil Displacement and Calculated Pipe Displacement under Different Soil Restraints
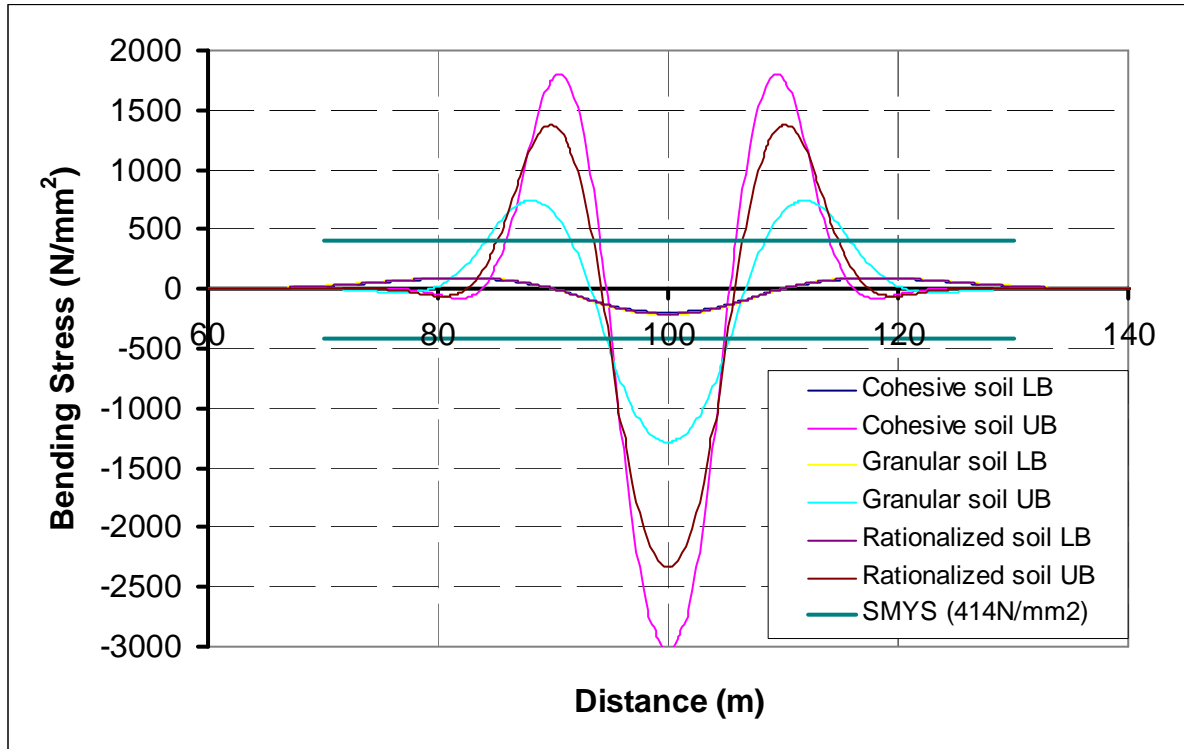
Figure 9. Calculated Bending Stress under Different Soil Restraints
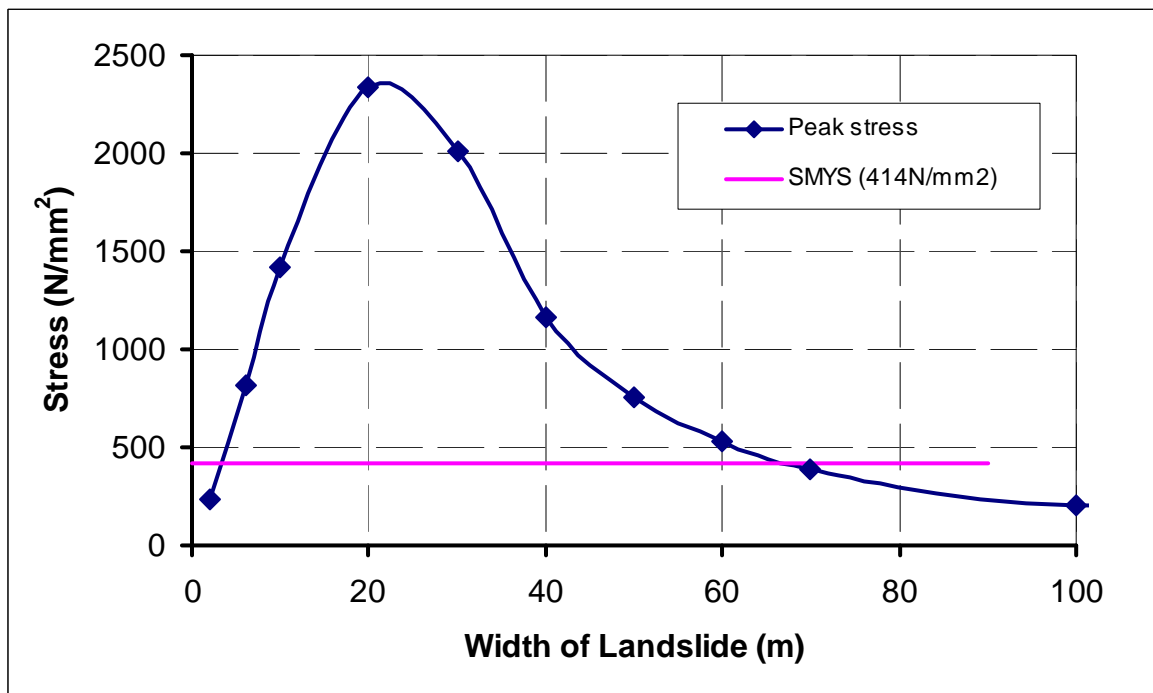
Figure 10. Calculated Maximum Bending Stress under Different Widths of Landslide
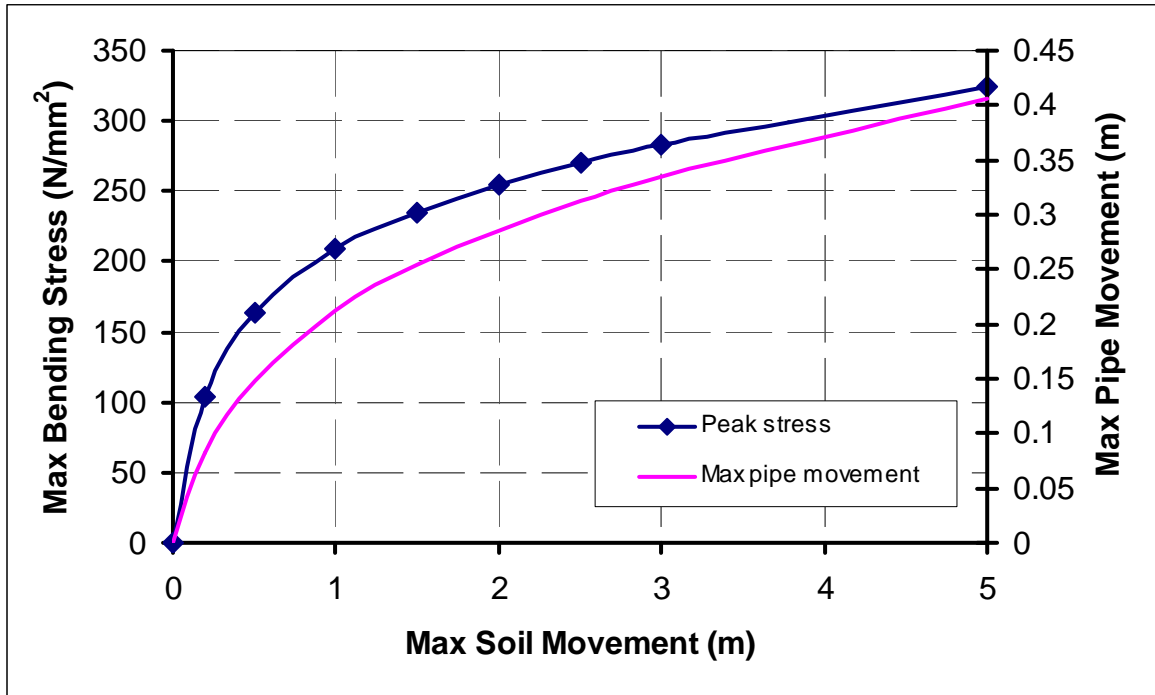
Figure 11. Calculated Maximum Bending Stress and Maximum Pipe Movement under Different Landslide Magnitudes
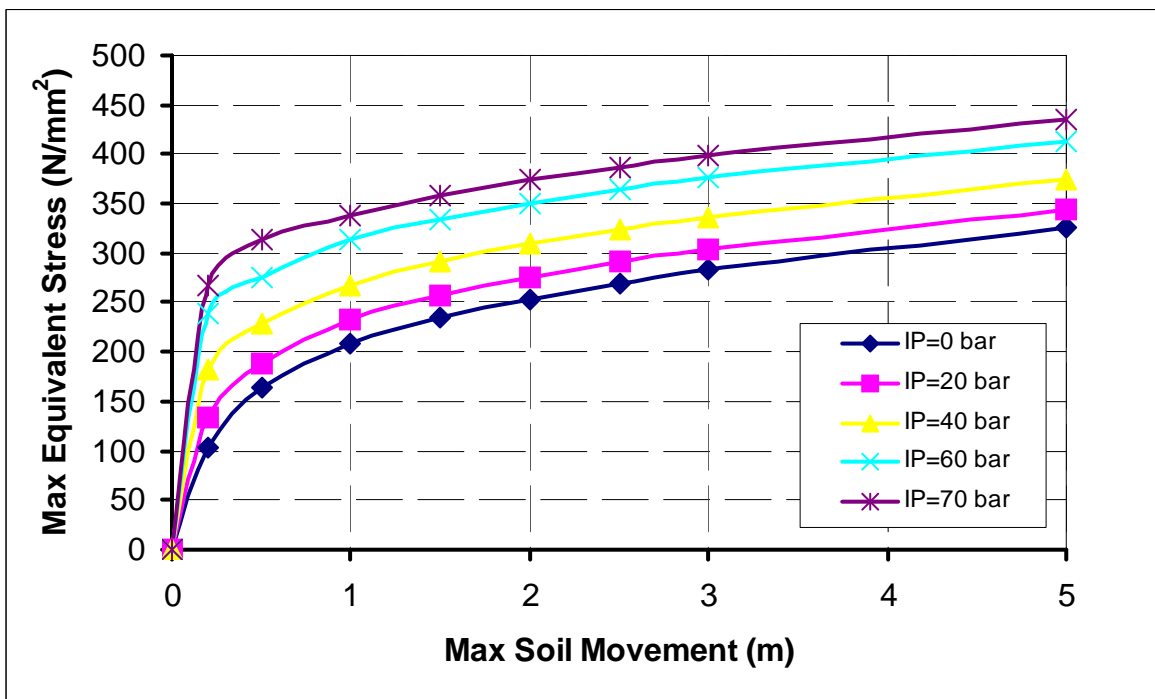
Figure 12. Calculated Maximum Equivalent Stresses under Different Internal Pressures
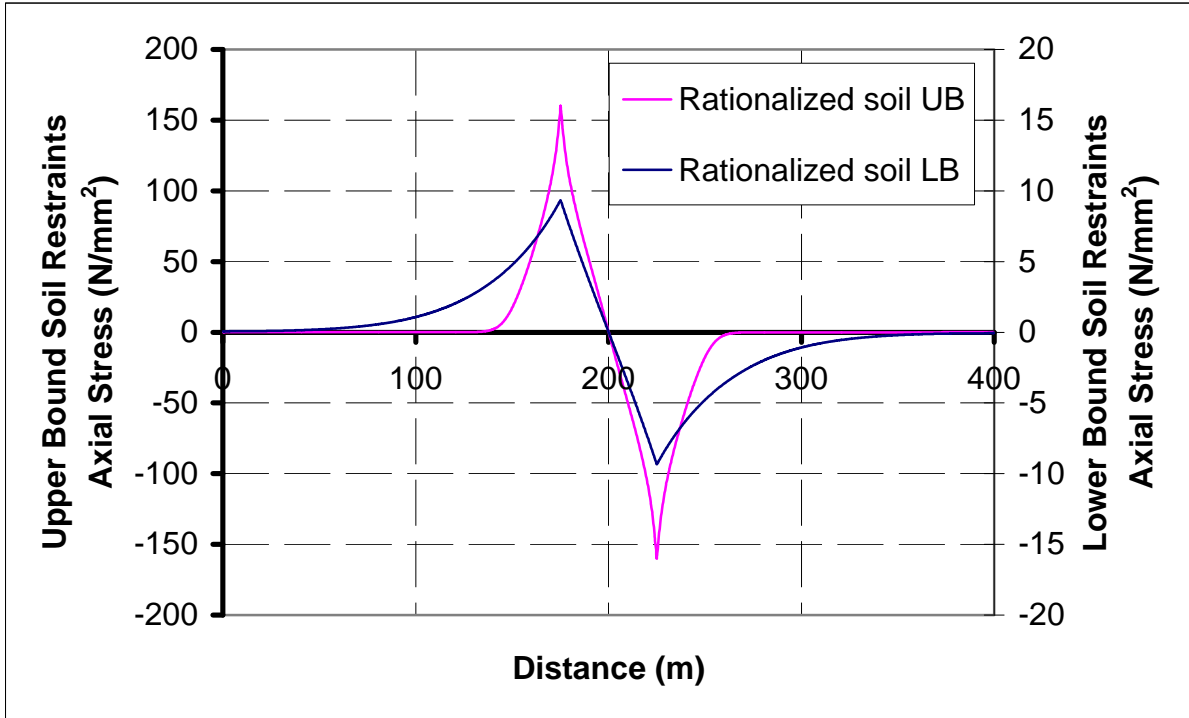
Figure 13. Calculated Axial Stresses Along Pipeline under Different Soil Restraints
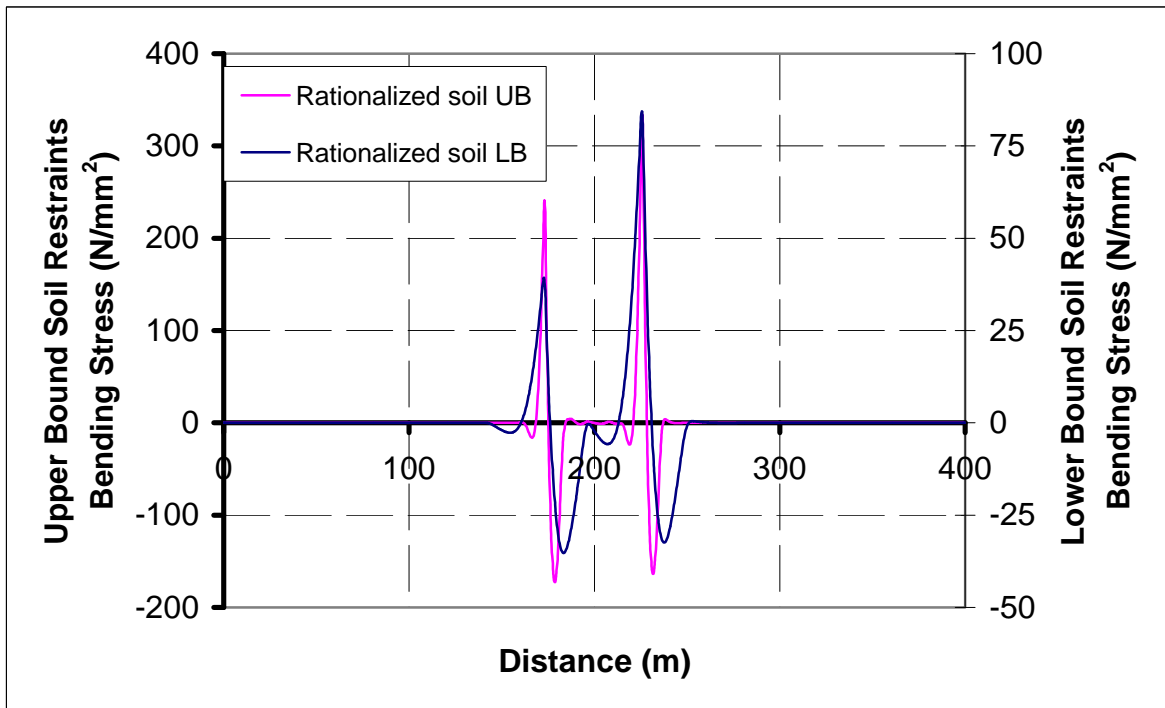
Figure 14. Calculated Vertical Bending Stresses under Different Soil Restraints
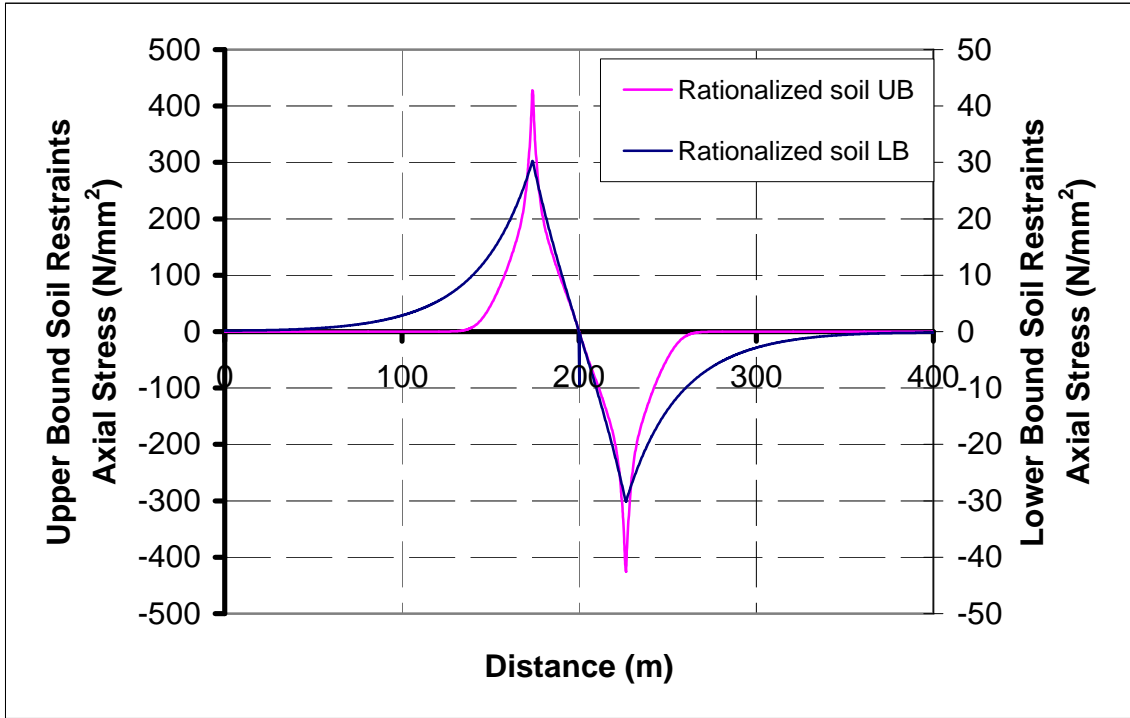
Figure 15. Calculated Axial Stresses under Different Soil Restraints
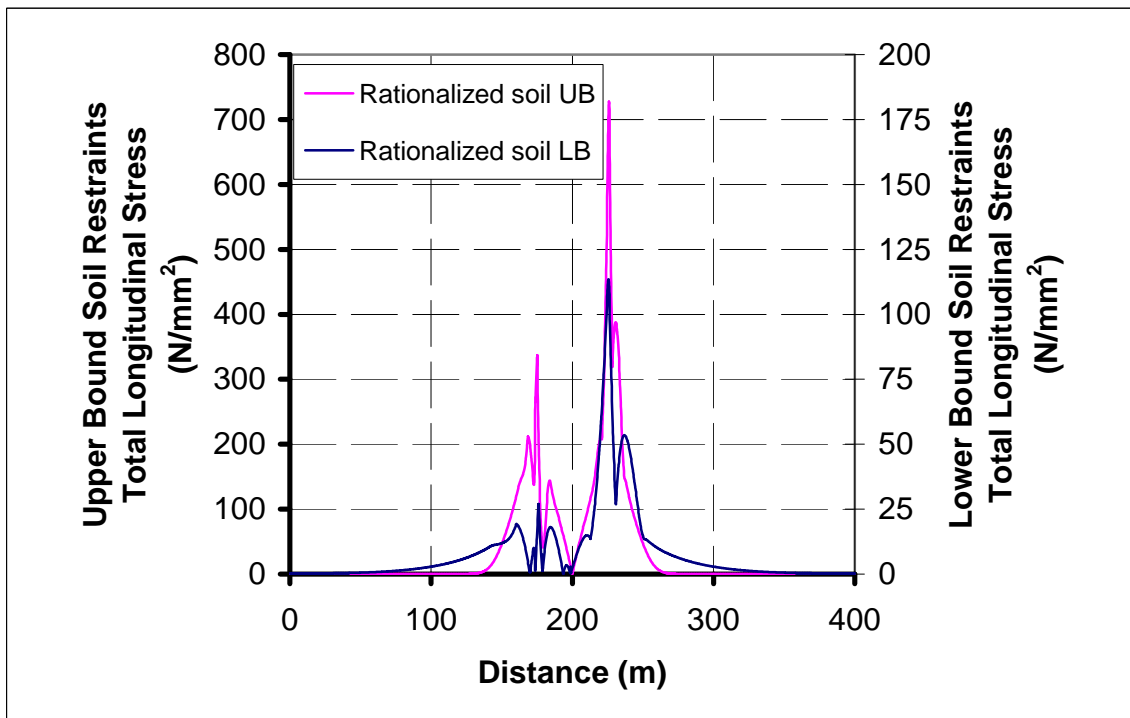
Figure 16. Calculated Total Equivalent Stresses under Different Soil Restraints
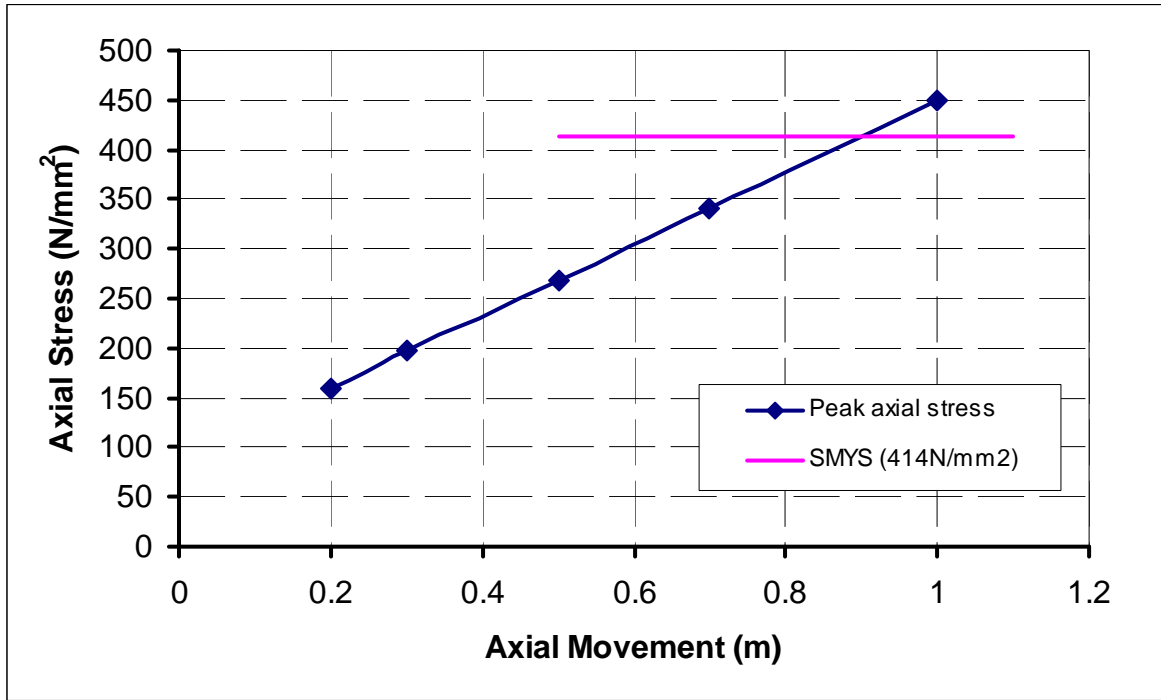
Figure 17. Calculated Axial Stresses under Different Movements of the Landslide
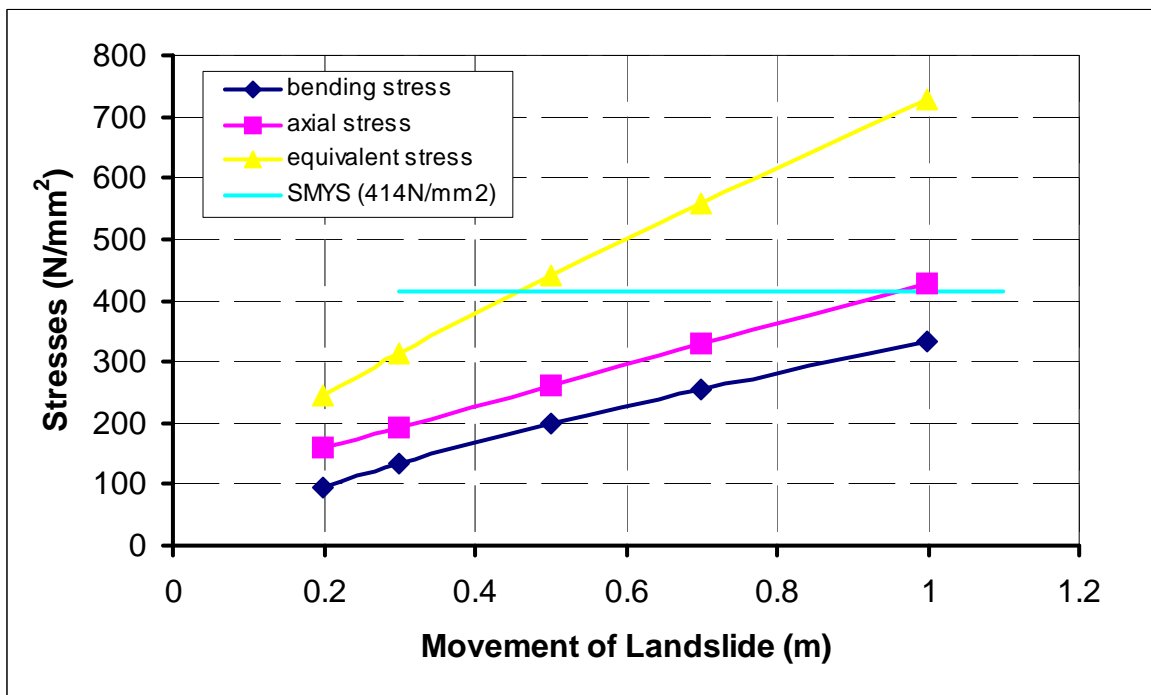
Figure 18. Calculated Stresses under Different Movements of the Landslide
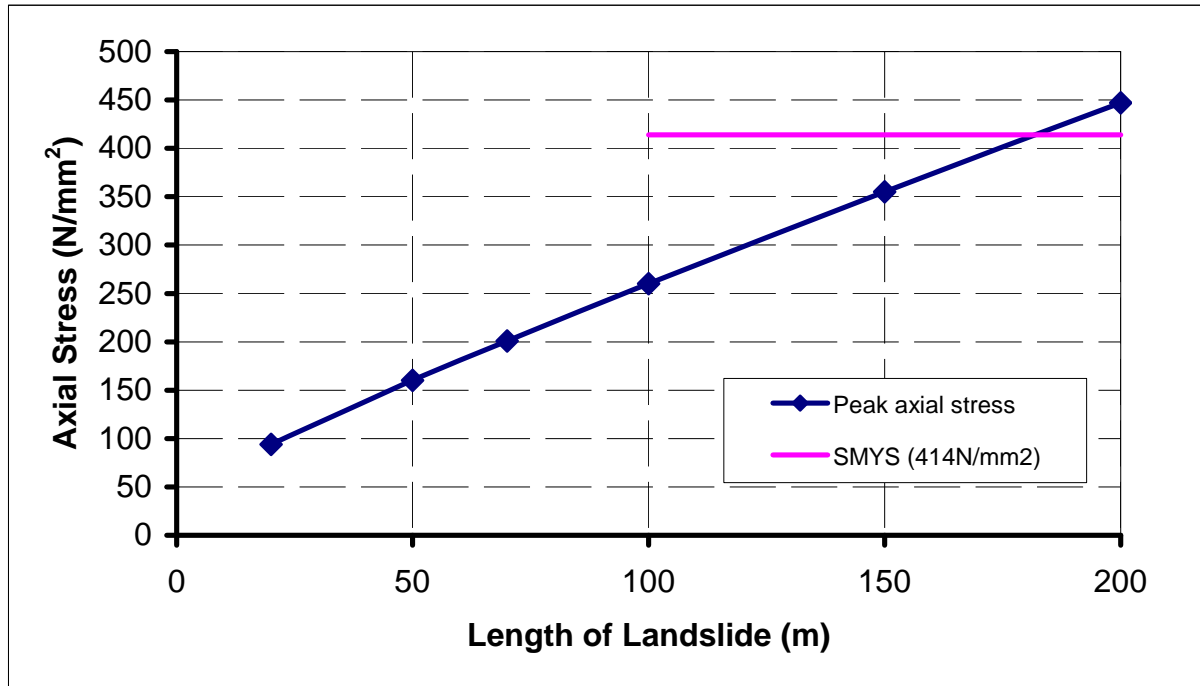
Figure 19. Calculated Axial Stresses under Different Lengths of Landslide
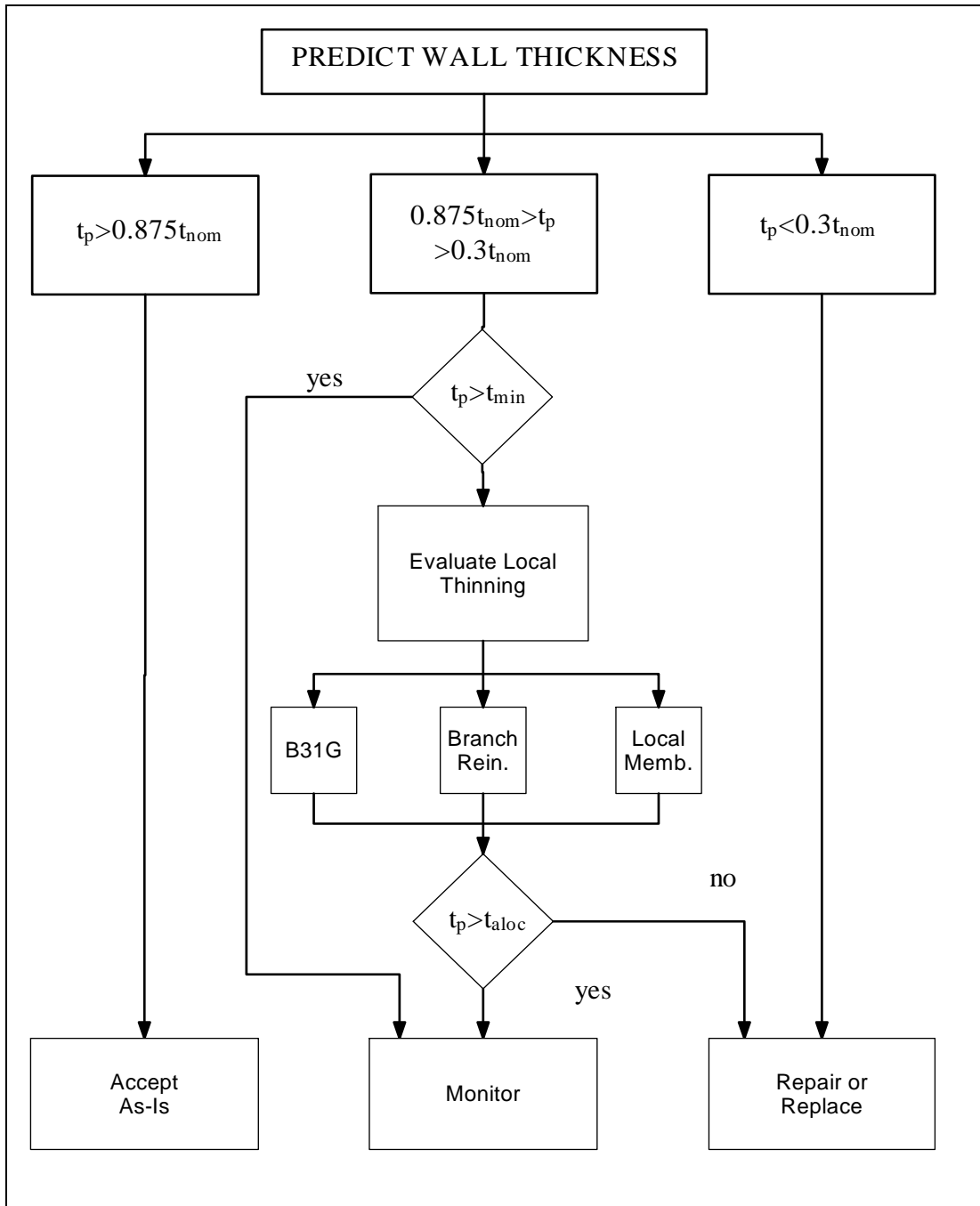
Figure 20. Flow Diagram for Evaluation of Wall Thinning in Pipework According to ASME Code Case N-597-2

Note: See Figure 21 for symbol definitions
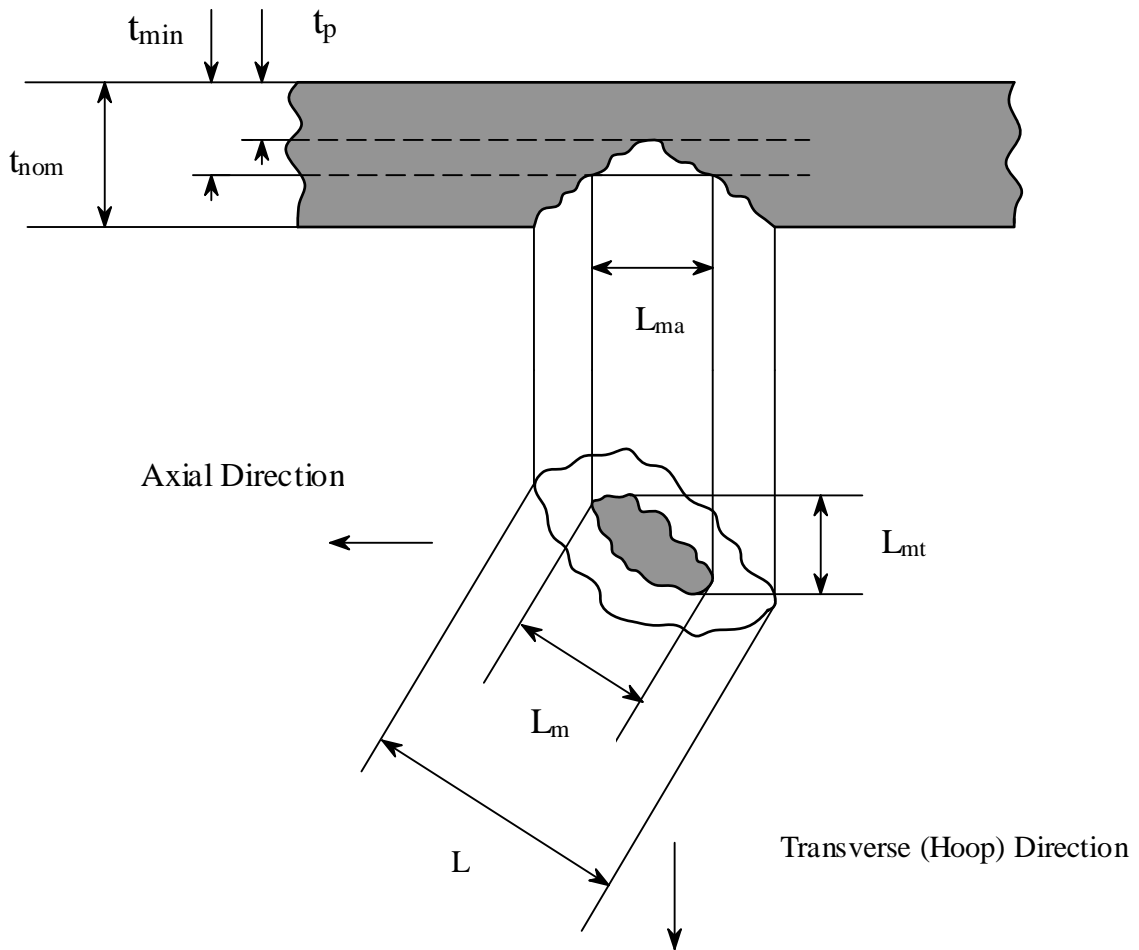
Figure 21. Diagram to Show Nomenclature Used to Define Depth and Extent of Wall Thinning in ASME Code Case N-597-2
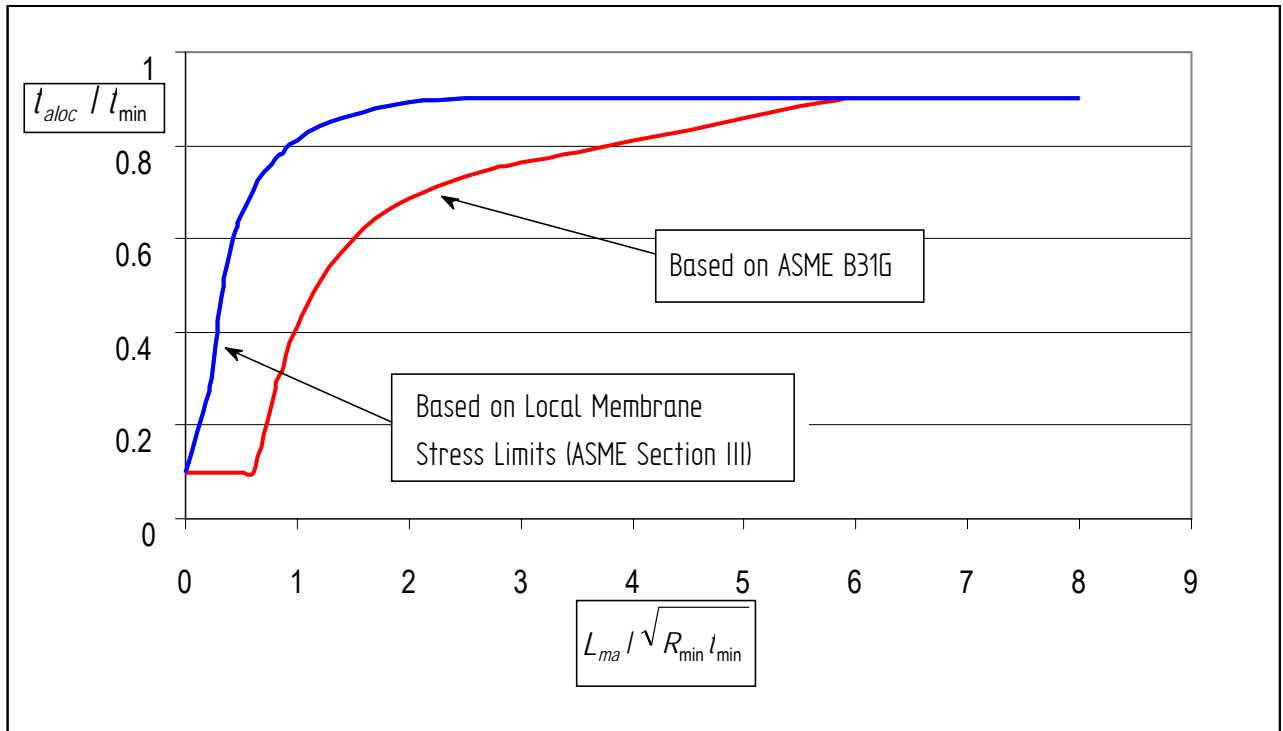
Figure 22. Allowable Depth and Length of Locally Thinned Area Based on the Local Membrane and Axial Corrosion Criteria of ASME Code Case N-597-2

Note: See Figure 21 for Symbol Definitions
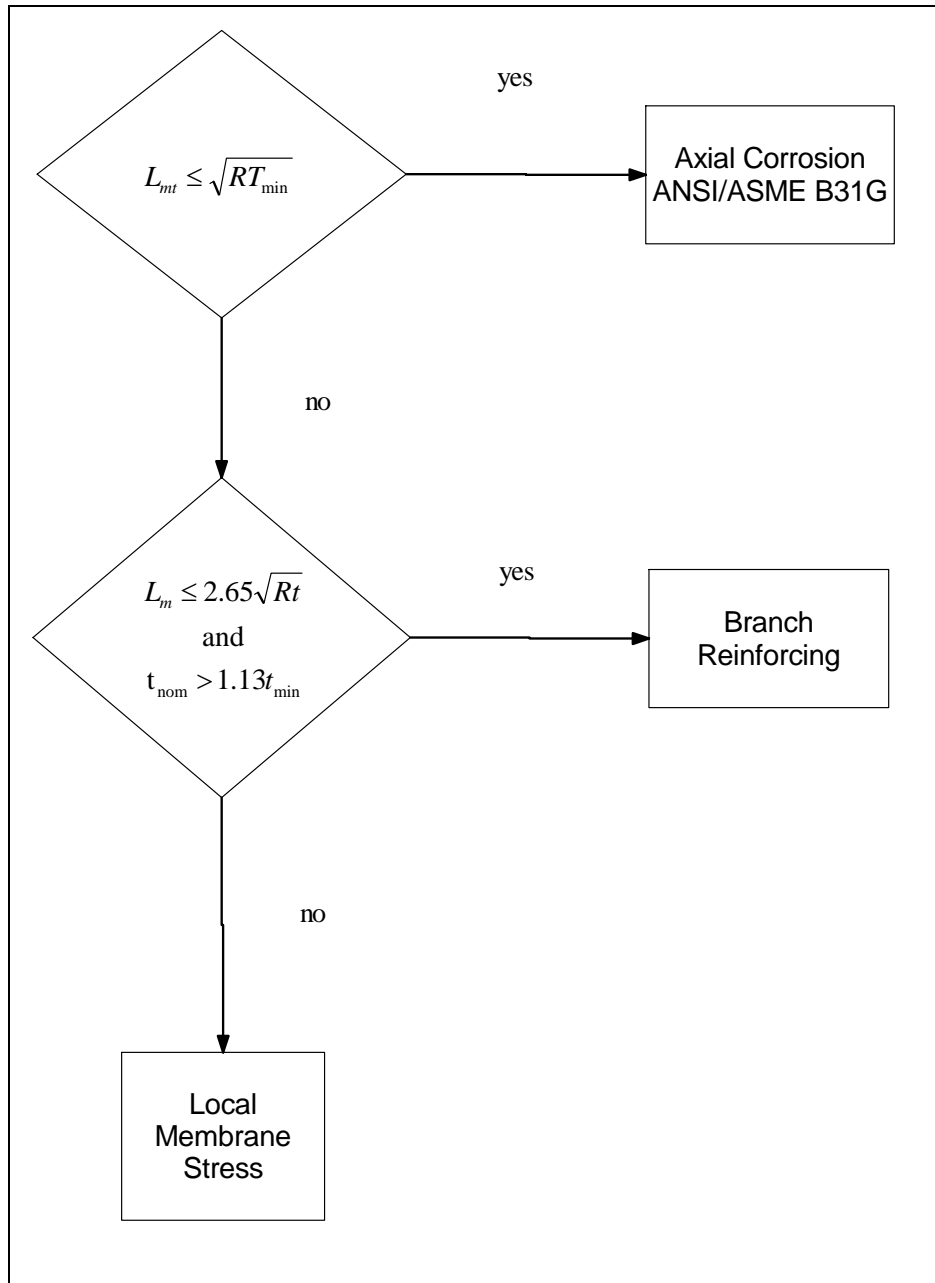
Figure 23. Flow Diagram to Select Appropriate Wall Thickness Evaluation Procedure According to ASME Code Case N-597-2

Note: See Figure 21 for Symbol Definitions
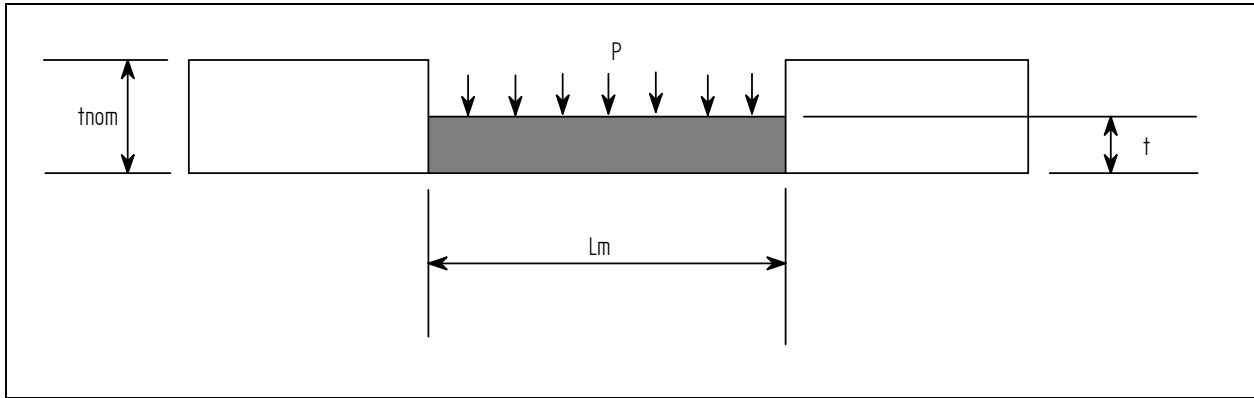
Figure 24. Local Thinned Region Idealized as a Circular Plate with Diameter Lm and Uniform Thickness
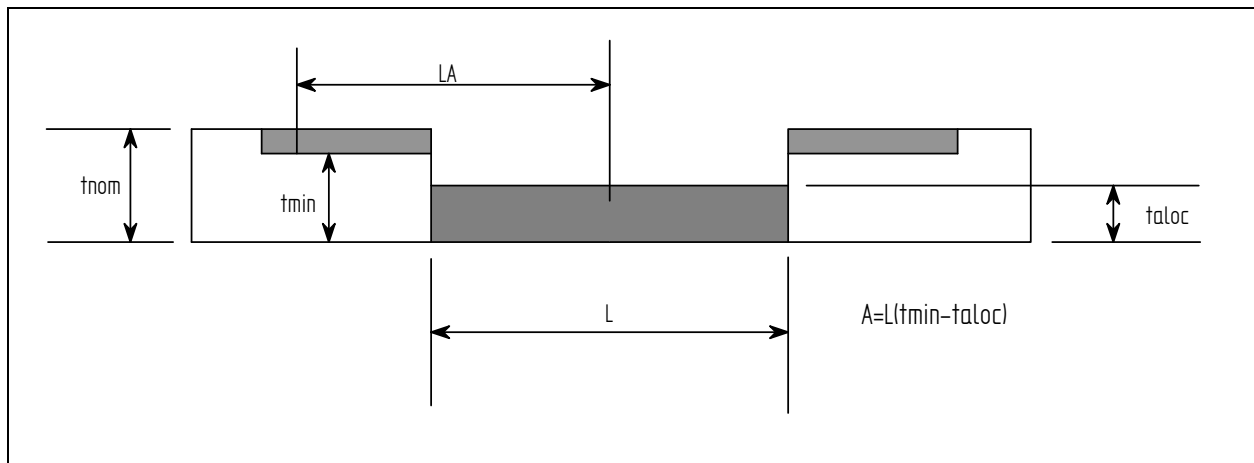
Figure 25. Area Reinforcement Rule from Section III of the ASME Boiler and Pressure Vessel Code for a Local Thinned Region in a Pipe of Diameter L and Uniform Thickness t_{aloc}

Note: $L_A = \dfrac{L}{2} + 0.5(R_{min}t_{min})^{1/2}$
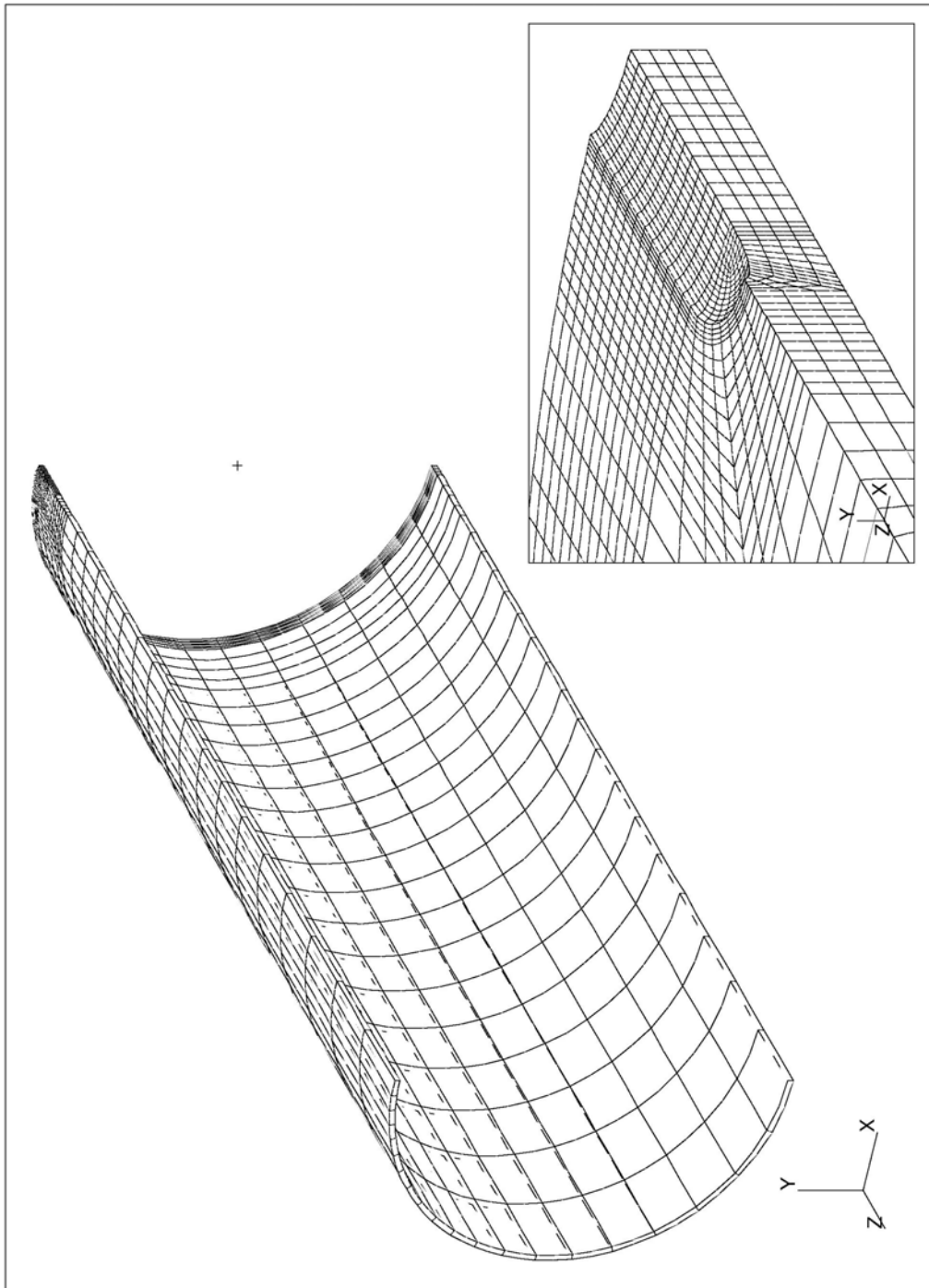
Figure 26. Quarter Symmetry FE Model of a 20% Deep Axial Groove in a 36-inch Diameter Pipe
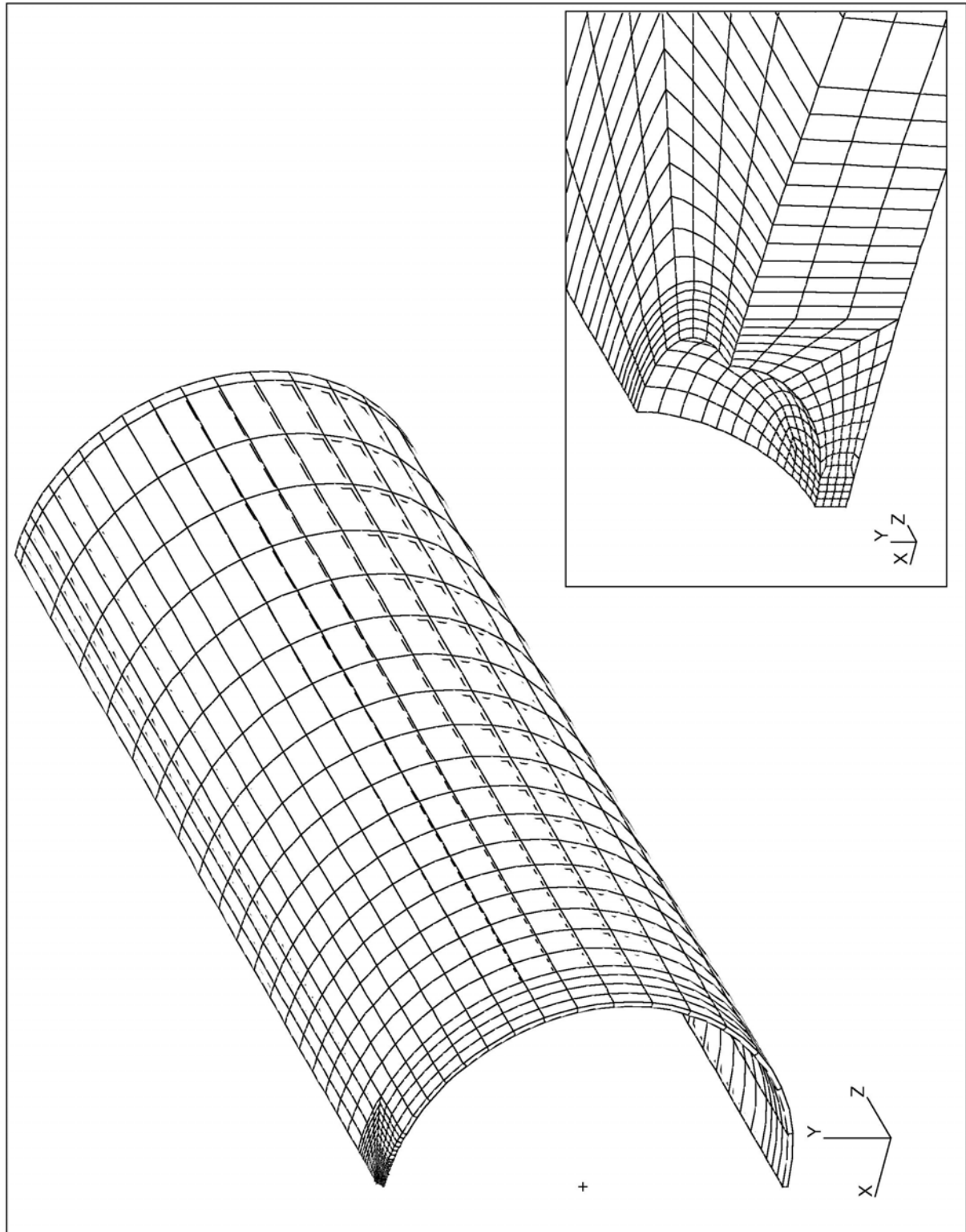
Figure 27. Quarter Symmetry FE Model of an 80% Deep Pit in an 18-inch Diameter Pipe
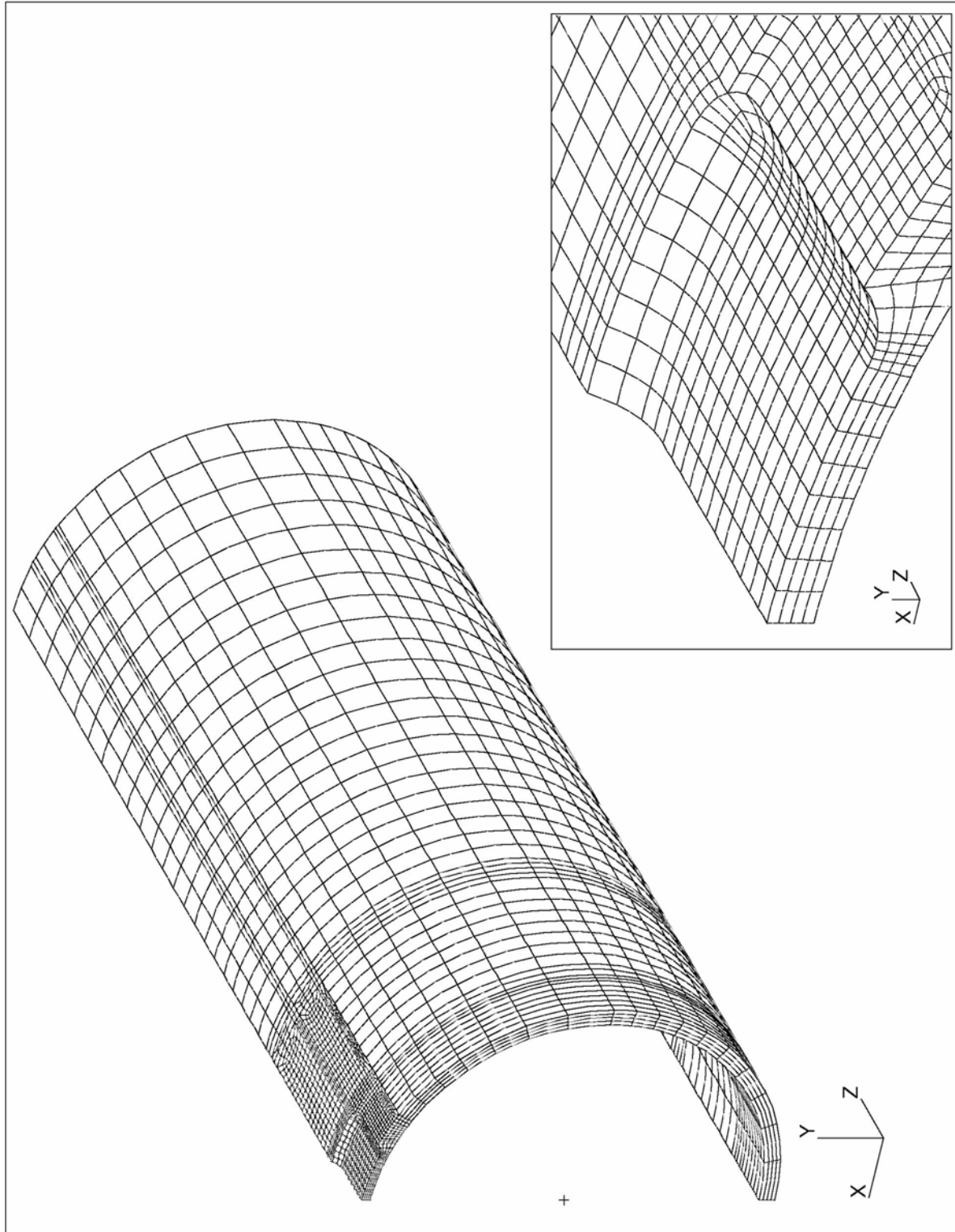
Figure 28. Quarter Symmetry FE Model of a 50% Deep Patch in a 203.2 mm (8-inch) Diameter Pipe
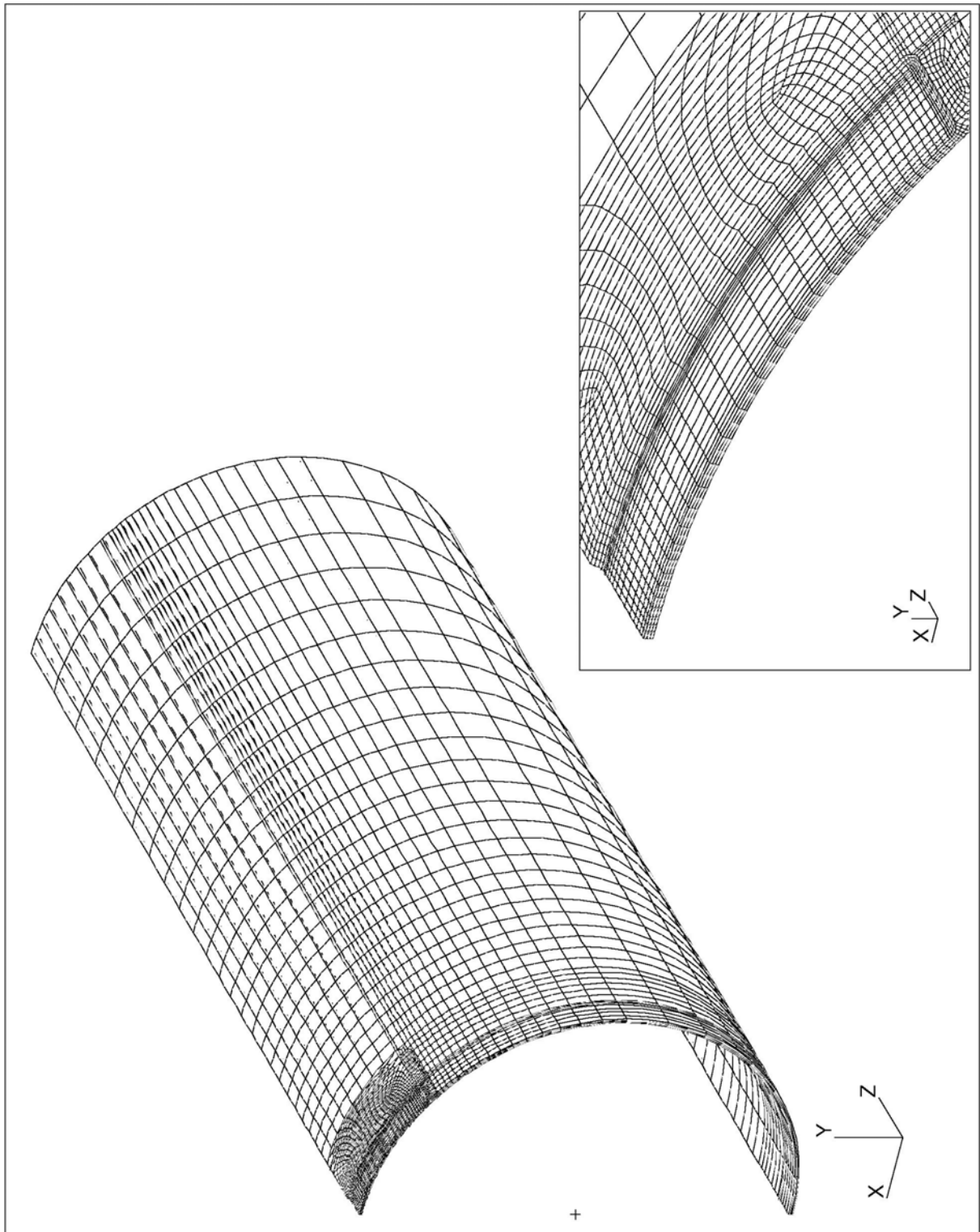
Figure 29. Quarter Symmetry FE Model of a 50% Deep Patch (152.4mm x 762mm /6-inch x 30-inch) in 1219.2 mm (48-inch) Diameter Pipe (Alyeska Test II-2)
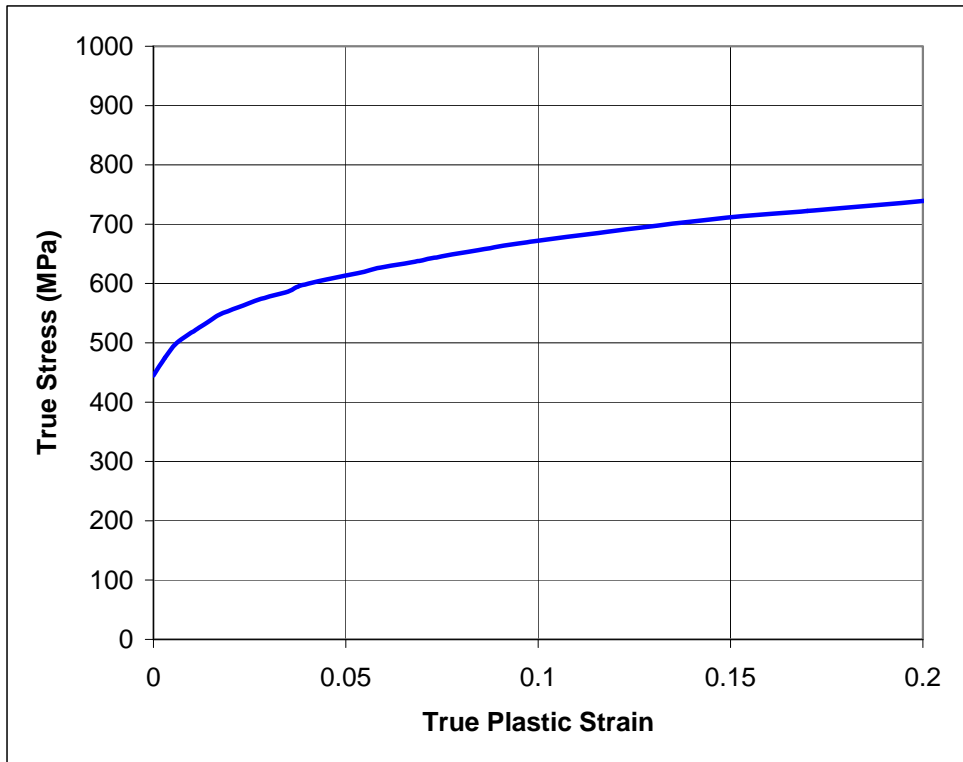
Figure 30. True Stress Versus True Strain Curve for 914.4 mm (36-inch) Diameter Grade X65 Pipe
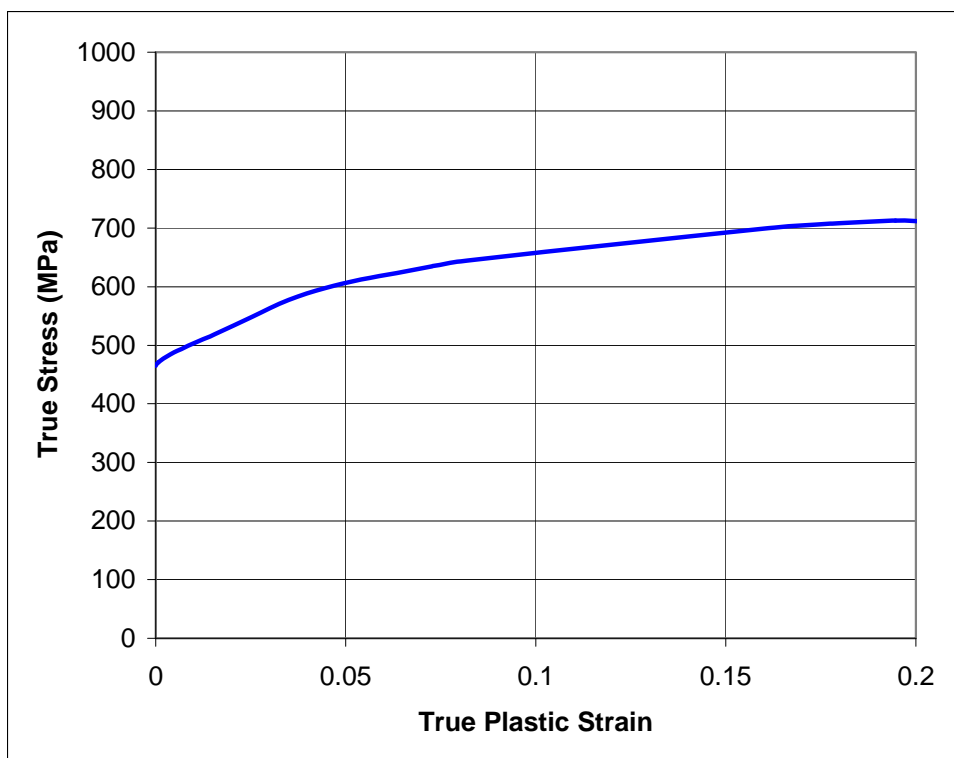
Figure 31. True Stress Versus True Strain Curve for 1219.2 mm (48-inch) Diameter Grade X65 Pipe
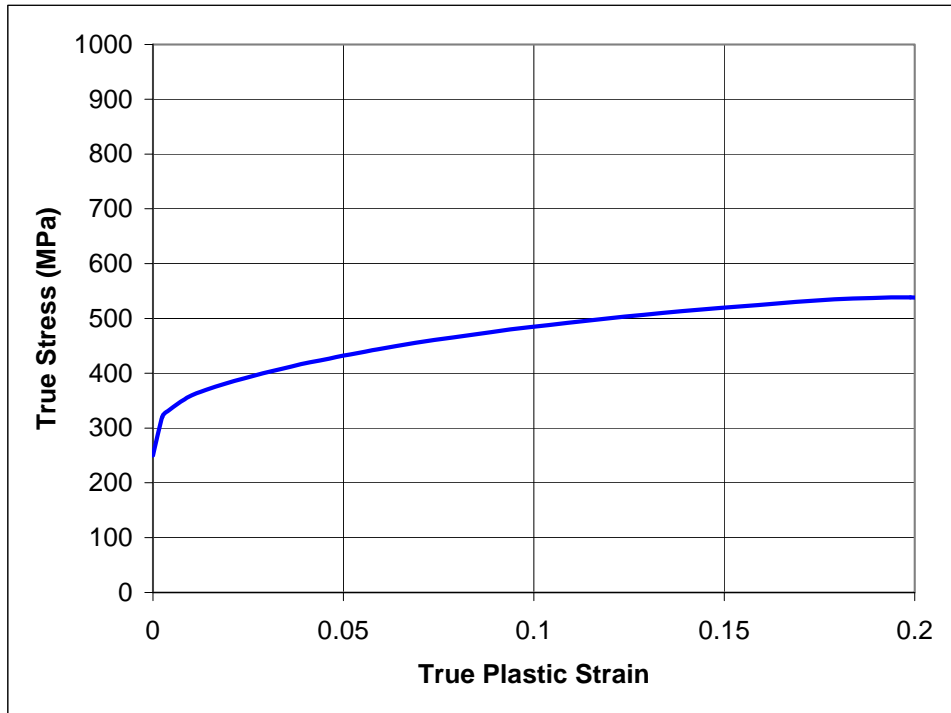
Figure 32. True Stress Versus True Strain Curve for 457.2mm (18-inch) Diameter Grade B/X42 Pipe
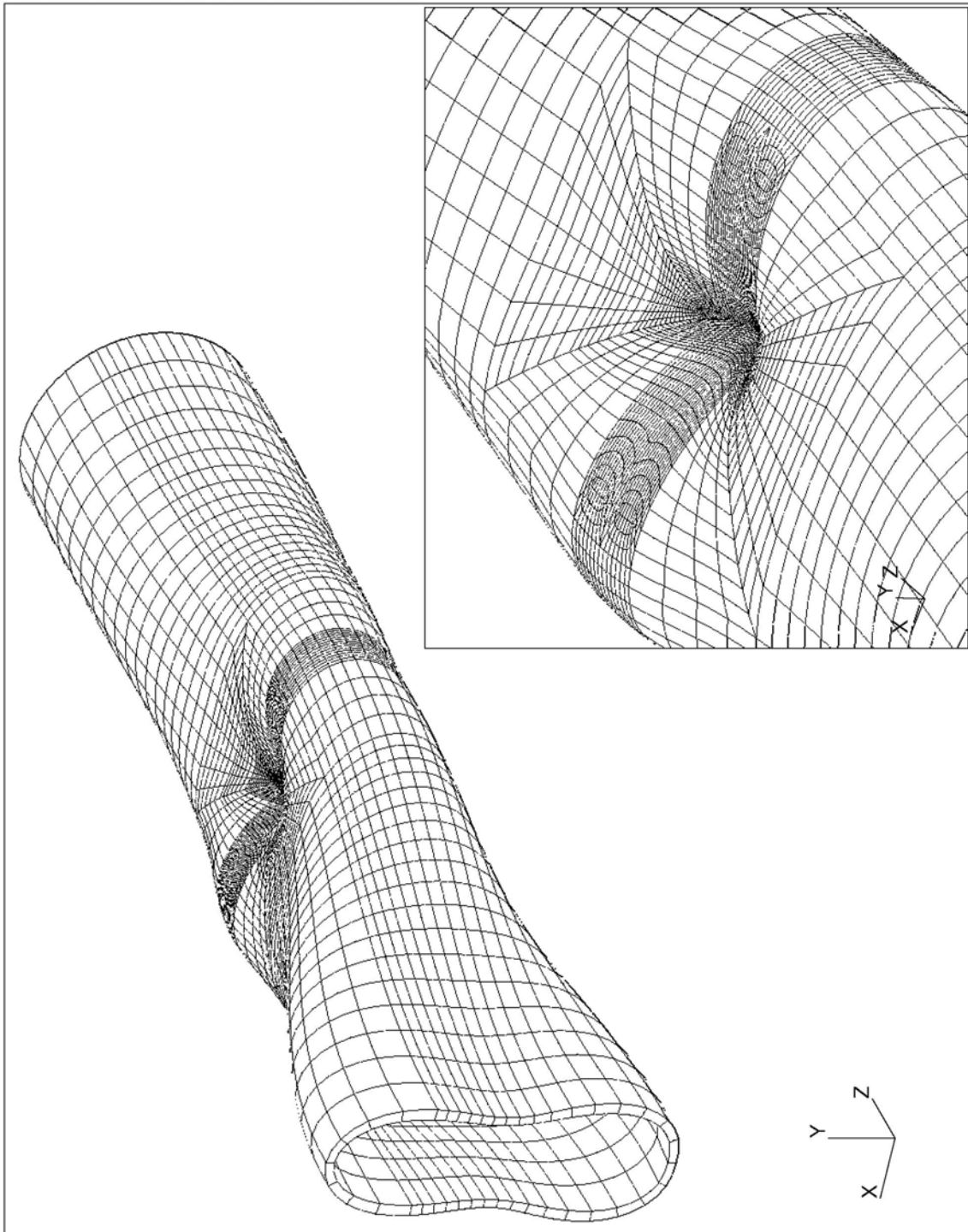
Figure 33. Typical eigenmode for 203.2 mm (8-inch) diameter pipe with an 80% deep axial groove (highly magnified)
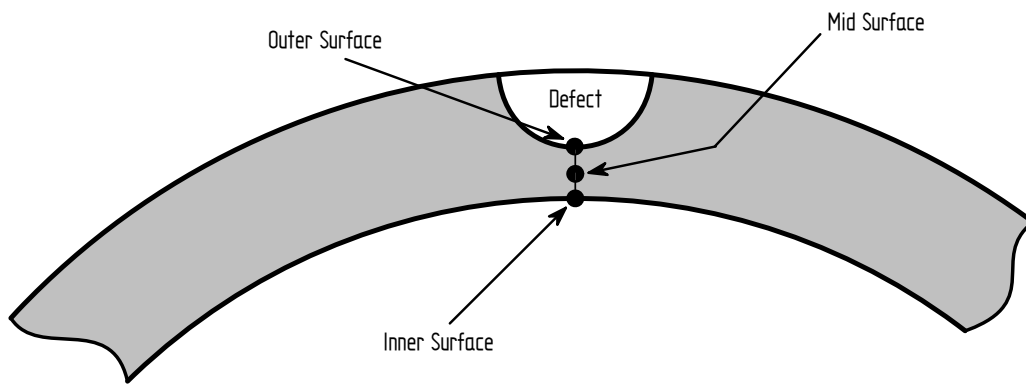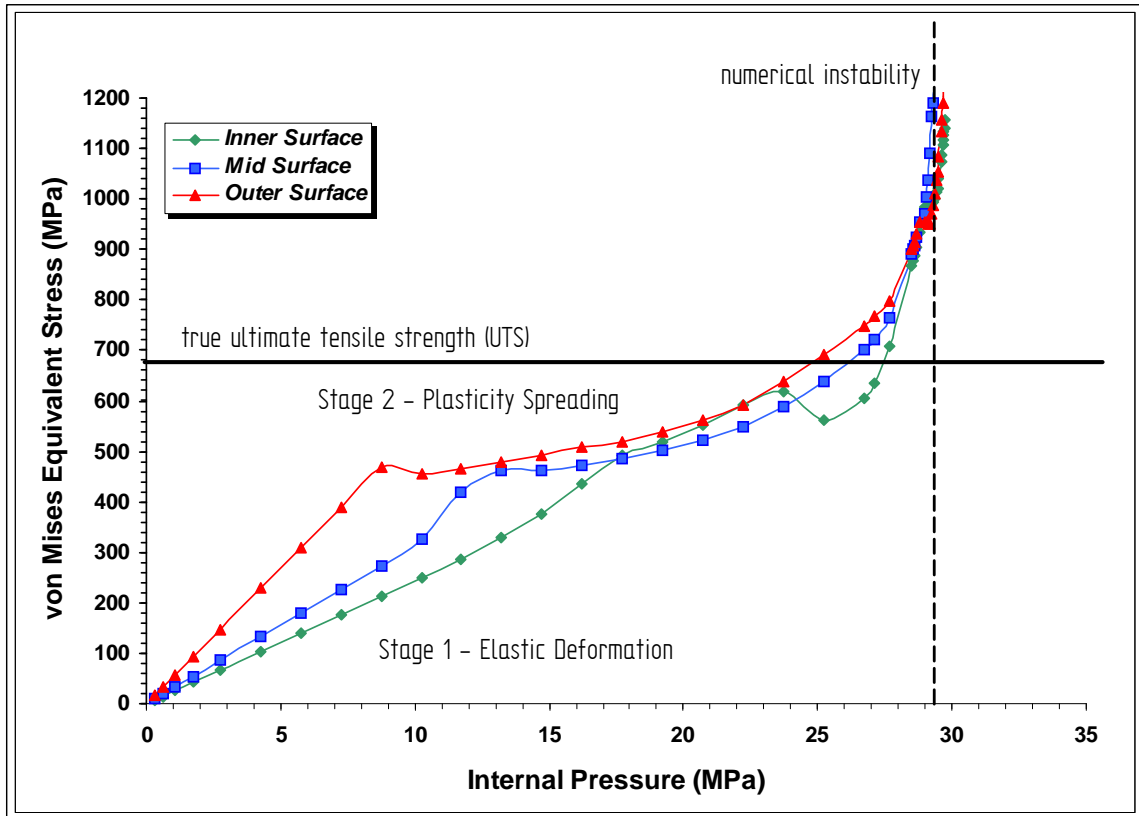
Figure 34. Method of Predicting the Failure Pressure of Corroded Pipe Using Non-Linear FE Analysis
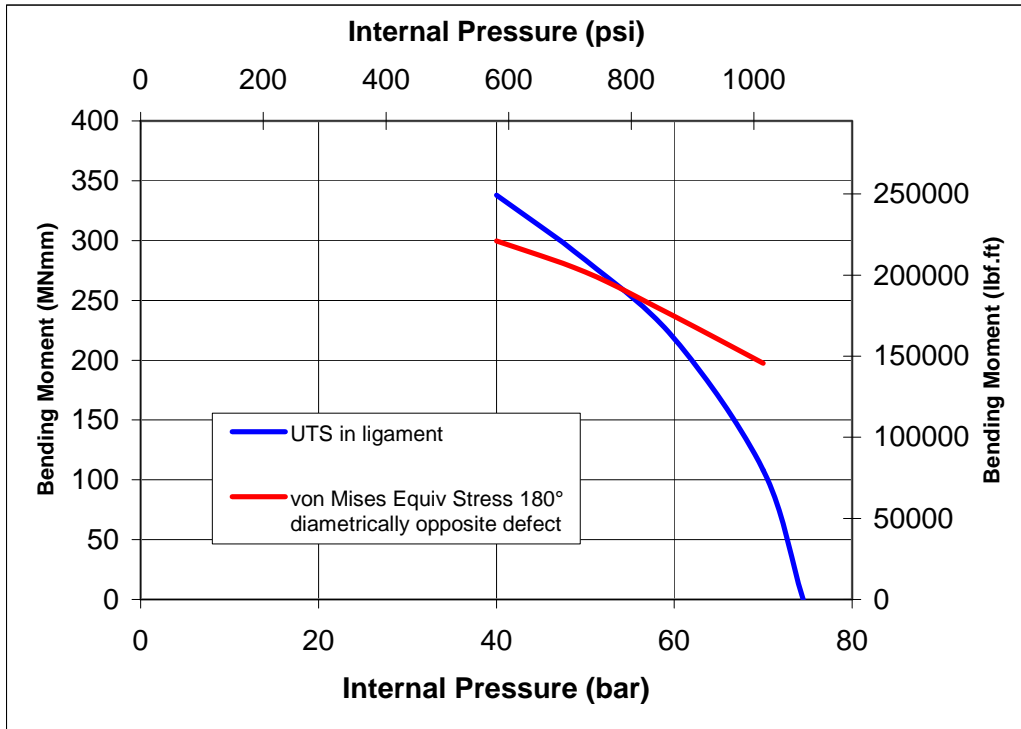
Figure 35. Derivation of Failure Locus. 457.2 mm (18-inch) Diameter 5.56 mm (0.219-inch) Wall Grade B/X42 Pipe with an 80% Deep Axial Groove
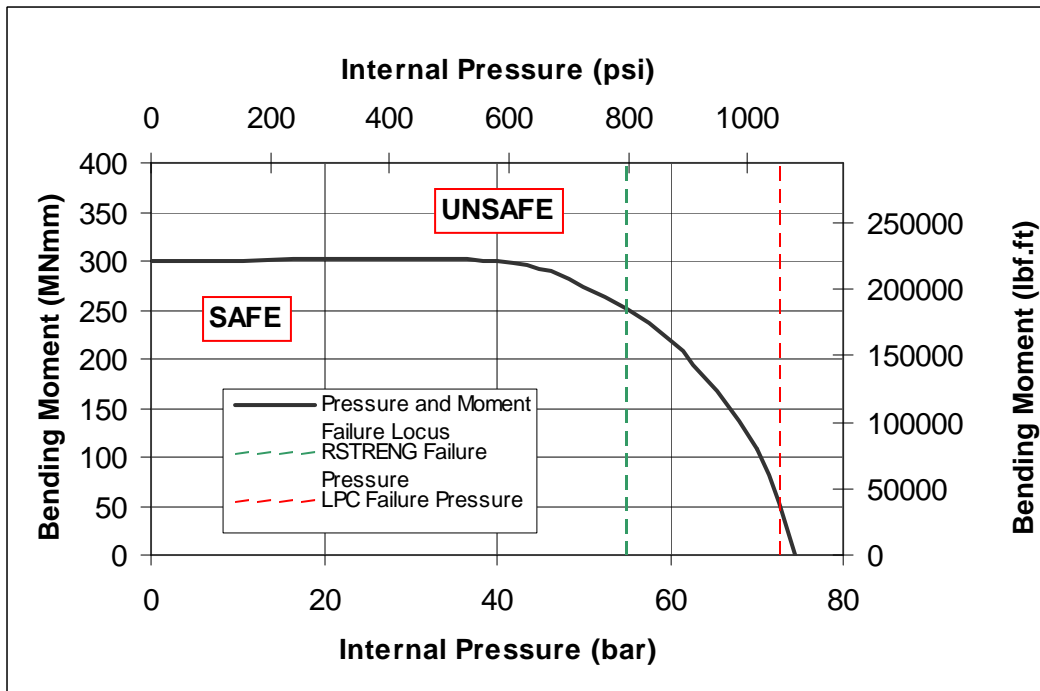
Figure 36. Failure Locus for 457.2 mm (18-inch) Diameter 5.56 mm (0.219-inch) Wall Grade B/X42 Pipe with an 80% Deep Axial Groove
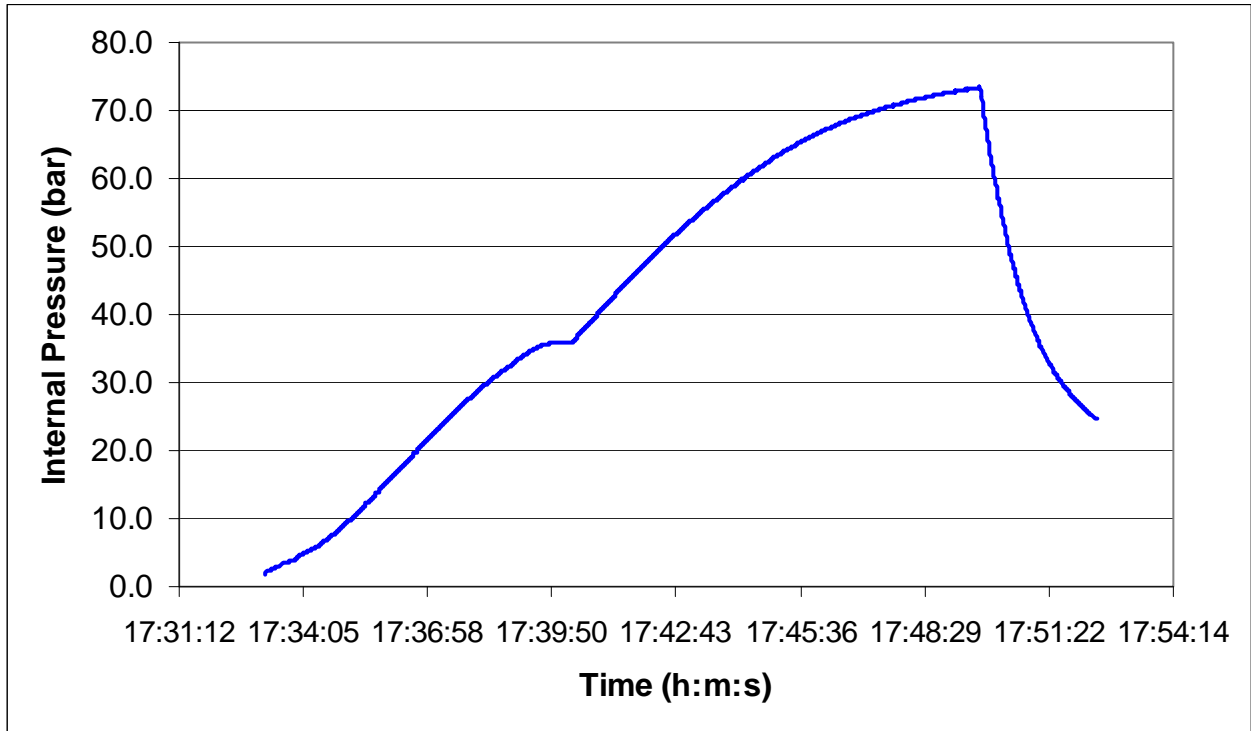
Figure 37. Pressure versus Time Plot for Vessel 1 (Failure Pressure 73.4bar)
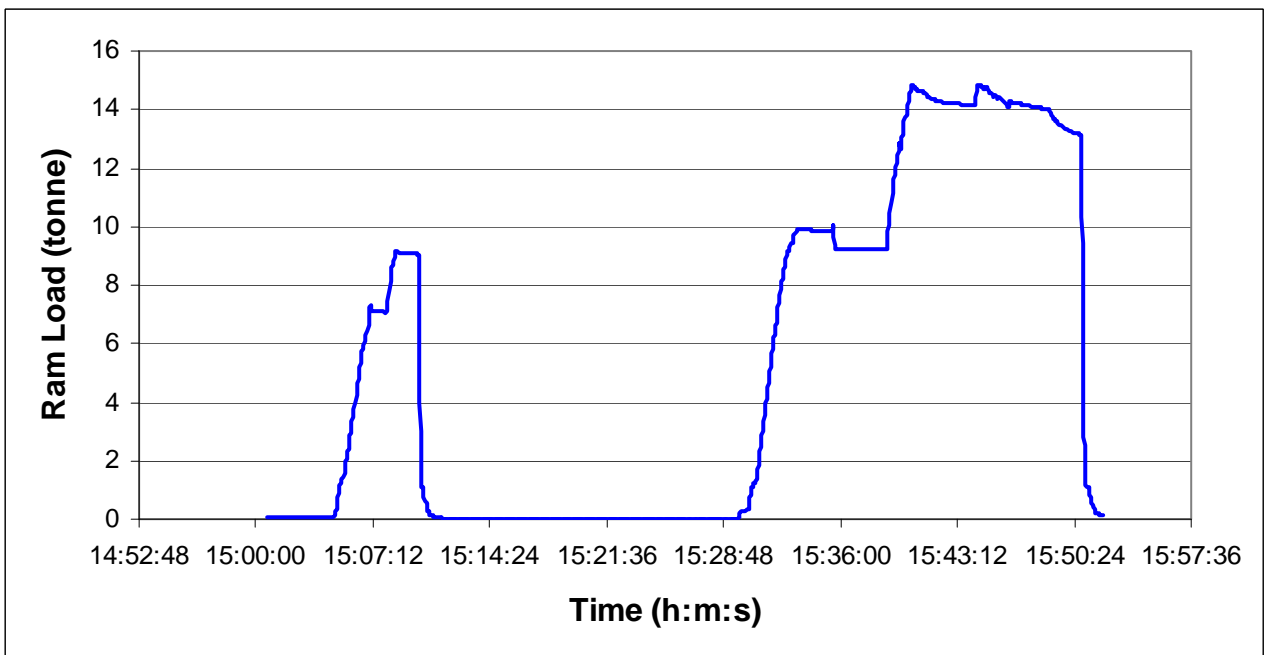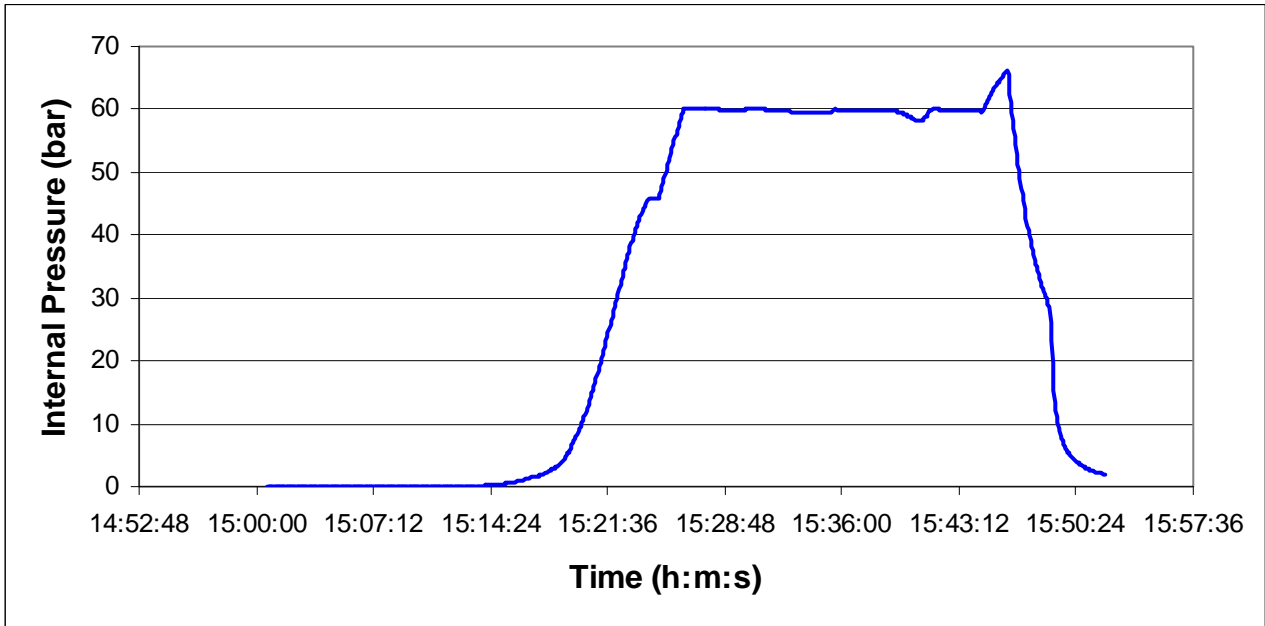
Figure 38. Pressure/Ram Load versus Time Plot for Vessel 2

Figure 39. Vessel 2 After Completion of Test
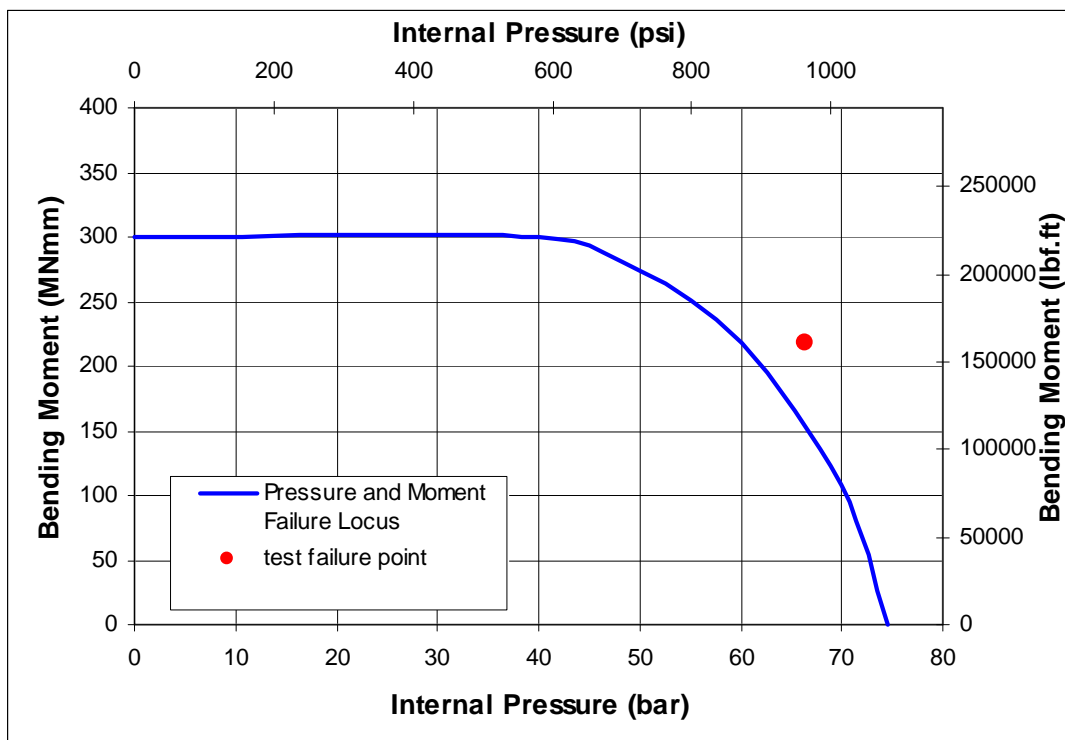
Figure 40. Vessel 2 Failure Point on Internal Pressure-Bending Moment Failure Locus for 457.2 mm (18-inch) Diameter Pipe with an 80% Deep Axial Groove
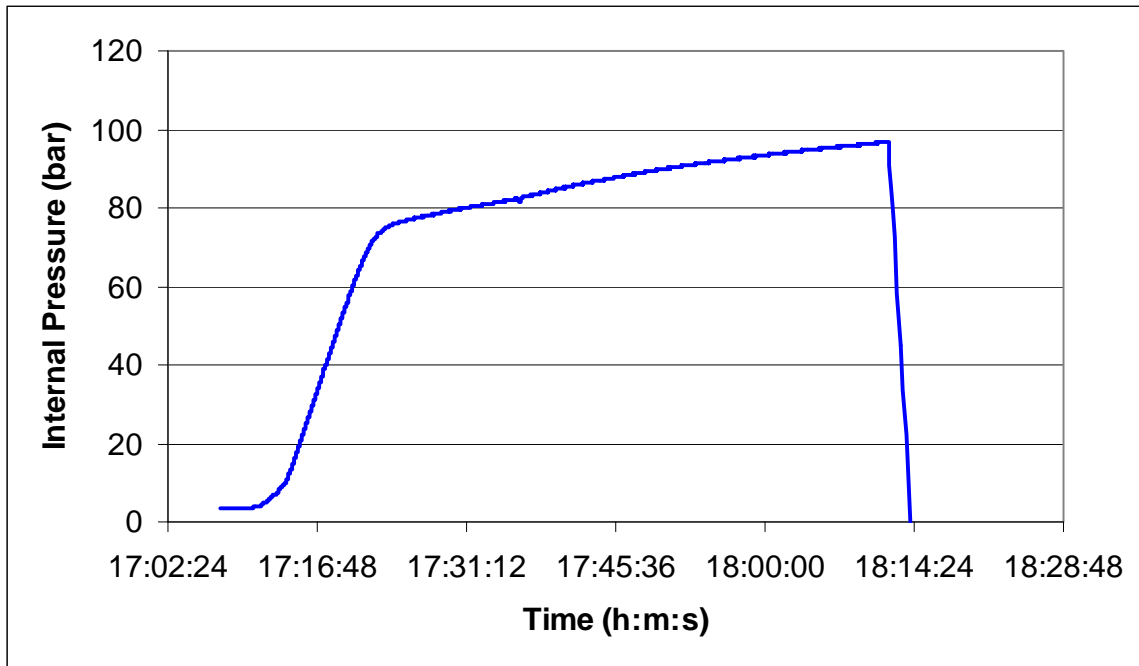
Figure 41. Pressure versus Time Plot for Vessel 3 (Test Terminated at Pressure of 96.8bar)
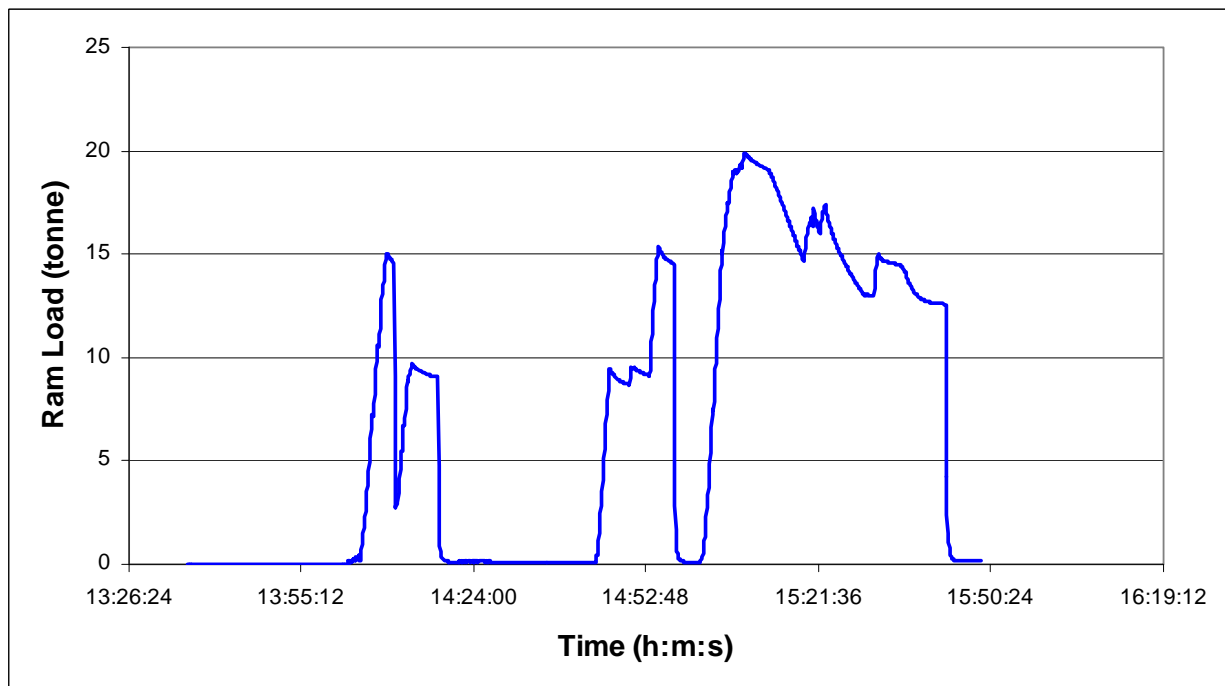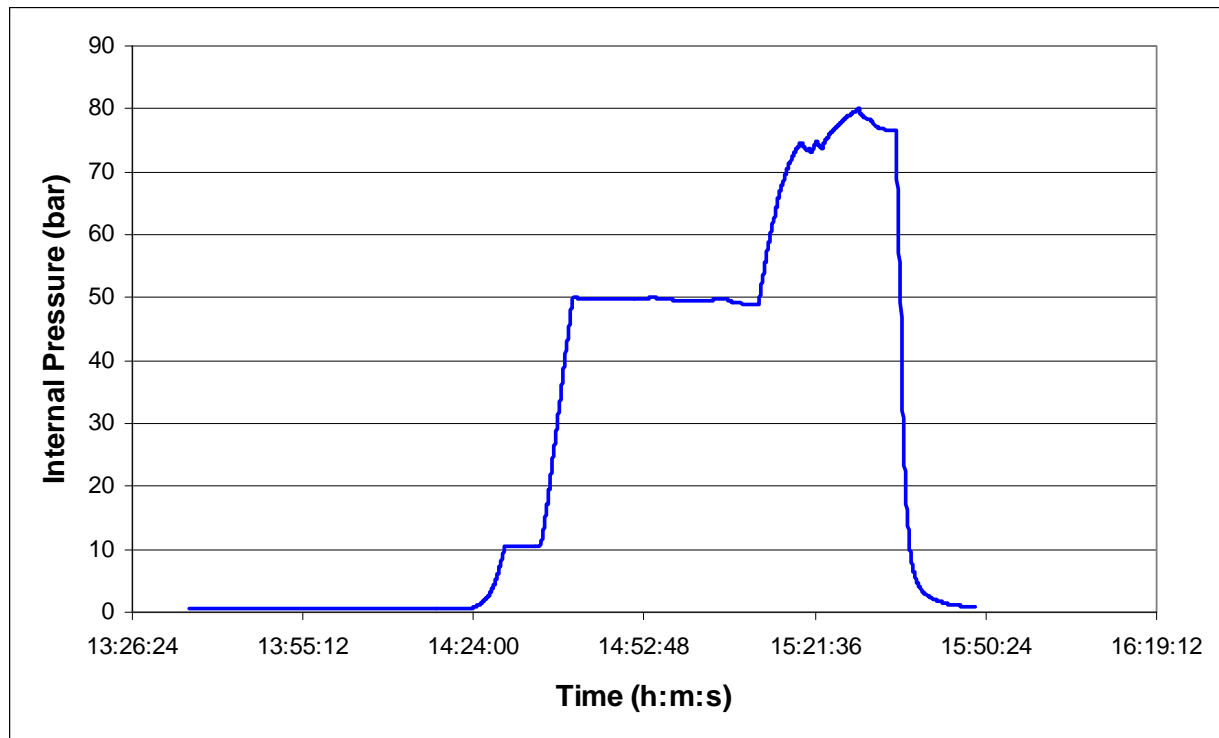
Figure 42. Pressure/Ram Load versus Time Plot for Vessel 4

Figure 43. Vessel 4 after Completion of Test
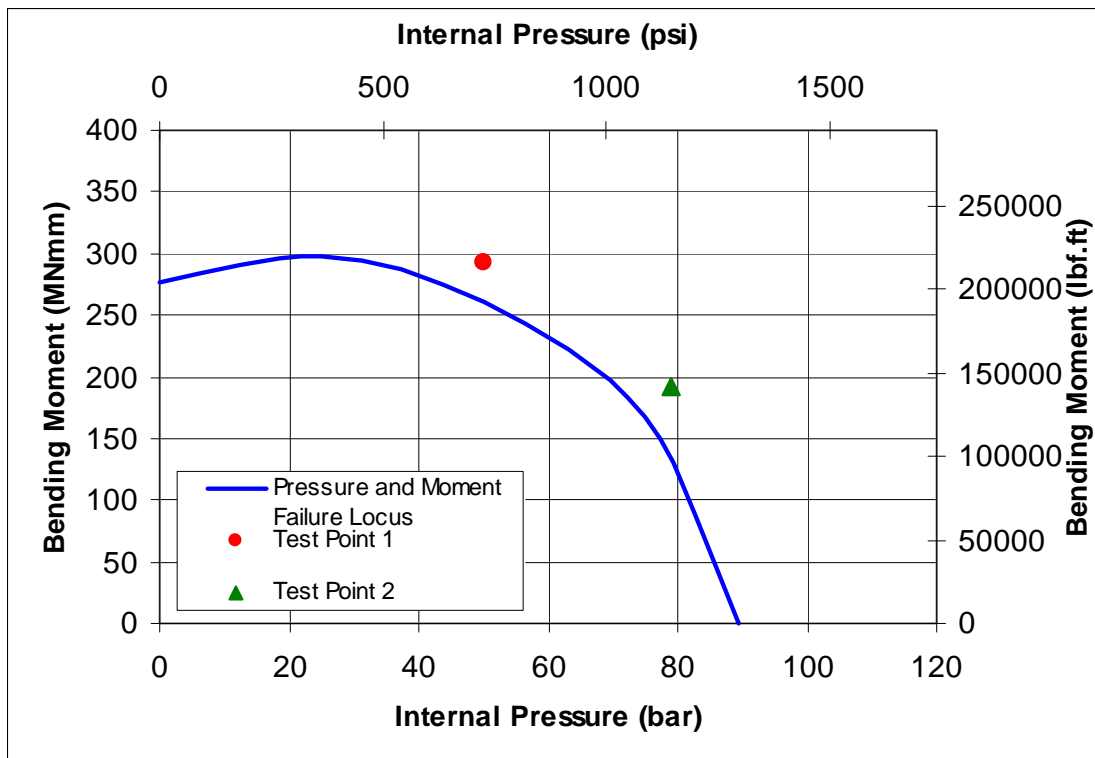
Figure 44. Vessel 4 Test Points on Internal Pressure-Bending Moment Failure Locus for 457.2 mm (18-inch) Diameter Pipe with an 80% Deep Circumferential Groove
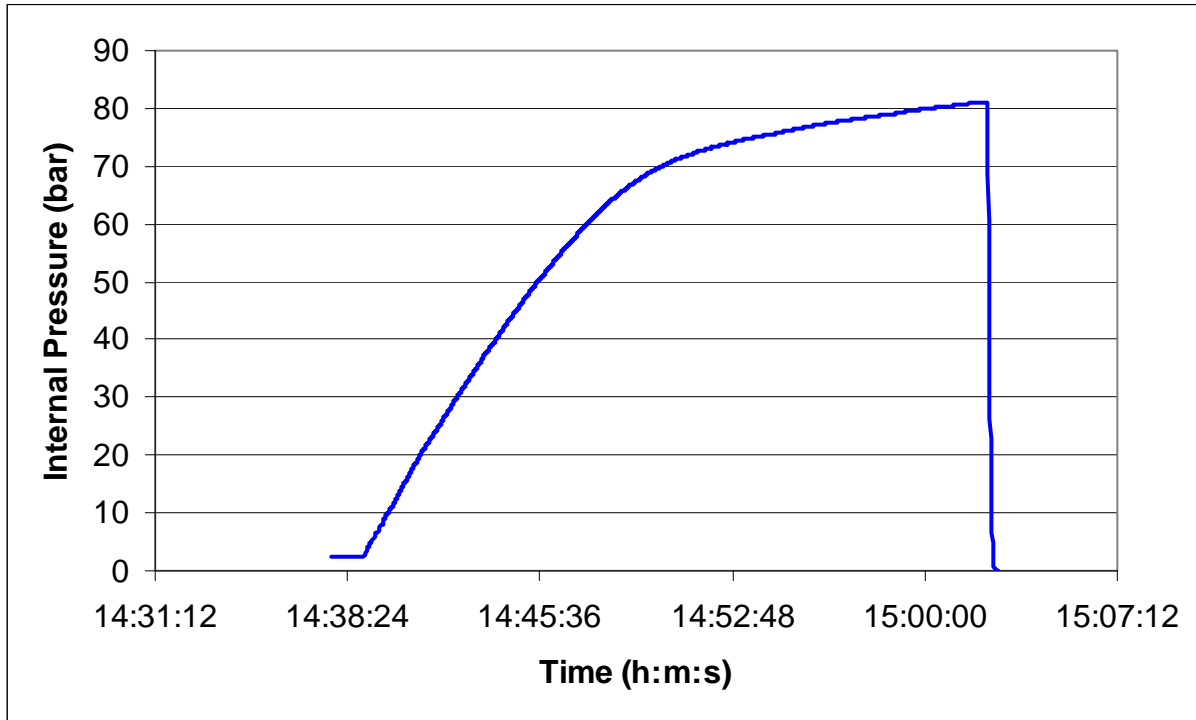
Figure 45. Pressure versus Time Plot for Vessel 5 (Failure Pressure of 81.1bar)
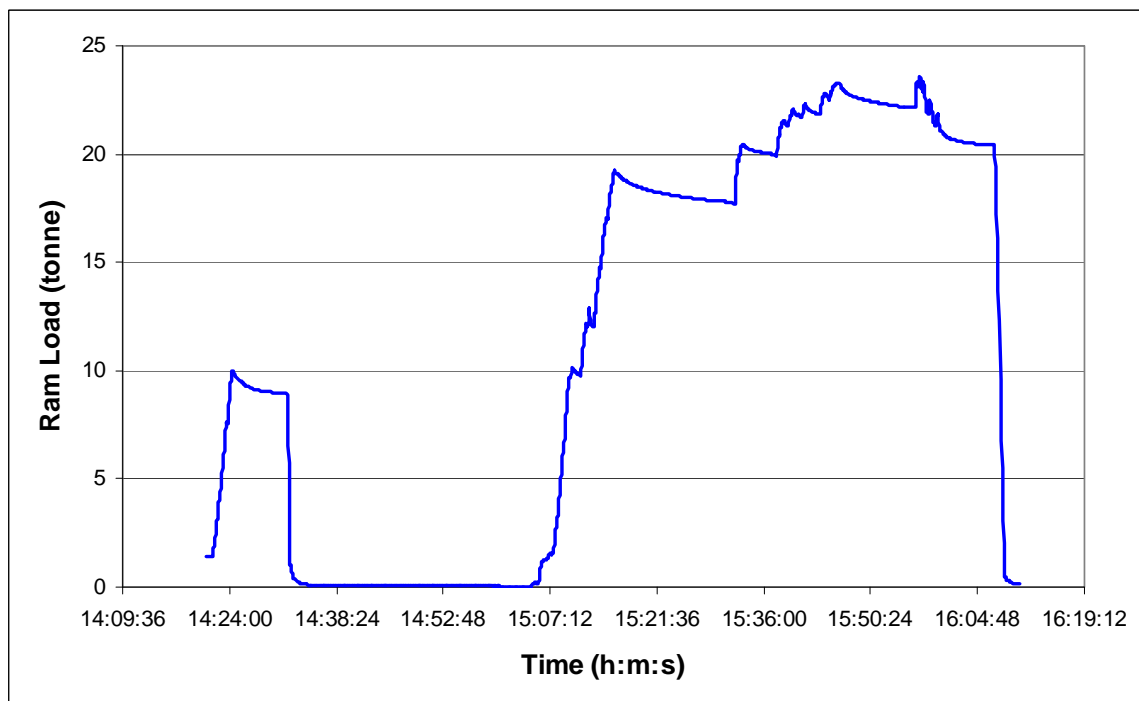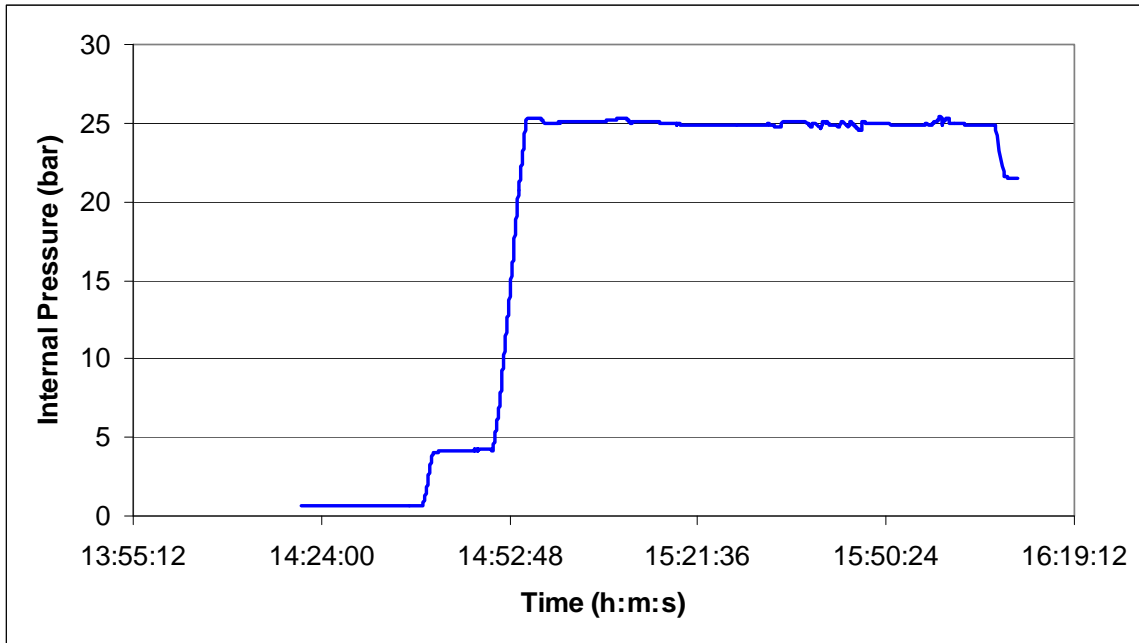
Figure 46. Pressure/Ram Load versus Time Plot for Vessel 6

Figure 47. Vessel 6 after Completion of Test
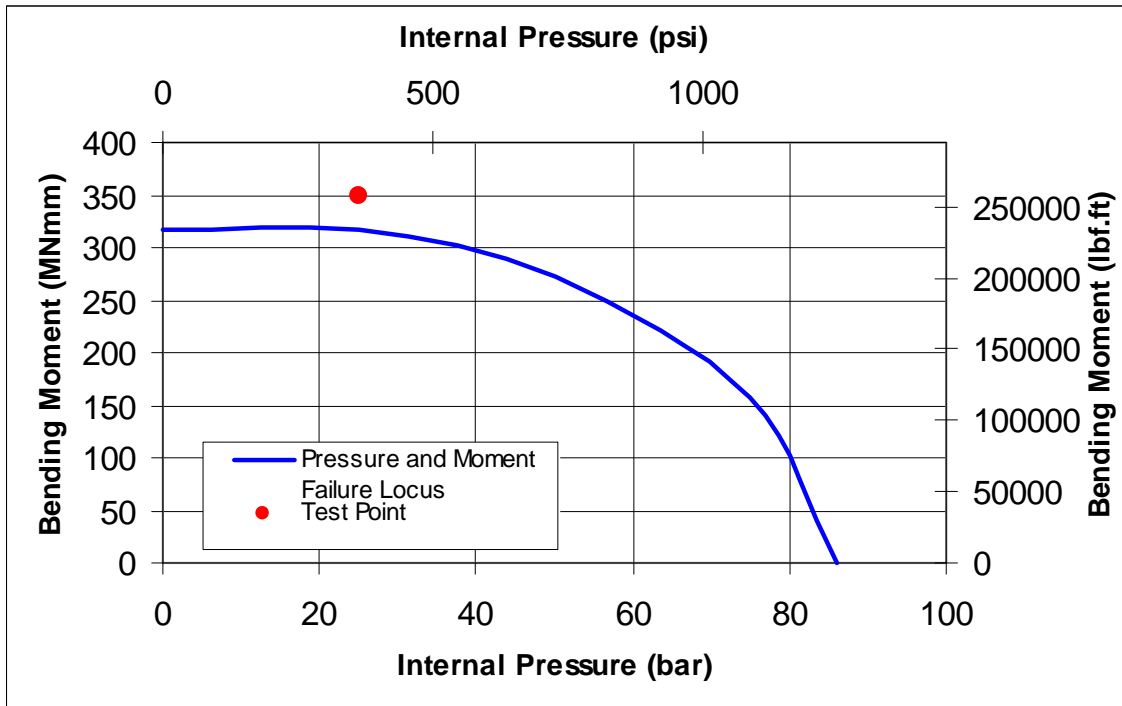
Figure 48. Vessel 6 Test Point on Internal Pressure-Bending Moment Failure Locus for 457.2 mm (18-inch) Diameter Pipe with an 80% Deep Patch

GL⊛

Appendix A   Pipe Mill Certificate for 457.2 mm (18-Inch) Diameter Grade B/X42 Pipe

Corus UK Limited
Corus Tubes

20" H.F.I Mill
Brenda Road
Hartlepool Cleveland UK TS25 2EG

Telephone: +44 (0)1429 266611
Fax: +44 (0)1429 527256

INSPECTION CERTIFICATE
(EN10204 Type 3.1)

Date	25/04/05
Cert No.	280/0517/01B9
Dd. Note	

Page No. 01 of 02

Customer

P.VAN LEEUWEN JRS
BULZENHANDEL NV

LINDTSEDIJK 100
P.O.BOX 1
3330 A A ZWIJNDRECHT
THE NETHERLANDS

Approval No. 0840080

Corus Tubes Ref.No. GXA233542   Sales Works 9103

Customer Order No.   P/O: 3234684 OF 04/FEB/05

Product Description
ELECTRIC WELDED STEEL TUBES TO API 5L GRADE B PSL1, API 5L GRADE X42
PSL1,ASTM A53 GRADE B AND VAN LEEUWEN SPECIFICATION 28.500R REVISION 6
APRIL 2004 WITH AGREED COMMENTS AND EXCEPTIONS.
PIPES MARKED 3234684

L=Longitudinal   T=Transverse   B=Body   W=Weld   KV=Charpy V-Notch   HV=Hardness Vickers(10 Kg Load)   DT=Drop Weight Tear Test

Item No.	Number of Pieces	Product Dimensions
7141	9	MADE FROM BOS KILLED STEEL. NO HEAT TREATMENT WELD ANNEALED. PIPES HARD STAMPED WITH LOW STRESS STAMPS CORUS AND API STAMP WIDTH OF TENSILE TEST SPECIMEN 1.5 INCH NOMINAL. ENDS BEVELLED TO API 5L

Steel Making Process   BASIC OXYGEN STEEL

Other Tests
WELD FACTOR V=1.0
FLATTENING TEST SATISFACTORY
ALSO IN ACCORDANCE WITH NACE
STD MR-01-75
SURFACE AND DIMENSIONAL INSPECTION
CARRIED OUT IN ACCORDANCE
WITH API 5L.
ULTRASONIC TESTING CARRIED OUT
IN ACCORDANCE WITH API 5L
SECTION 9.7.2.2

Analysis %

Cast No.		C	SI	MN	P	S	CR	MO	NI	AL	CU	N	NB	SN	TI	V	CEV
7B32757	LADLE	.14	.145	.84	.013	.008	.020	.002	.016	.034	.013	.0063	.001	.001	.002	.001	.28
7B32757	CHECK	.14	.149	.85	.012	.008	.019	.003	.016	.033	.009	.0059	.001	.001	.001	.001	.29

Code Numbers in this document are in accordance with EN10168 (see overleaf).

Alterations to this document or its use for other products shall be regarded as falsification of documents and be subject to criminal jurisdiction.

The products covered by this inspection document are certified by Corus UK Limited
and comply with the requirements of the Product Description.
Corus Tubes Quality System complies with Pressure Equipment Directive
(PED) 97/23/EC Annex I Para. 4.3.

DAVID EVANS
Section Manager Metallurgy

This document has been prepared by a

| Corus Tubes HARTLEPOOL |
| EN 10210 |
| EN 10219 |
| DIN 6x6 |

GL

Corus UK Limited
Corus Tubes

20" H.F.I Mill
Brenda Road
Hartlepool Cleveland UK TS25 2EG

Telephone: +44 (0)1429 266611
Fax: +44 (0)1429 527256

INSPECTION CERTIFICATE
(EN10204 Type 3.1)

Date: 25/04/05
Cert No. 280/0517/01B9
Del. Note

Page No. 02 of 02

Customer
P.VAN LEEUWEN JRS
BUIZENHANDEL NV
LINDTSEDIJK 100
P.O.BOX 1
3330 A A ZWIJNDRECHT
THE NETHERLANDS

Approval No. 0840080

Corus Tubes Ref.No. Sales GXA233542   Works 9103

Customer Order No.   P/O: 3234684 OF 04/FEB/05

Product Description
ELECTRIC WELDED STEEL TUBES TO API 5L GRADE B PSL1, API 5L GRADE X42
PSL1,ASTM A53 GRADE B AND VAN LEEUWEN SPECIFICATION 28.500E REVISION 6
APRIL 2004 WITH AGREED COMMENTS AND EXCEPTIONS.
PIPES MARKED 3234684

L=Longitudinal   T=Transverse   B=Body   W=Weld   KV=Charpy V-Notch   HV=Hardness Vickers(10 Kg Load)   DT=Drop Weight Tear Test

Item No.	Number of Pieces	Product Dimensions	Cast/Heat No.	Pipe No.		Tensile Test					Hydro Pressure		Impact/Hardness Tests								Other Tests
						C11 Yield Stress Re N/mm2	C12 Tensile Strength Rm N/mm2	C13 Elong A% 50mm	D02 Hydro Pressure BAR		C01 C02 C10	C00 C30 Test Type	C41 Width mm	C03 Temp °C	C42 C31 Values J	C43 C32 Ave J				
714 9																				
	31	457.0MM OD X 5.60 MM 11.800-11.950 367.17M	7B32757	1600433	W T B T	307	506 466	40	60 5.0 SECS		HV				170				
					END OF TEST CERTIFICATE														

Steel Making Process   BASIC OXYGEN STEEL

Cast No.	C	SI	MN	P	S	CR	MO	NI	AL	CU	N	NB	SN	TI	V	CEV

Analysis %

The products covered by this inspection document are certified by Corus UK Limited
and comply with the requirements of the Product Description.
Corus Tubes Quality System complies with Pressure Equipment Directive
(PED) 97/23/EC Annex 1 Part. 4.3.

DAVID EVANS
Section Manager Metallurgy

This document has been approved by a .

Corus Tubes
HARTLEPOOL
EN 10210
EN 10219
DIN 1626

Code Numbers in accordance with EN10168 (see overleaf).

Alterations to this document or its use for other products shall be regarded
as falsification of documents and be subject to criminal jurisdiction.

30-SEP-2005 10:20   VAN LEEUWEN PROCESS   01142578437   P.03

GL⬤

# Appendix B   Failure Loci 8-Inch Diameter Grade B/X42 Pipe
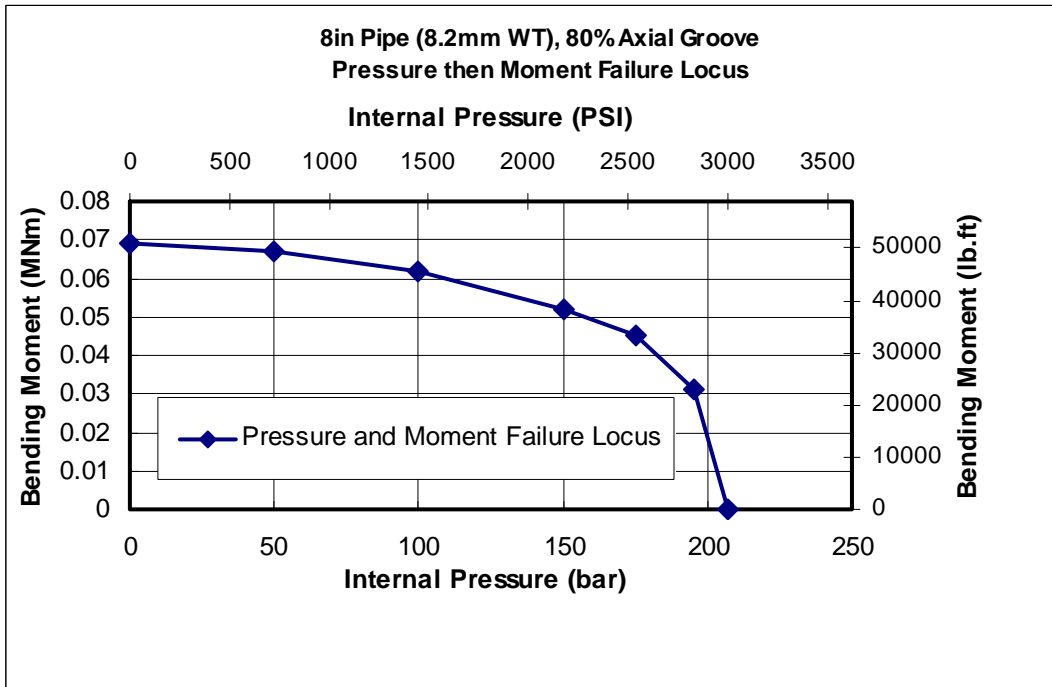

Figure B1. 203.2mm (8-inch) Diameter Grade B/X42 Pipe 80% Deep Axial Groove. Moment-Pressure Failure Locus
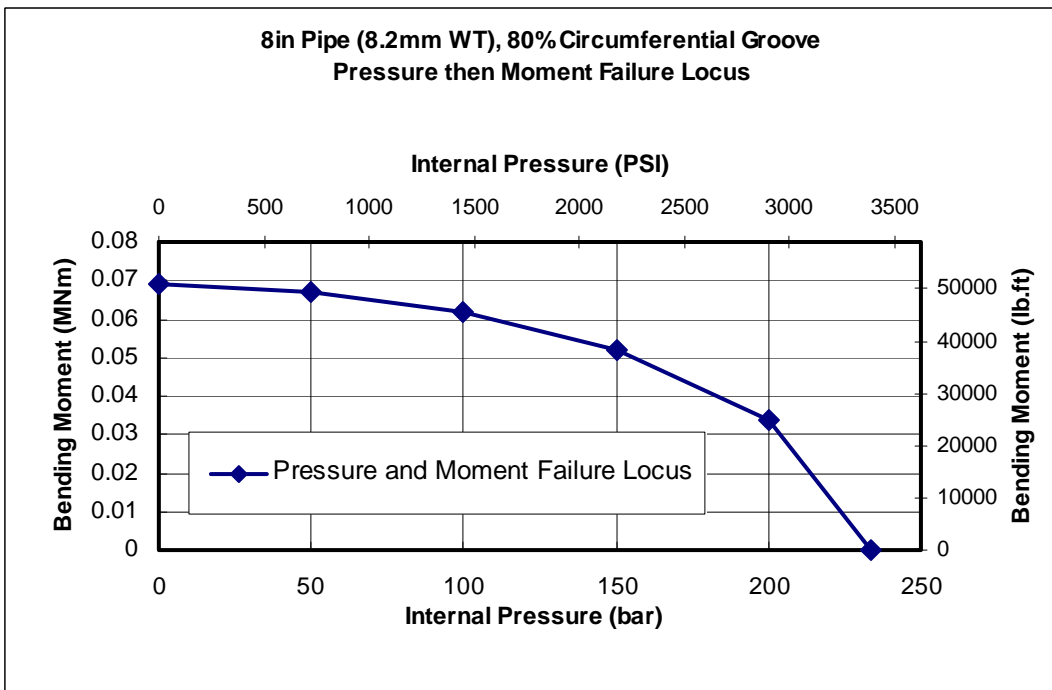
Figure B2. 203.2mm (8-inch) Diameter Grade B/X42 Pipe 80% Deep Circumferential Groove. Moment-Pressure Failure Locus

**8in Pipe (8.2mm WT), 80% Pit
Pressure then Moment Failure Locus**
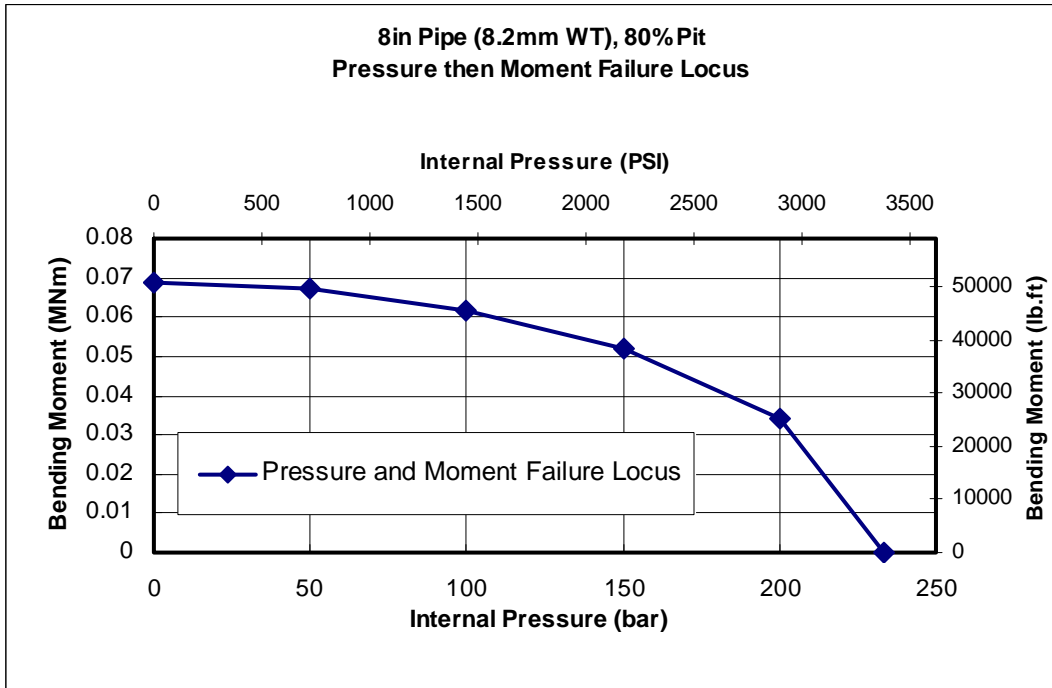
Figure B3. 203.2mm (8-inch) Diameter Grade B/X42 Pipe 80% Deep Pit. Moment-Pressure Failure Locus

**8in Pipe (8.2mm WT), 80% Patch
Pressure then Moment Failure Locus**
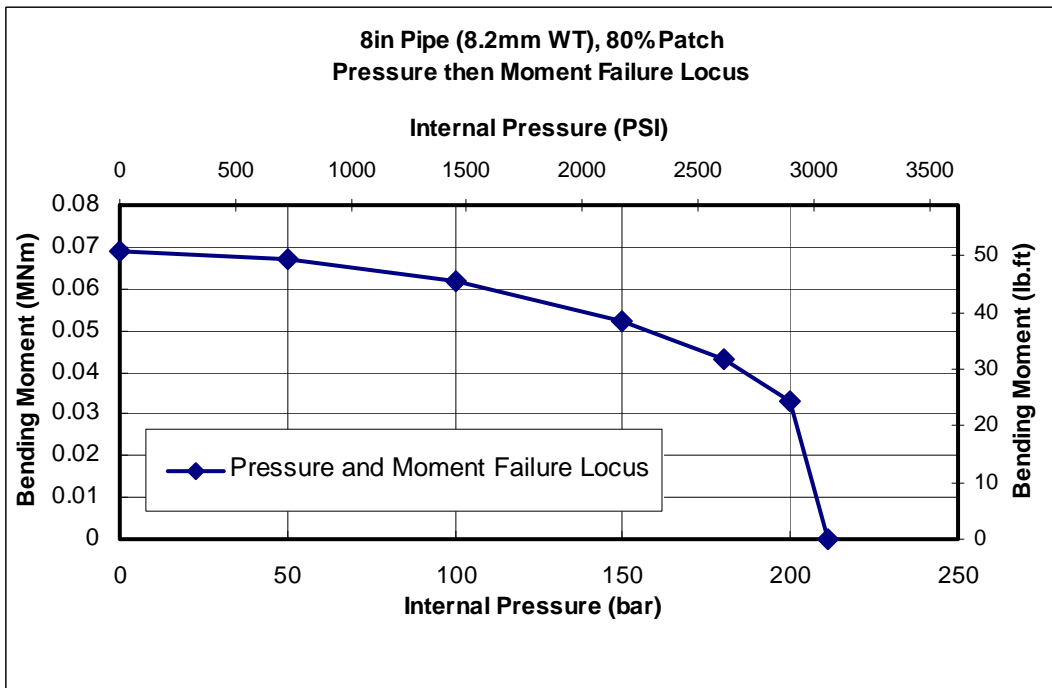
Figure B4. 203.2mm (8-inch) Diameter Grade B/X42 Pipe 80% Deep Patch. Moment-Pressure Failure Locus
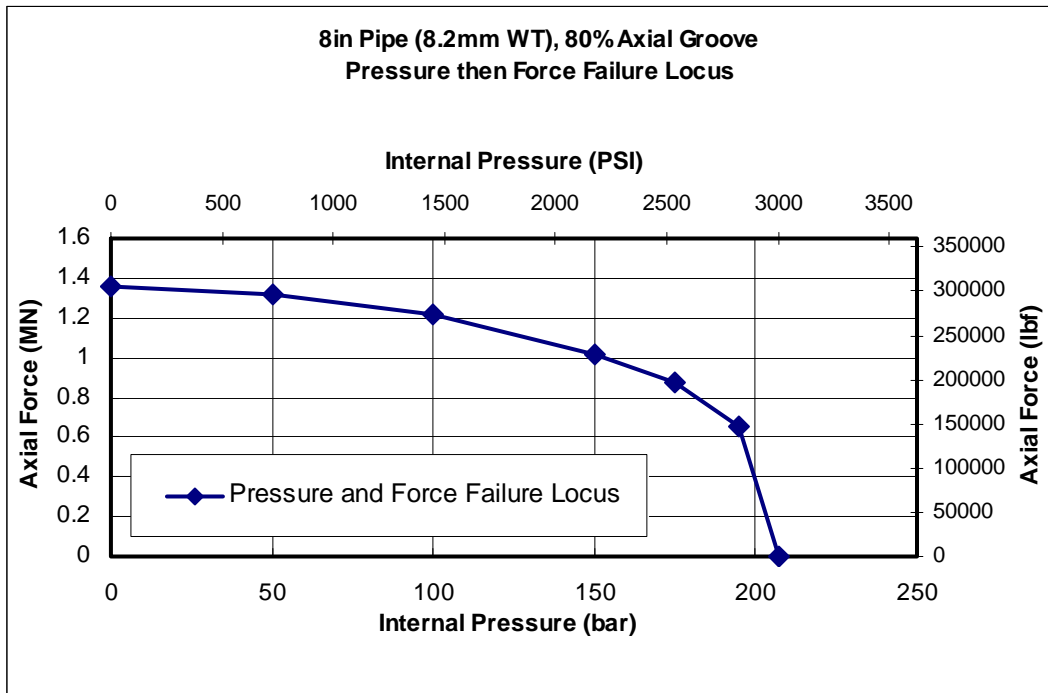
Figure B5. 203.2mm (8-inch) Diameter Grade B/X42 Pipe 80% Deep Axial Groove. Compressive Force-Pressure Failure Locus
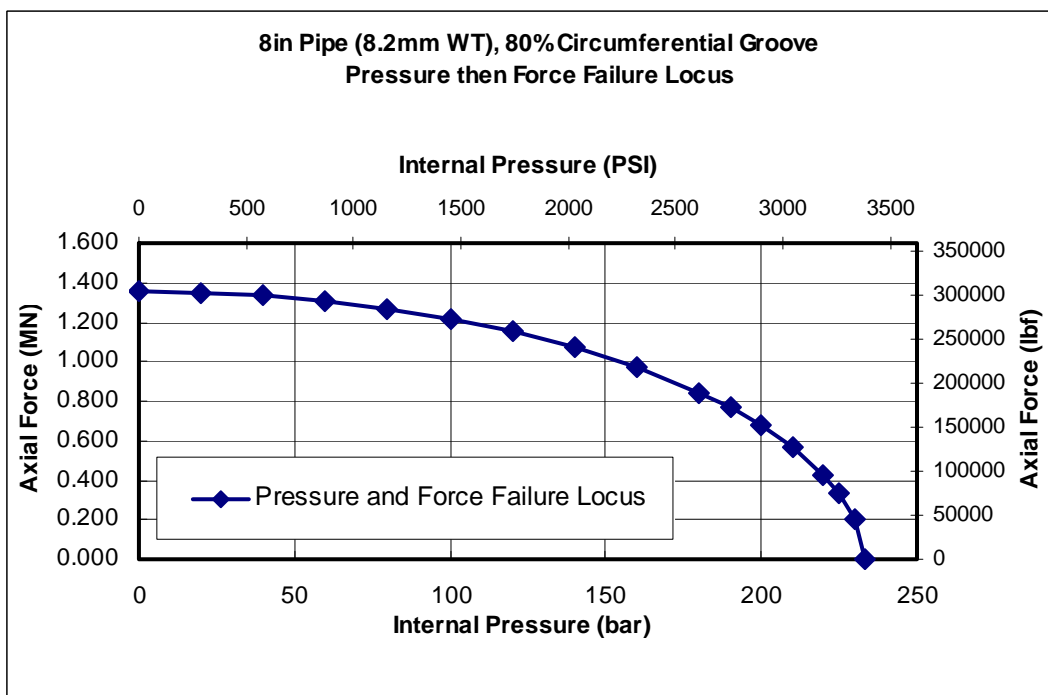
Figure B6. 203.2mm (8-inch) Diameter Grade B/X42 Pipe 80% Deep Circumferential Groove. Compressive Force-Pressure Failure Locus

GL⬤
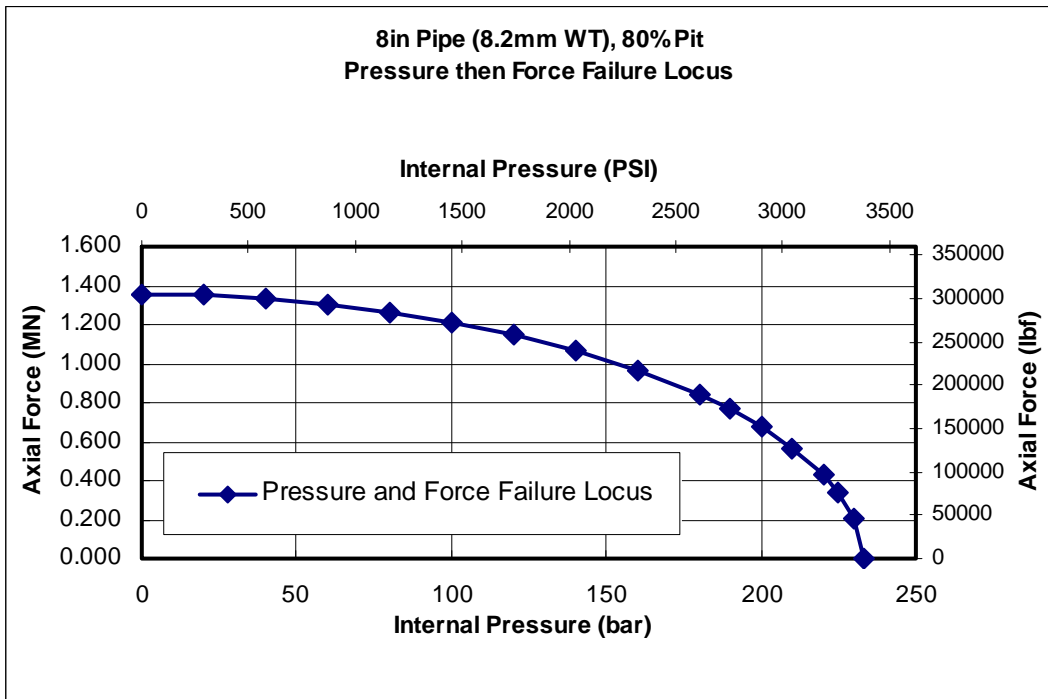
Figure B7. 203.2mm (8-inch) Diameter Grade B/X42 Pipe 80% Deep Pit. Compressive Force-Pressure Failure Locus
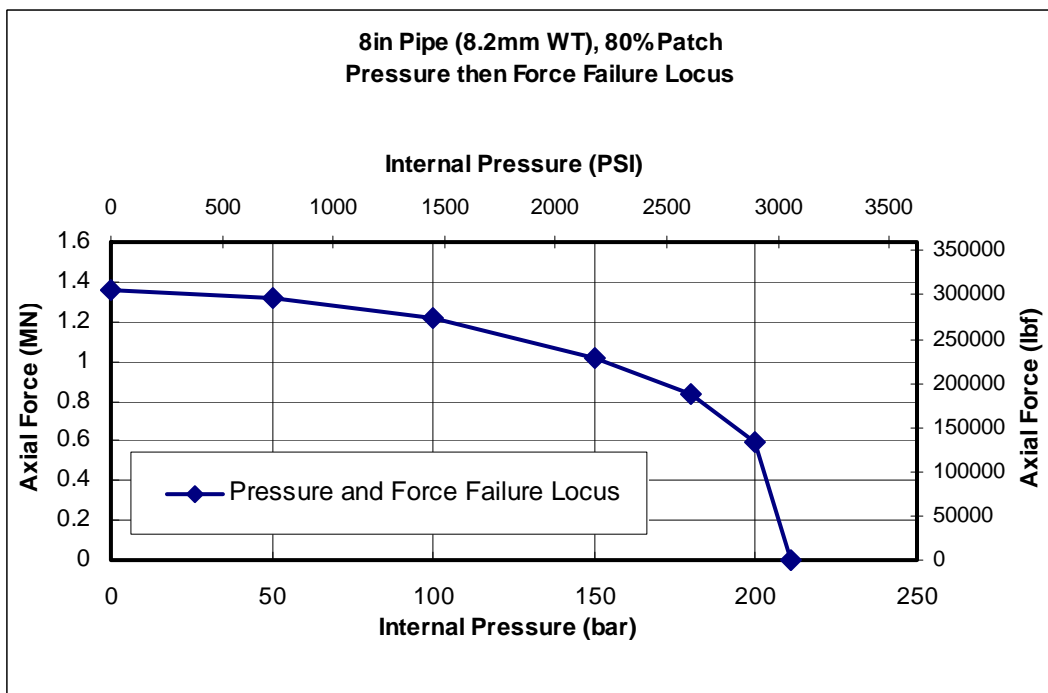
Figure B8. 203.2mm (8-inch) Diameter Grade B/X42 Pipe 80% Deep Patch. Compressive Force-Pressure Failure Locus

8in Pipe (8.2mm WT), 50% Axial Groove
Pressure then Moment Failure Locus
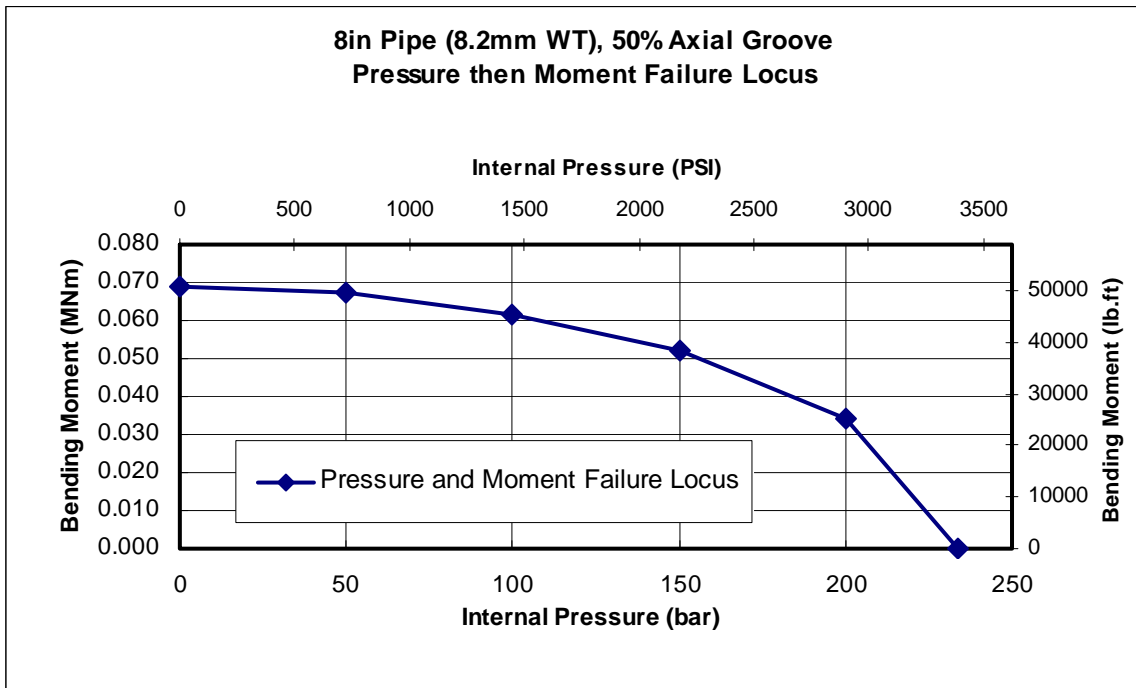
Figure B9. 203.2mm (8-inch) Diameter Grade B/X42 Pipe 50% Deep Axial Groove. Moment-Pressure Failure Locus

8in Pipe (8.2mm WT), 50% Circumferential Groove
Pressure then Moment Failure Locus
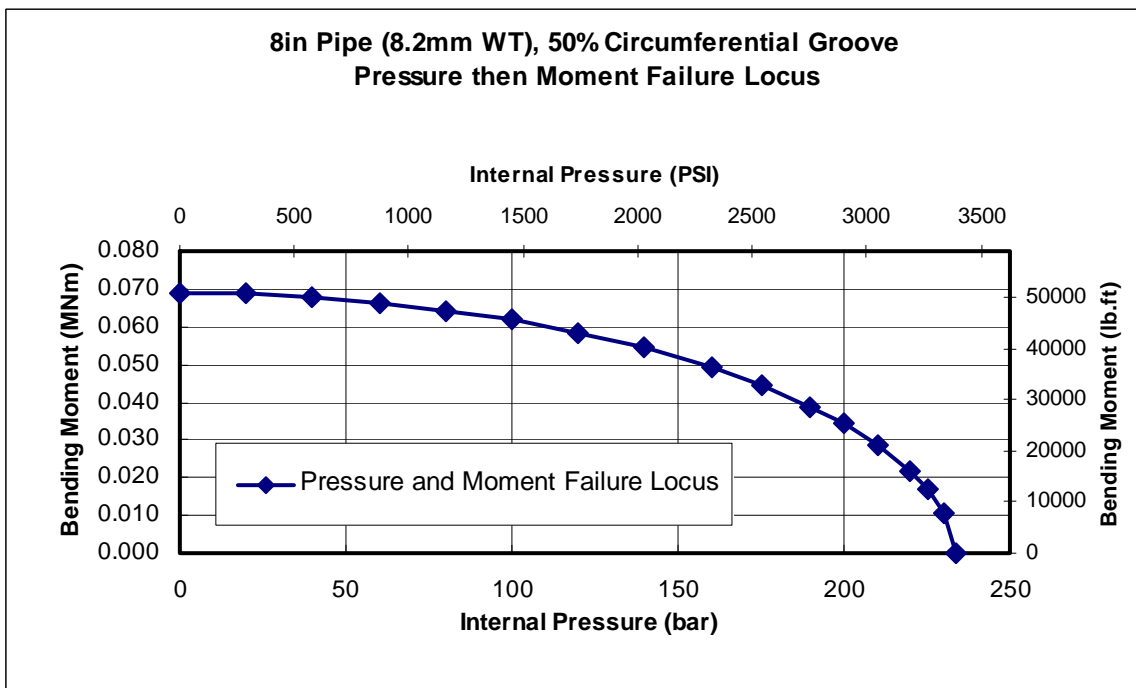
Figure B10. 203.2mm (8-inch) Diameter Grade B/X42 Pipe 50% Deep Circumferential Groove. Moment-Pressure Failure Locus

GL

**8in Pipe (8.2mm WT), 50% Pit
Pressure then Moment Failure Locus**
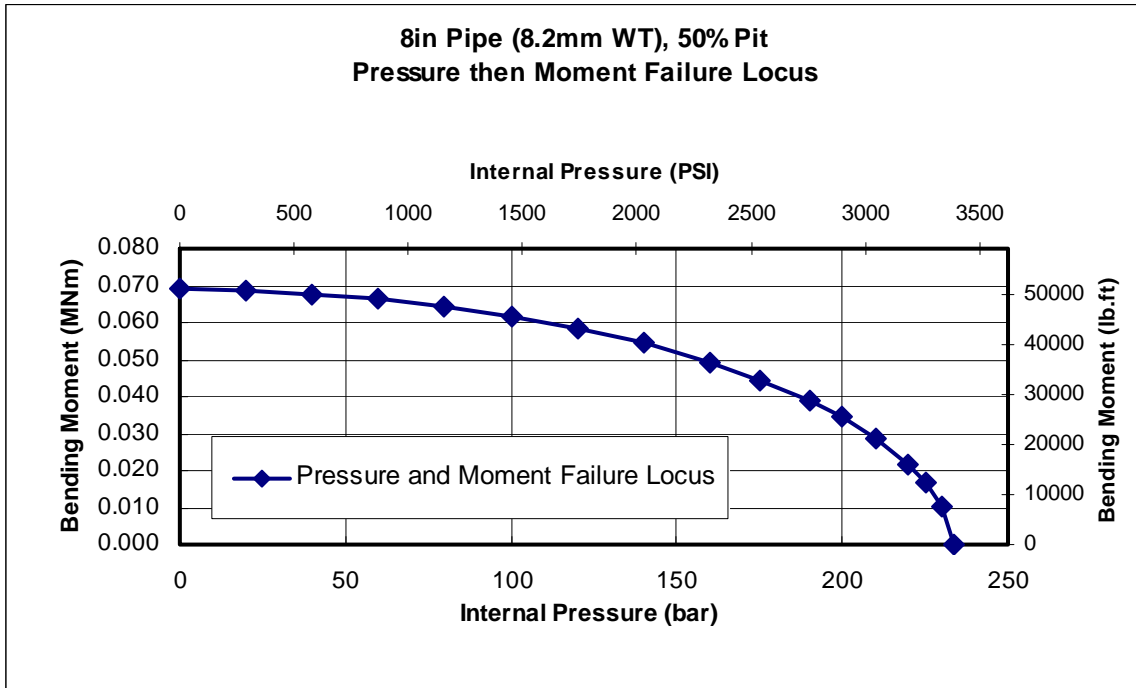
Figure B11. 203.2mm (8-inch) Diameter Grade B/X42 Pipe 50% Deep Pit. Moment-Pressure Failure Locus

**8in Pipe (8.2mm WT), 50% Patch
Pressure then Moment Failure Locus**
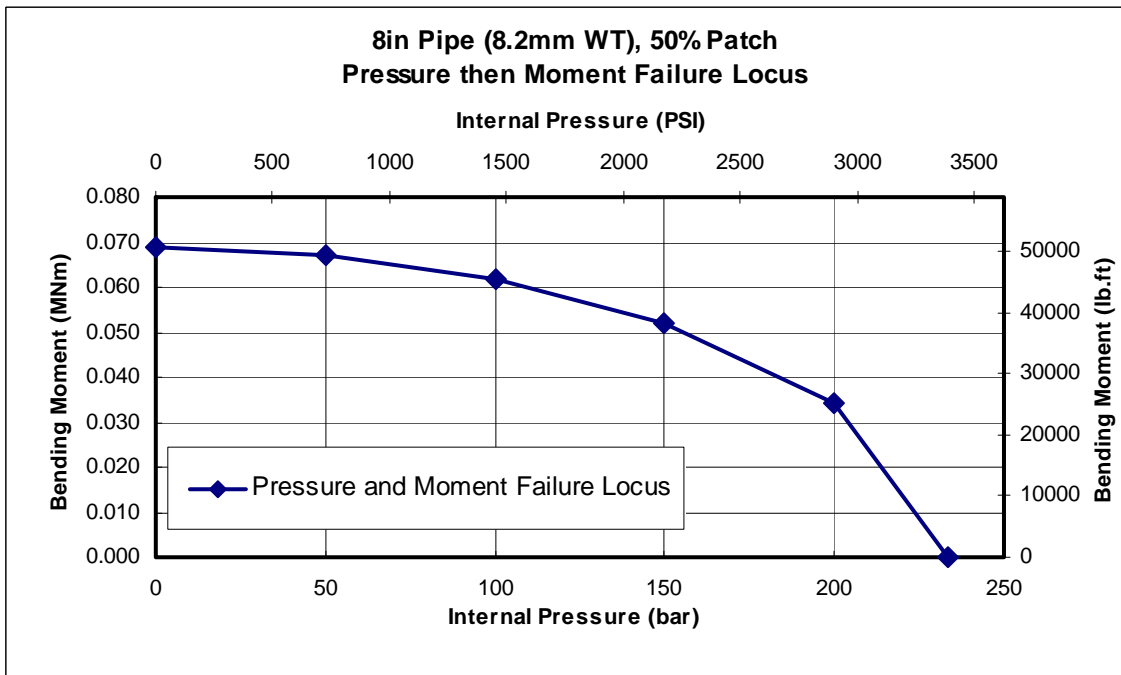
Figure B12. 203.2mm (8-inch) Diameter Grade B/X42 Pipe 50% Deep Patch. Moment-Pressure Failure Locus
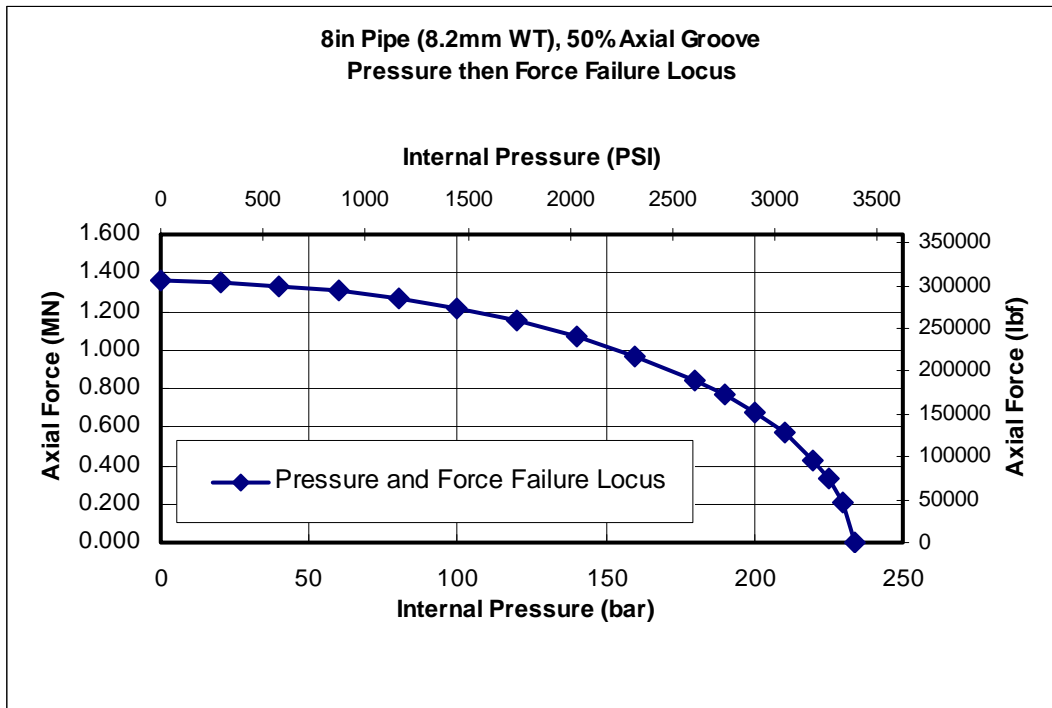
Figure B13. 203.2mm (8-inch) Diameter Grade B/X42 Pipe 50% Deep Axial Groove. Compressive Force-Pressure Failure Locus
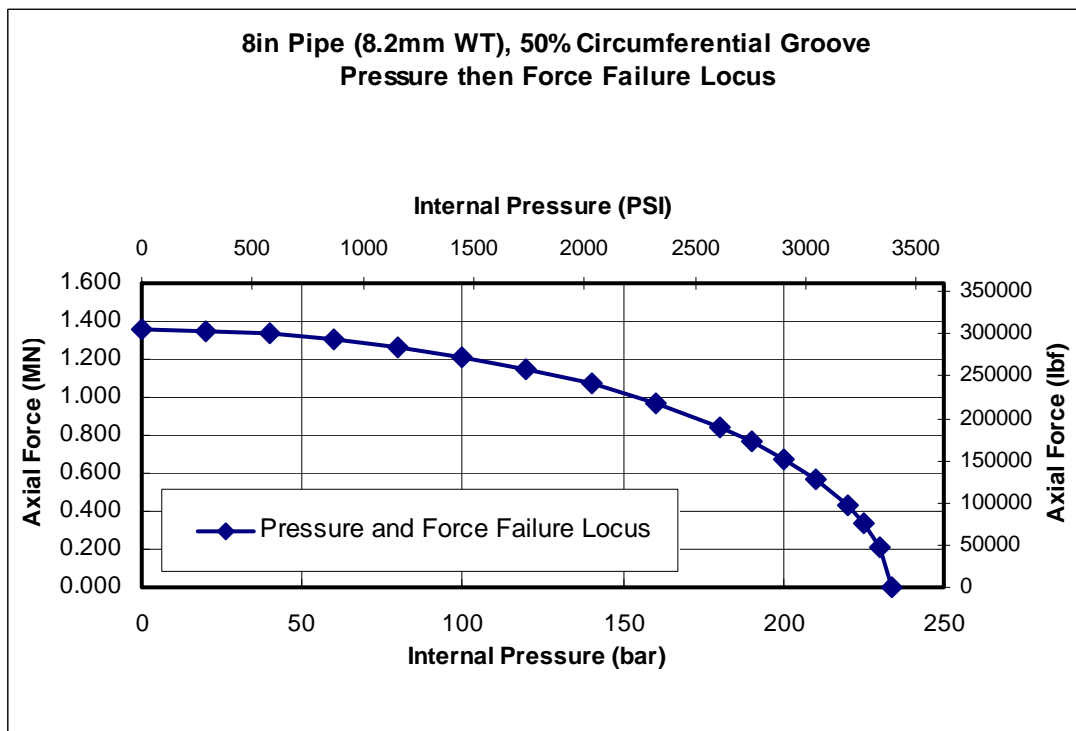
Figure B14. 203.2mm (8-inch) Diameter Grade B/X42 Pipe 50% Deep Circumferential Groove. Compressive Force-Pressure Failure Locus

8in Pipe (8.2mm WT), 50% Pit
Pressure then Force Failure Locus
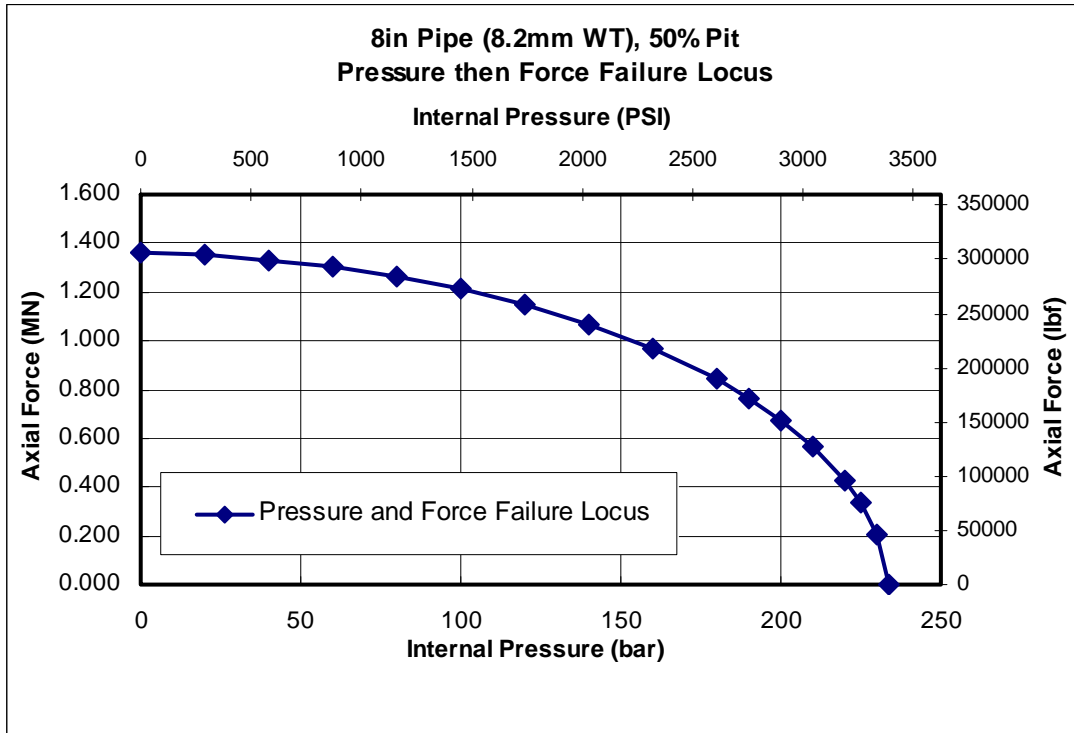
Figure B15. 203.2mm (8-inch) Diameter Grade B/X42 Pipe 50% Deep Pit. Compressive Force-Pressure Failure Locus

8in Pipe (8.2mm WT), 50% Patch
Pressure then Force Failure Locus
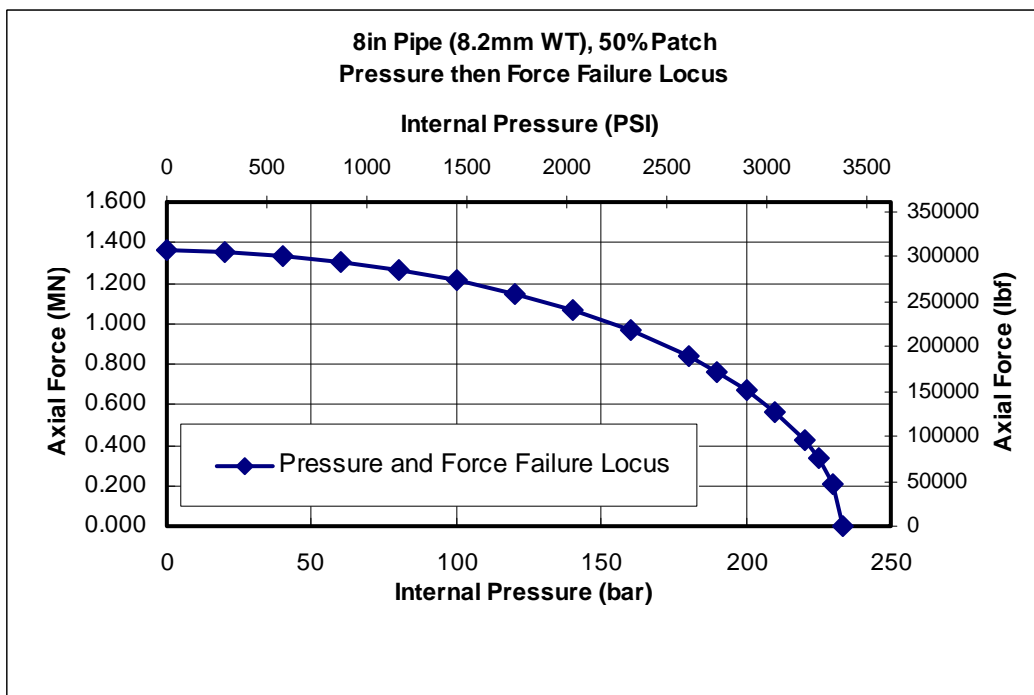
Figure B16. 203.2mm (8-inch) Diameter Grade B/X42 Pipe 50% Deep Patch. Compressive Force-Pressure Failure Locus
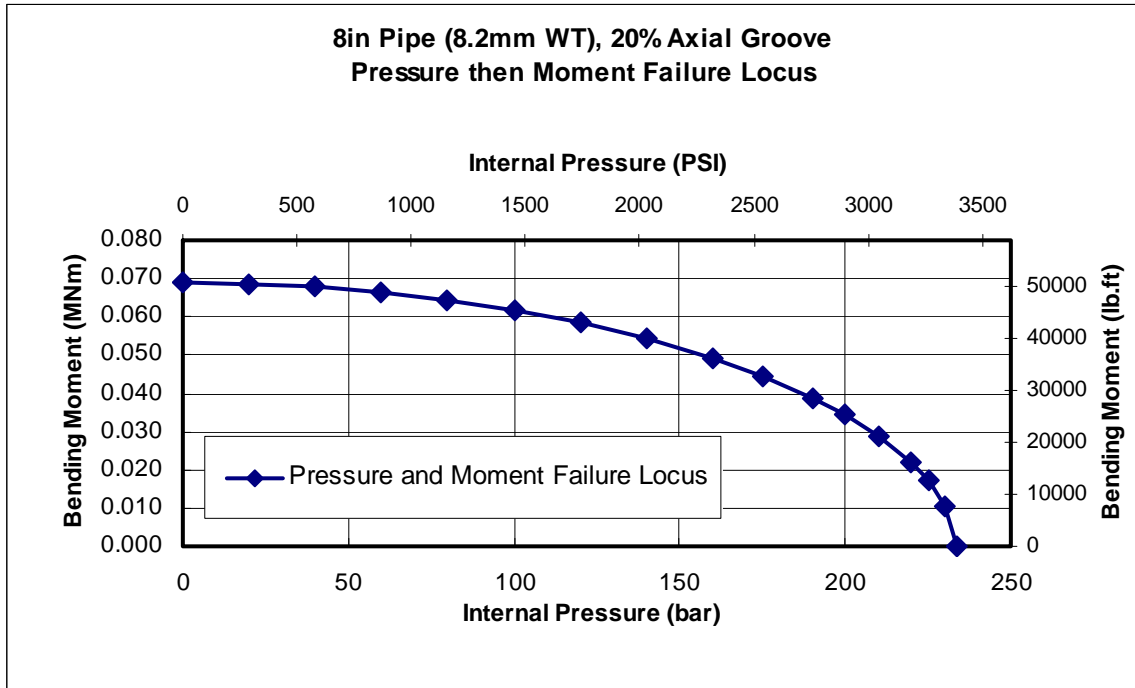
Figure B17. 203.2mm (8-inch) Diameter Grade B/X42 Pipe 20% Deep Axial Groove. Moment-Pressure Failure Locus
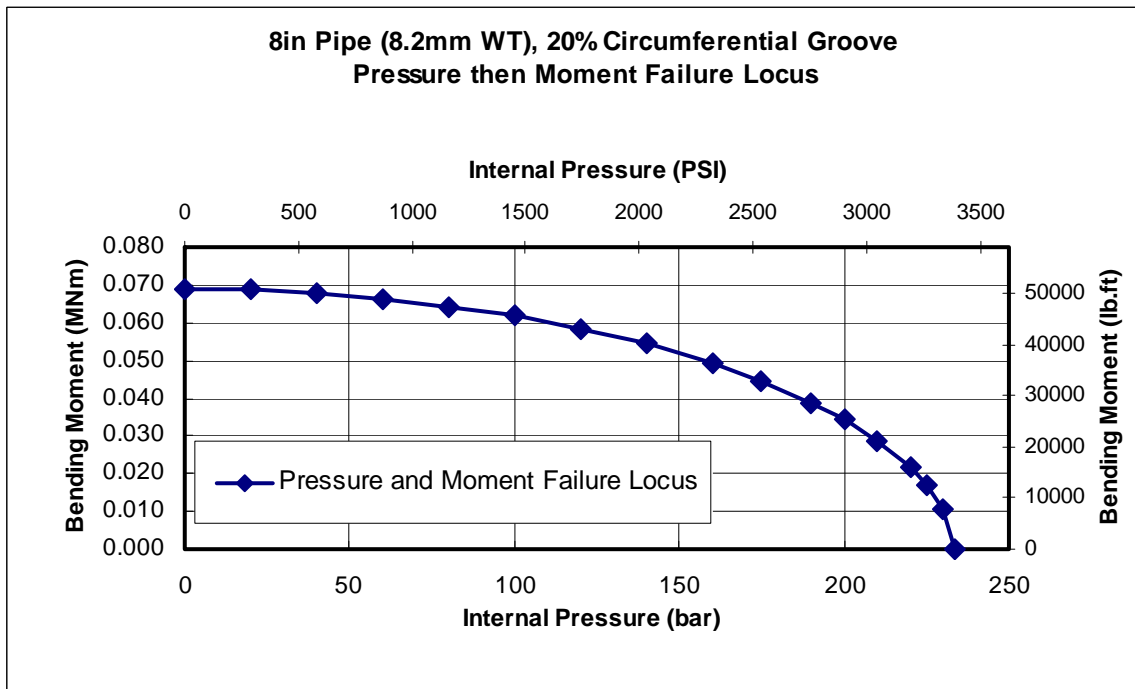
Figure B18. 203.2mm (8-inch) Diameter Grade B/X42 Pipe 20% Deep Circumferential Groove. Moment-Pressure Failure Locus
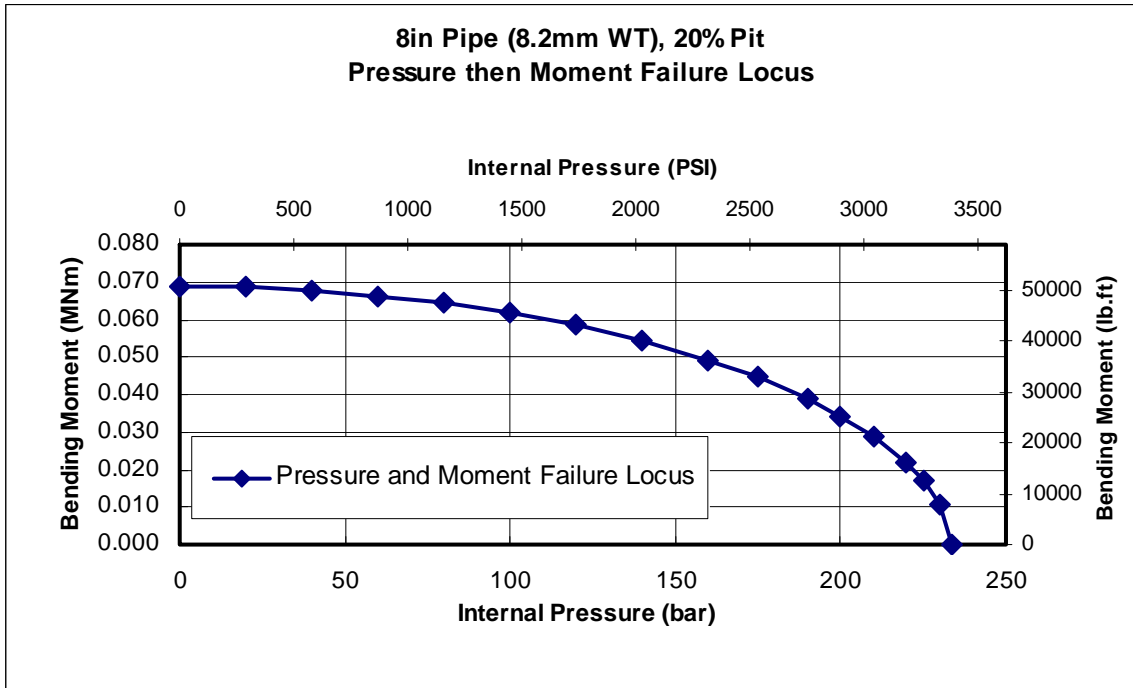
Figure B19. 203.2mm (8-inch) Diameter Grade B/X42 Pipe 20% Deep Pit. Moment-Pressure Failure Locus
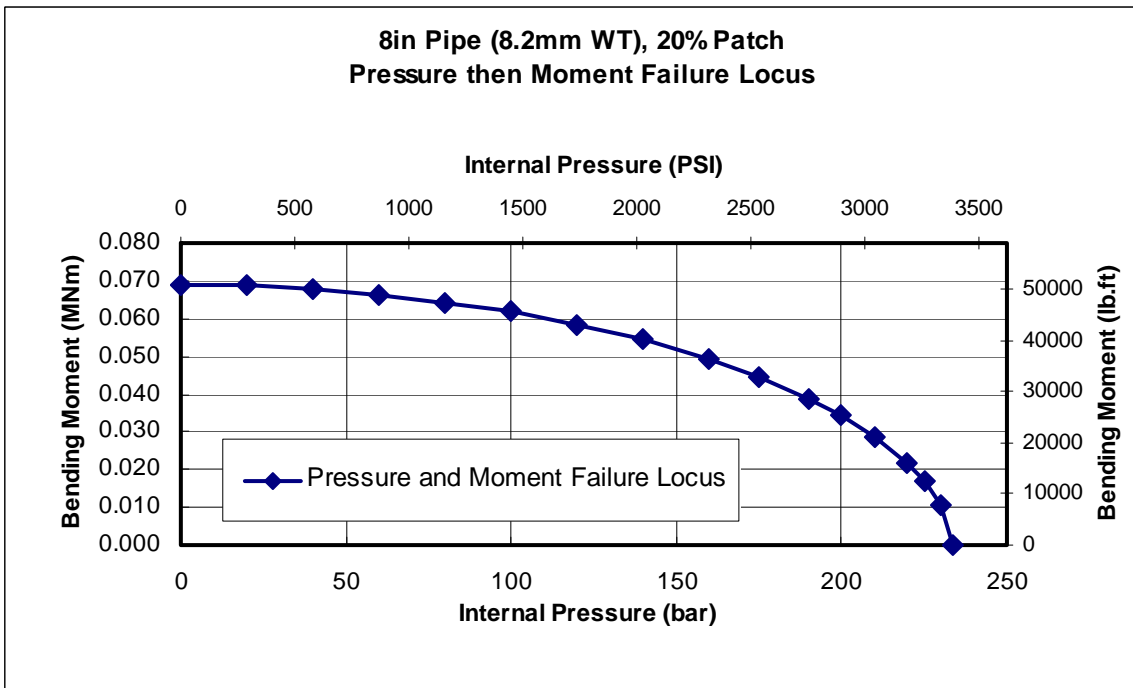

Figure B20. 203.2mm (8-inch) Diameter Grade B/X42 Pipe 20% Deep Patch. Moment-Pressure Failure Locus

8in Pipe (8.2mm WT), 20% Axial Groove
Pressure then Force Failure Locus
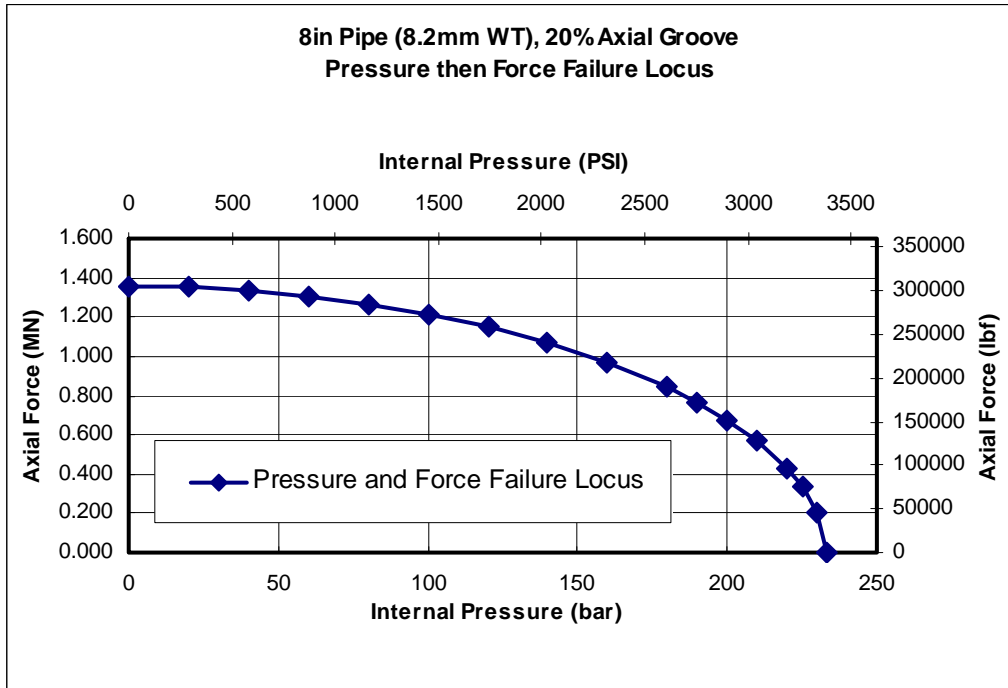
Figure B21. 203.2mm (8-inch) Diameter Grade B/X42 Pipe 20% Deep Axial Groove. Compressive Force-Pressure Failure Locus

8in Pipe (8.2mm WT), 20% Circumferential Groove
**Pressure then Force Failure Locus**
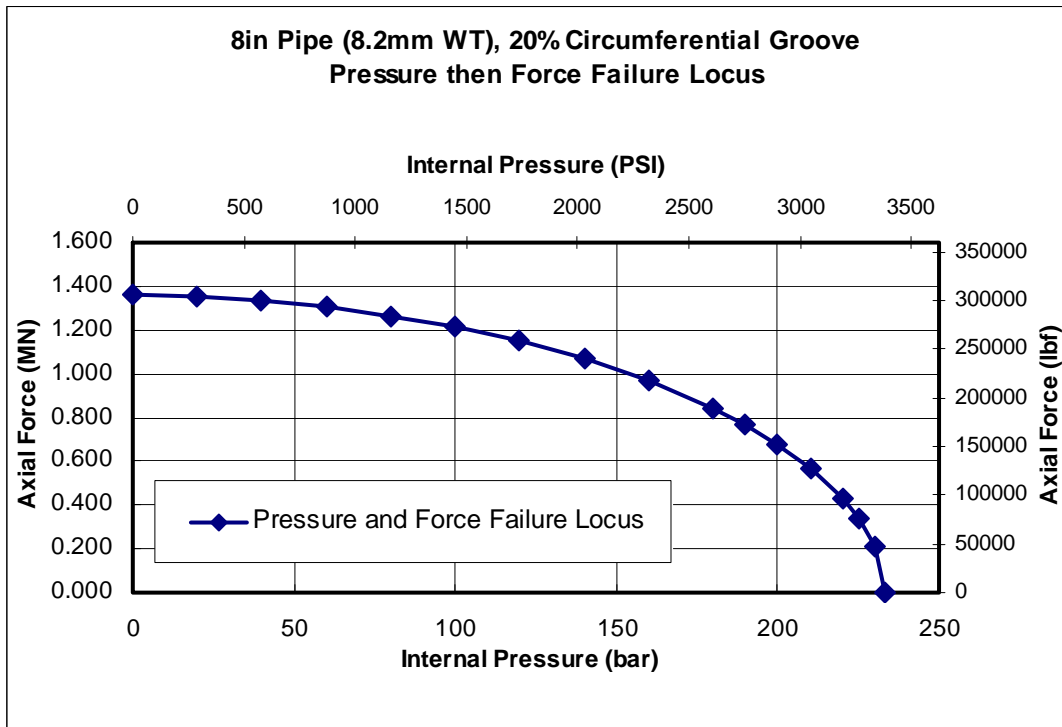
Figure B22. 203.2mm (8-inch) Diameter Grade B/X42 Pipe 20% Deep Circumferential Groove. Compressive Force-Pressure Failure Locus
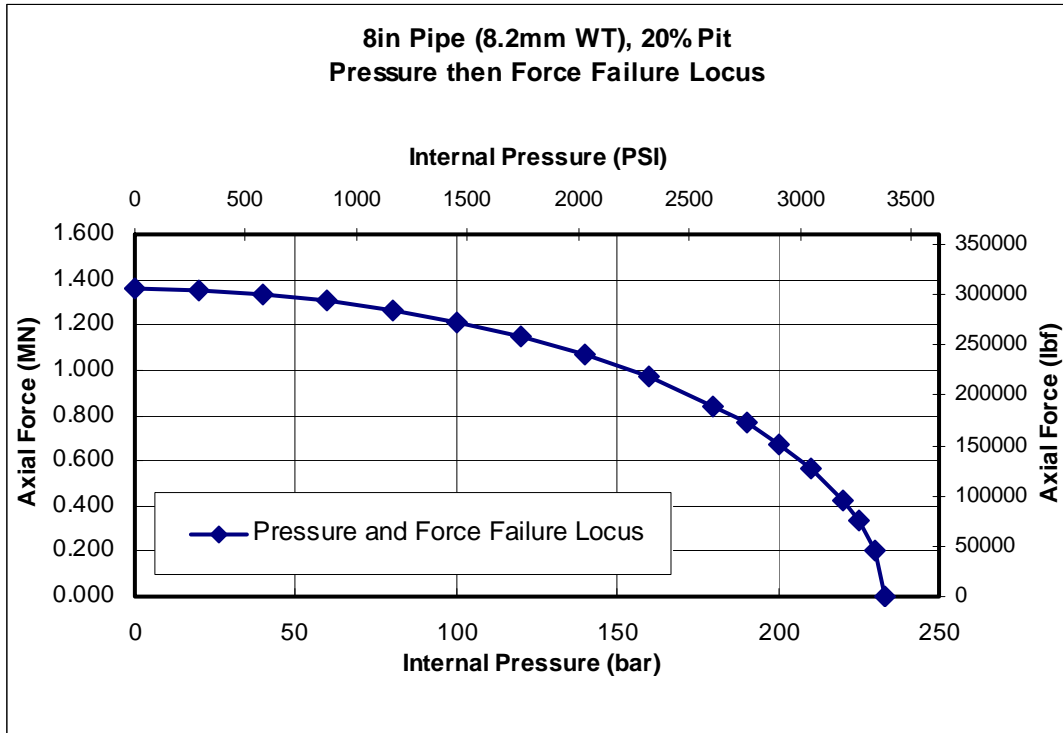
Figure B23. 203.2mm (8-inch) Diameter Grade B/X42 Pipe 20% Deep Pit. Compressive Force-Pressure Failure Locus
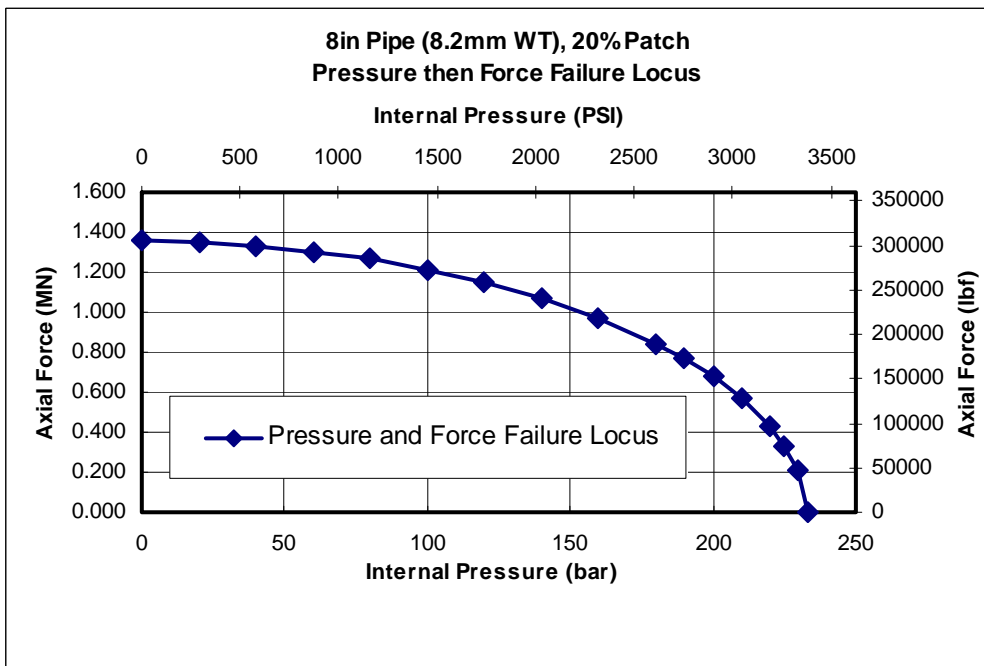

Figure B24. 203.2mm (8-inch) Diameter Grade B/X42 Pipe 20% Deep Patch. Compressive Force-Pressure Failure Locus

# Appendix C   457.2mm (18-Inch) Diameter Grade B/X42 Pipe Failure Loci

GL
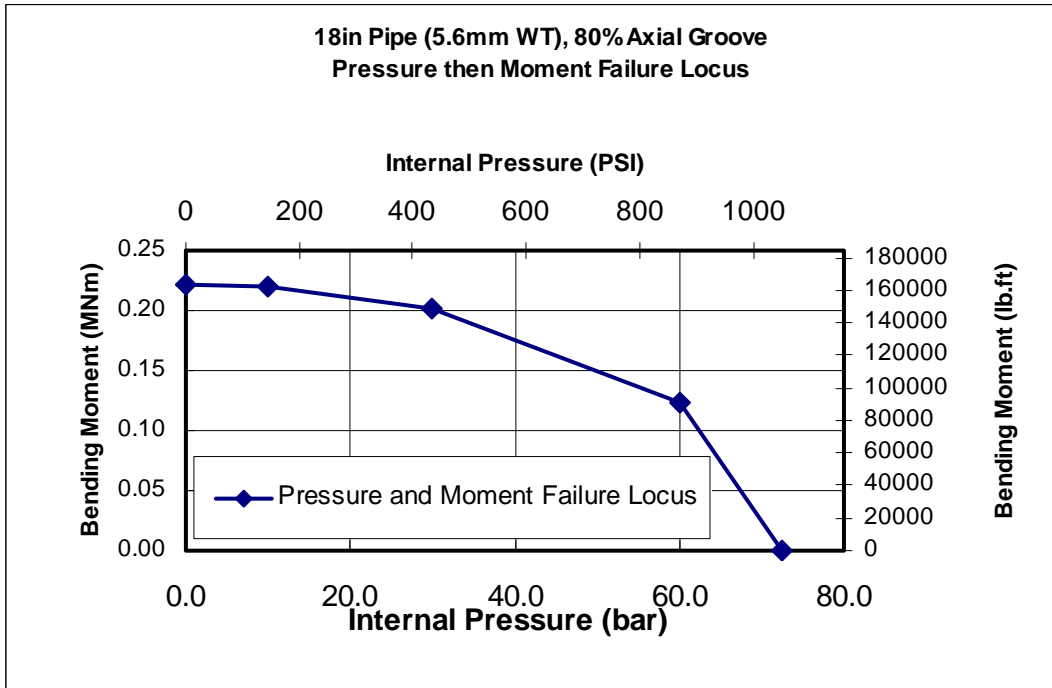
Figure C1. 457.2mm (18-inch) Diameter Grade B/X42 Pipe 80% Deep Axial Groove. Moment-Pressure Failure Locus
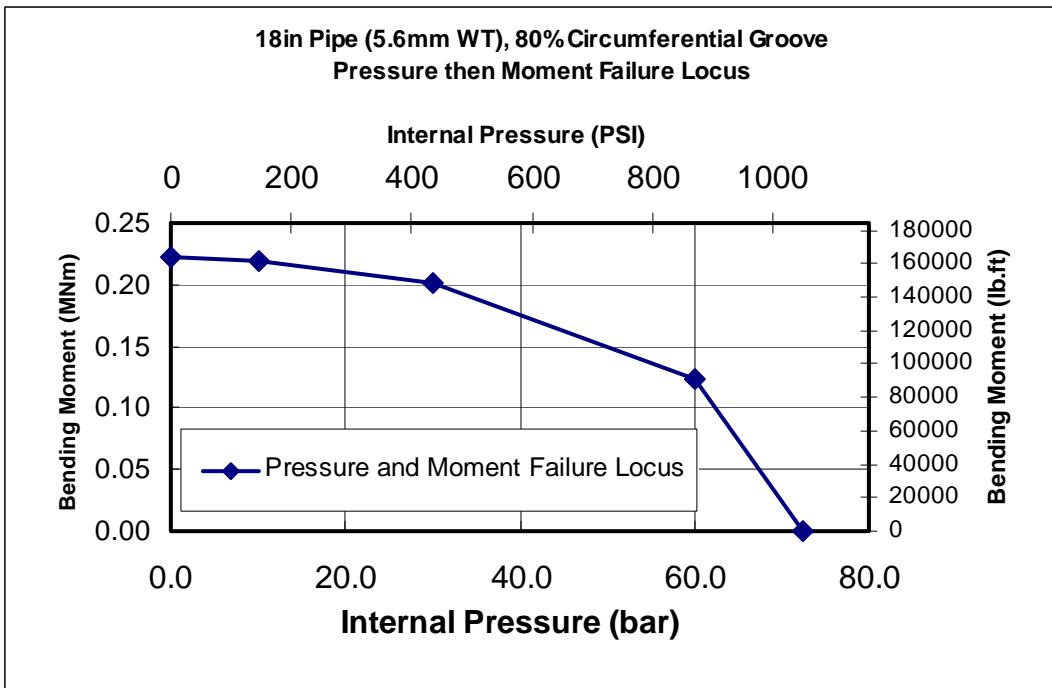
Figure C2. 457.2mm (18-inch) Diameter Grade B/X42 Pipe 80% Deep Circumferential Groove. Moment-Pressure Failure Locus

18in Pipe (5.6mm WT), 80%Pit
Pressure then Moment Failure Locus
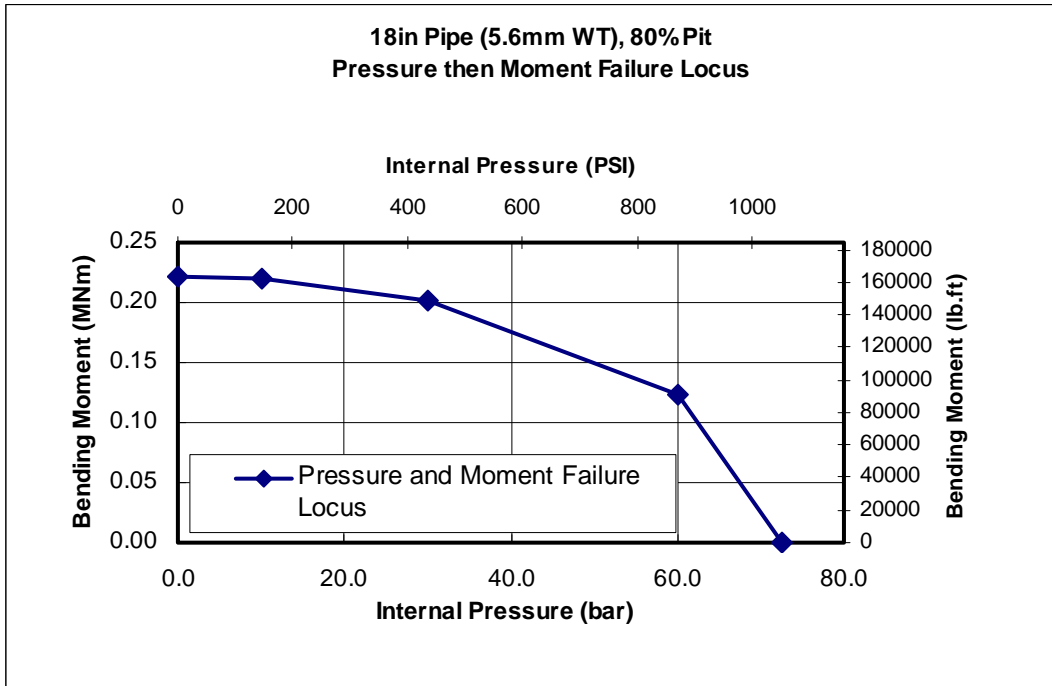
Figure C3. 457.2mm (18-inch) Diameter Grade B/X42 Pipe 80% Deep Pit. Moment-Pressure Failure Locus

18in Pipe (5.6mm WT), 80%Patch
Pressure then Moment Failure Locus
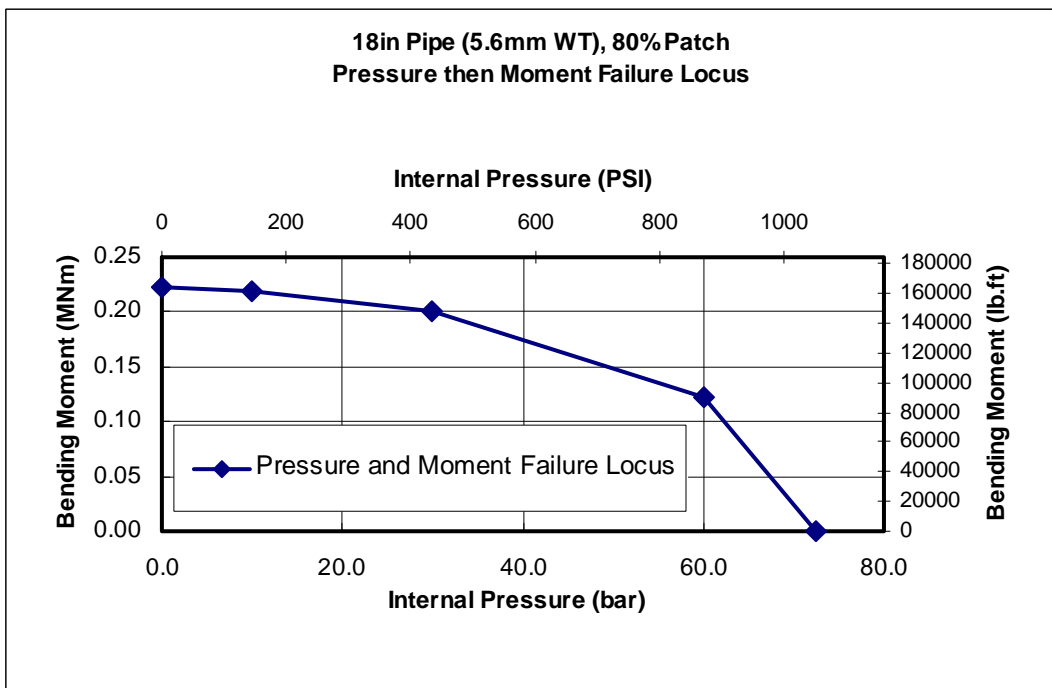
Figure C4. 457.2mm (18-inch) Diameter Grade B/X42 Pipe 80% Deep Patch. Moment-Pressure Failure Locus
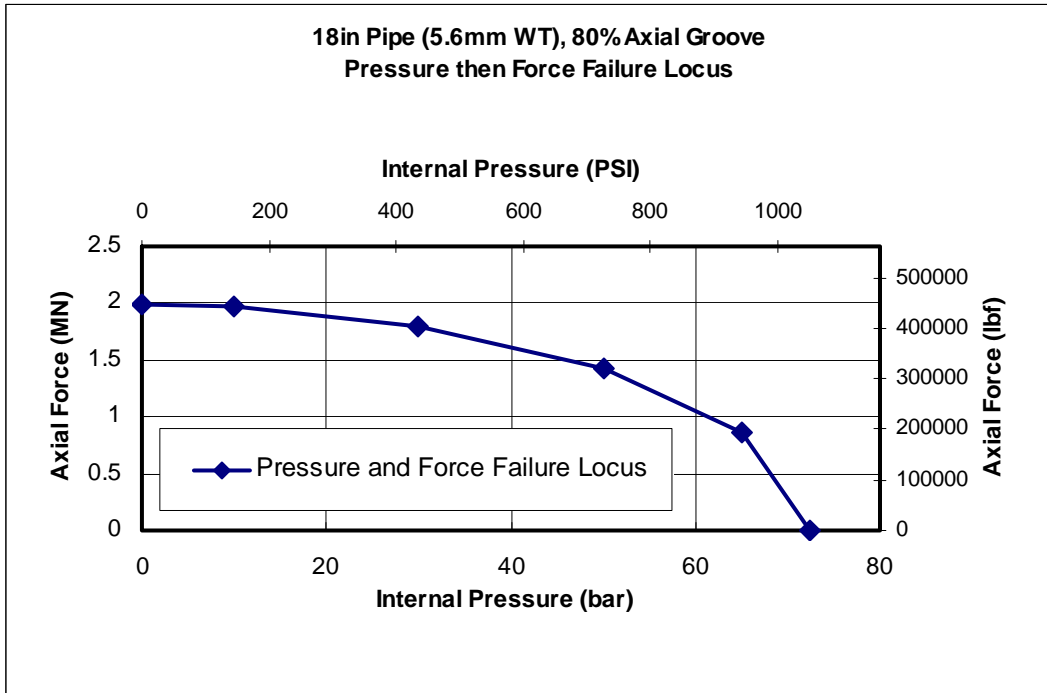
Figure C5. 457.2mm (18-inch) Diameter Grade B/X42 Pipe 80% Deep Axial Groove. Compressive Force-Pressure Failure Locus
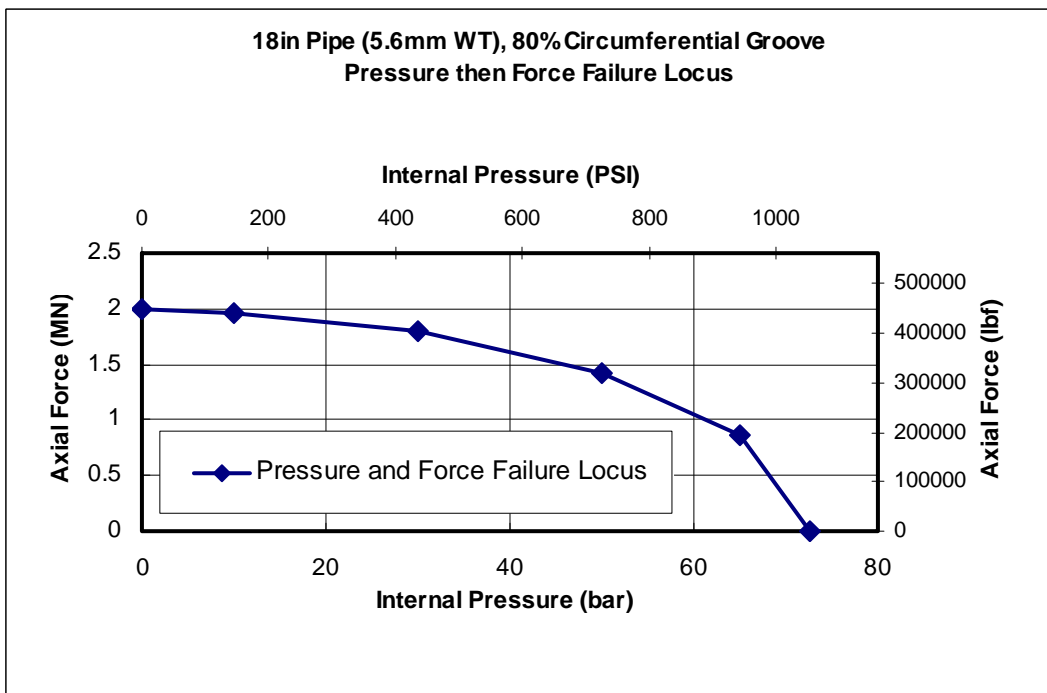
Figure C6. 457.2mm (18-inch) Diameter Grade B/X42 Pipe 80% Deep Circumferential Groove. Compressive Force-Pressure Failure Locus
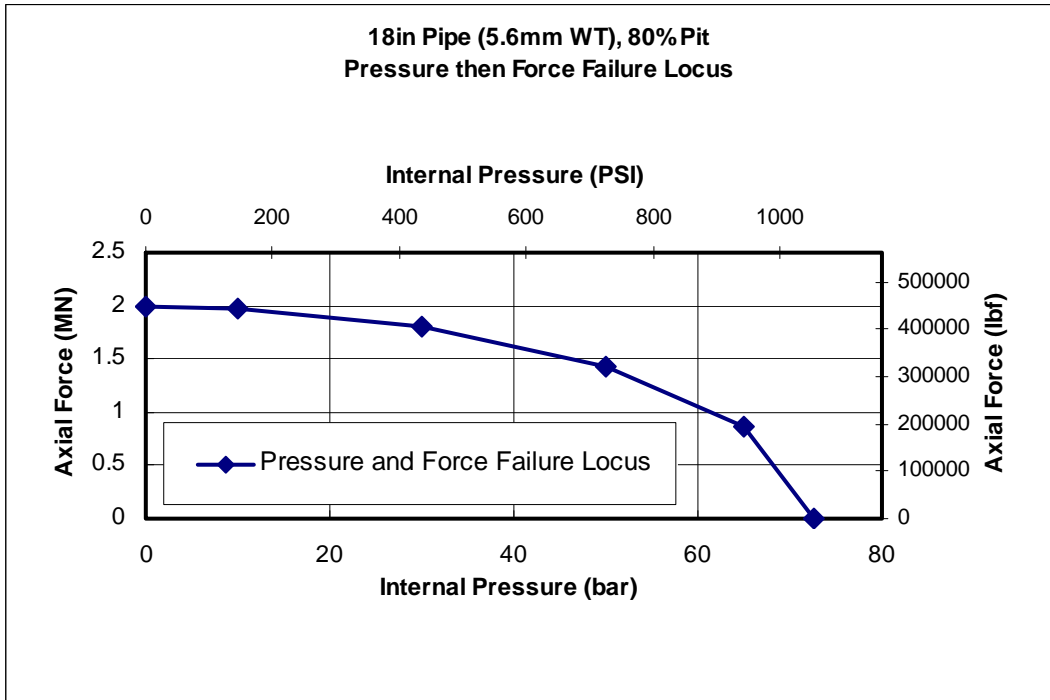
Figure C7. 457.2mm (18-inch) Diameter Grade B/X42 Pipe 80% Deep Pit. Compressive Force-Pressure Failure Locus
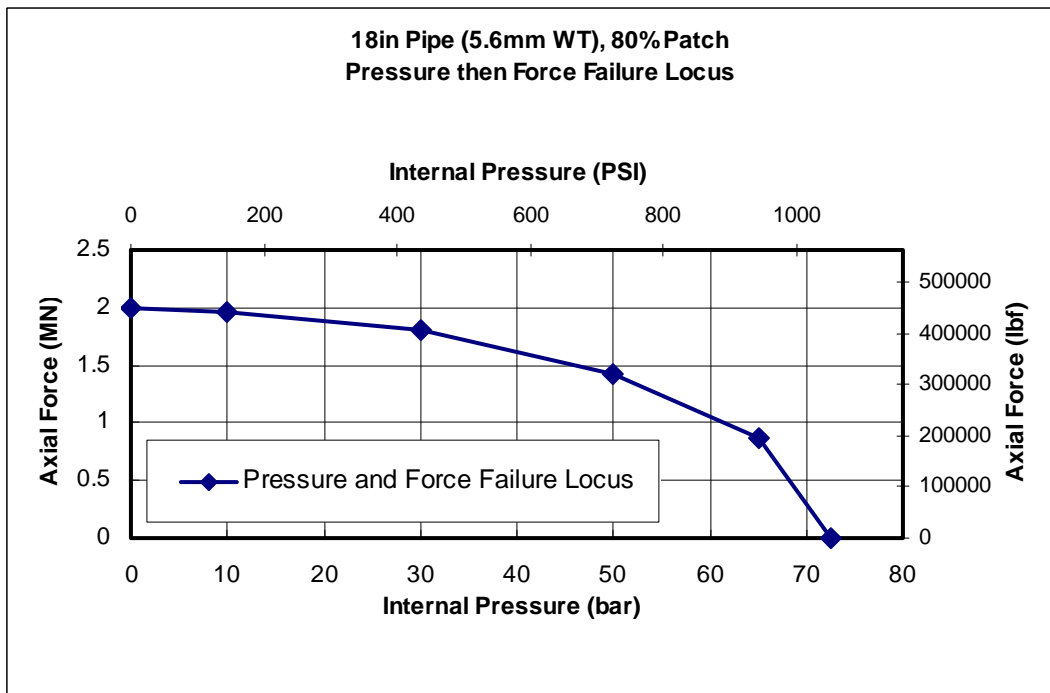
Figure C8. 457.2mm (18-inch) Diameter Grade B/X42 Pipe 80% Deep Patch. Compressive Force-Pressure Failure Locus
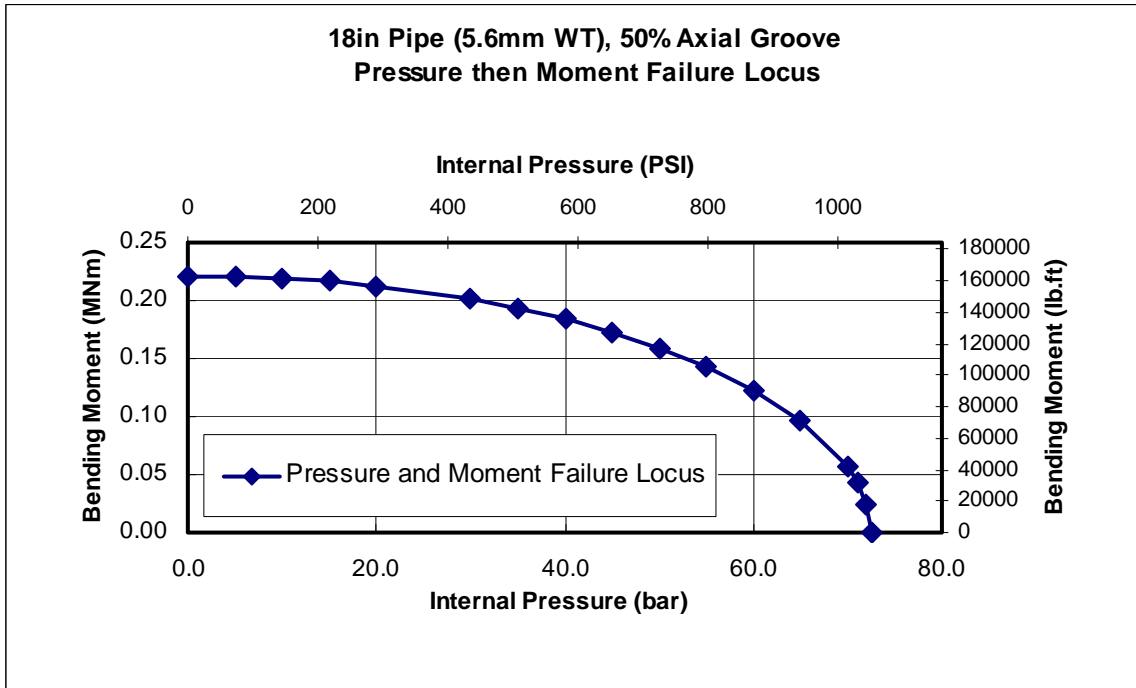
Figure C9. 457.2mm (18-inch) Diameter Grade B/X42 Pipe 20%/50% Deep Axial Groove. Moment-Pressure Failure Locus
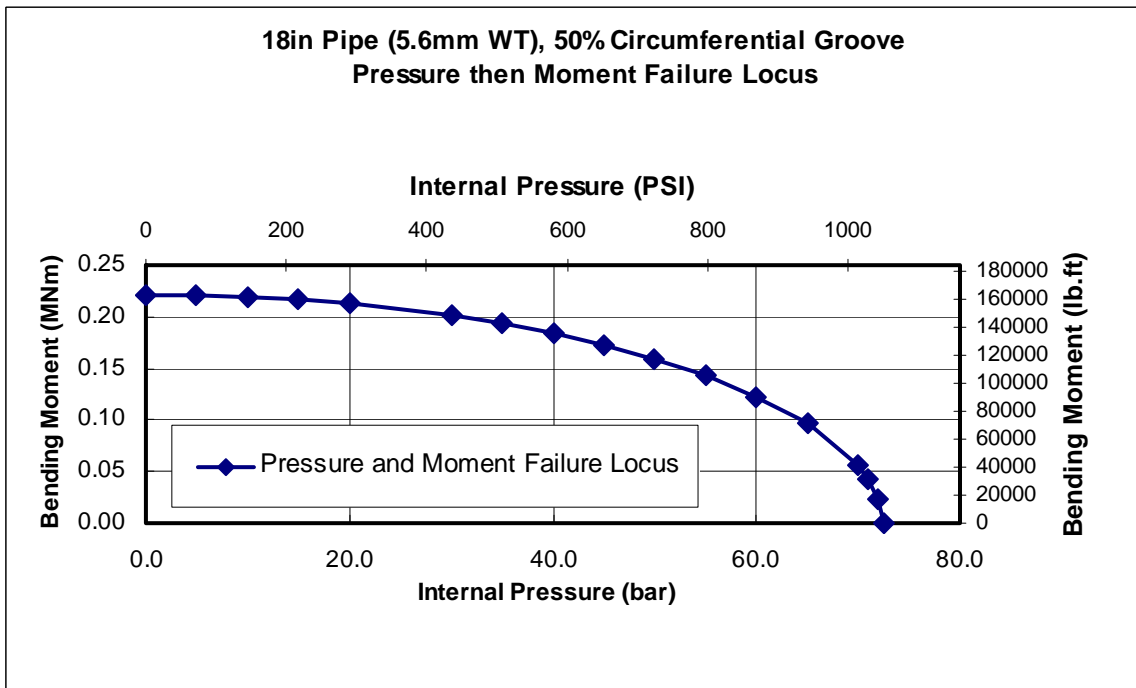
Figure C10. 457.2mm (18-inch) Diameter Grade B/X42 Pipe 20%/50% Deep Circumferential Groove. Moment-Pressure Failure Locus

18in Pipe (5.6mm WT), 50% Patch
Pressure then Moment Failure Locus
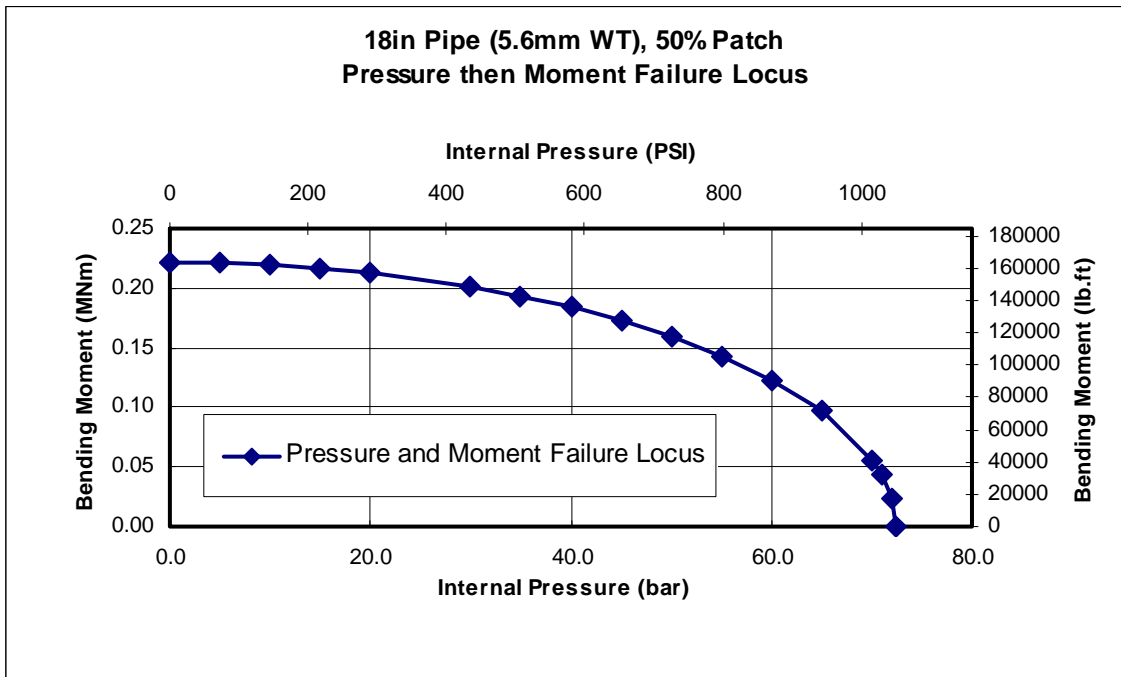
Figure C11. 457.2mm (18-inch) Diameter Grade B/X42 Pipe 20%/50% Deep Patch. Moment-Pressure Failure Locus

18in Pipe (5.6mm WT), 50% Axial Groove
Pressure then Force Failure Locus
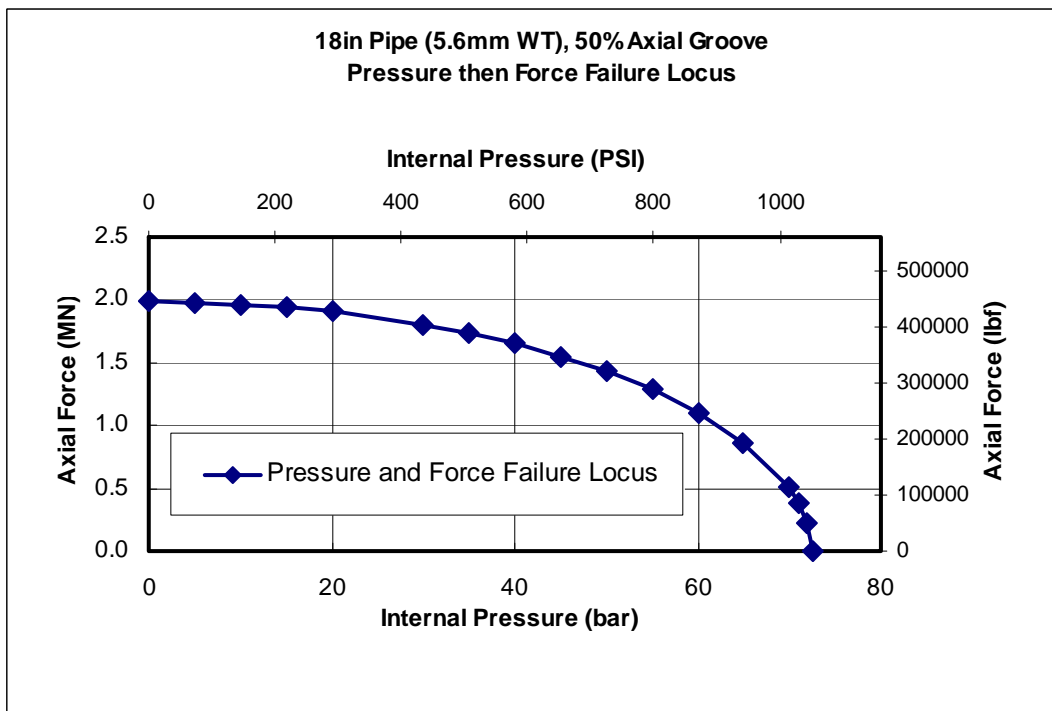
Figure C12. 457.2mm (18-inch) Diameter Grade B/X42 20%/50% Deep Axial Groove. Compressive Force-Pressure Failure Locus
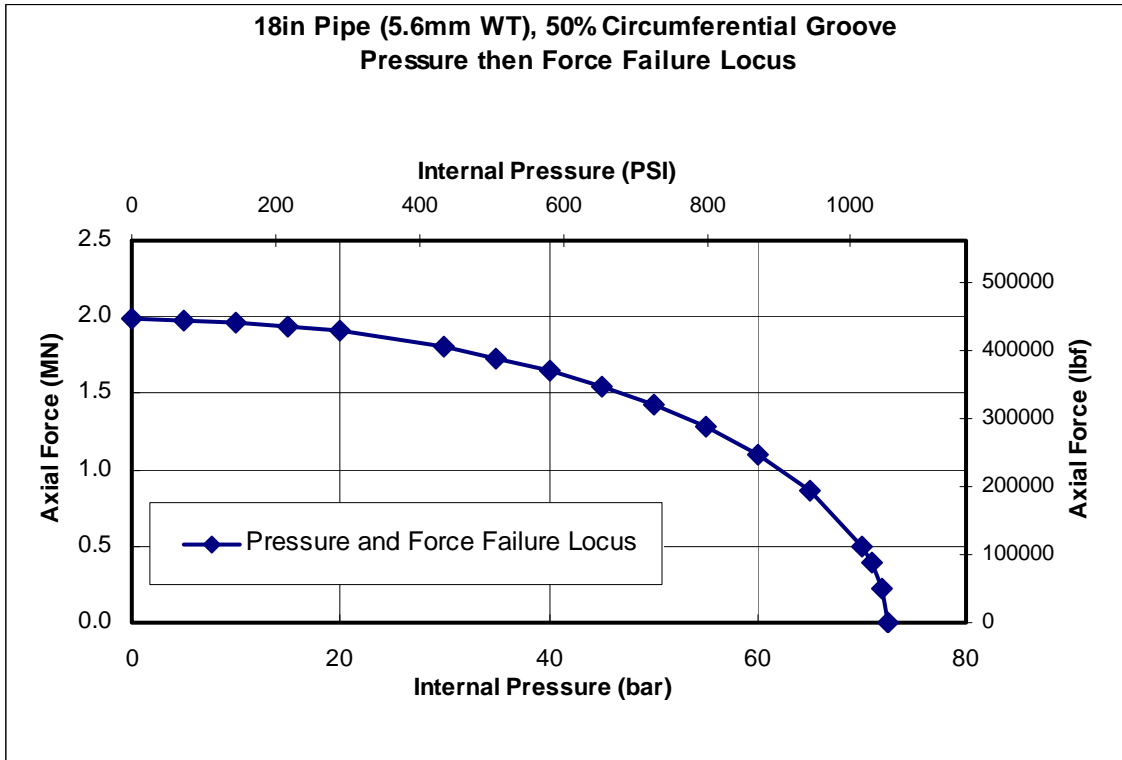
Figure C13. 457.2mm (18-inch) Diameter Grade B/X42 Pipe. 20%/50% Deep Circumferential Groove. Compressive Force-Pressure Failure Locus
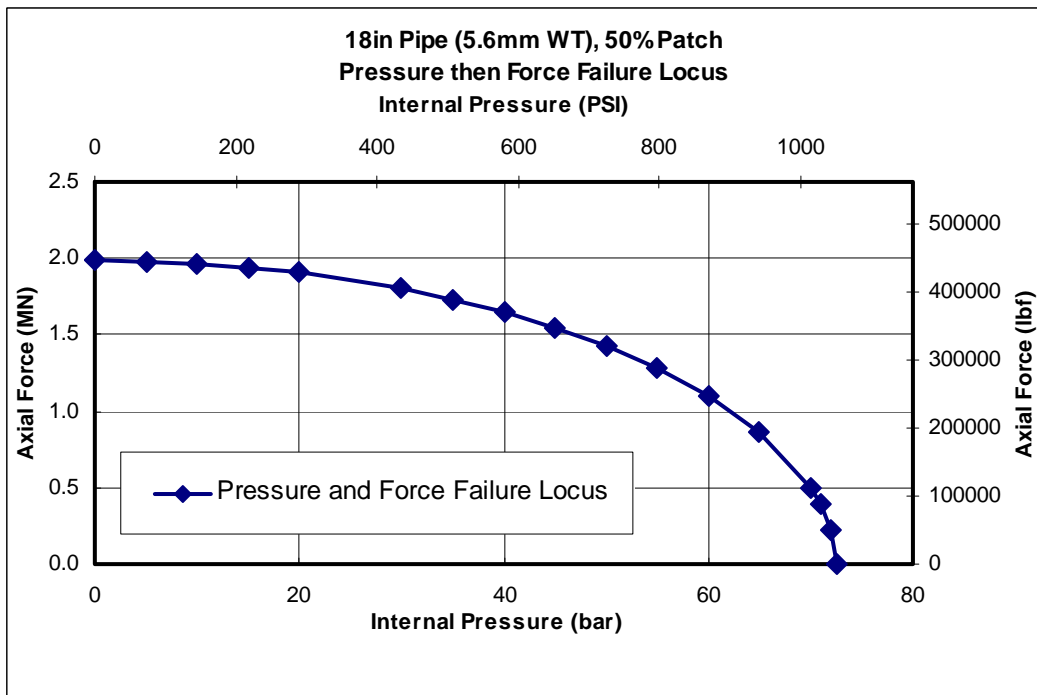
Figure C14. 457.2mm (18-inch) Diameter Grade B/X42 Pipe. 20%/50% Deep Patch. Compressive Force-Pressure Failure Locus

## Appendix D   914.4mm (36-Inch) Diameter Grade X65 Pipe Failure Loci
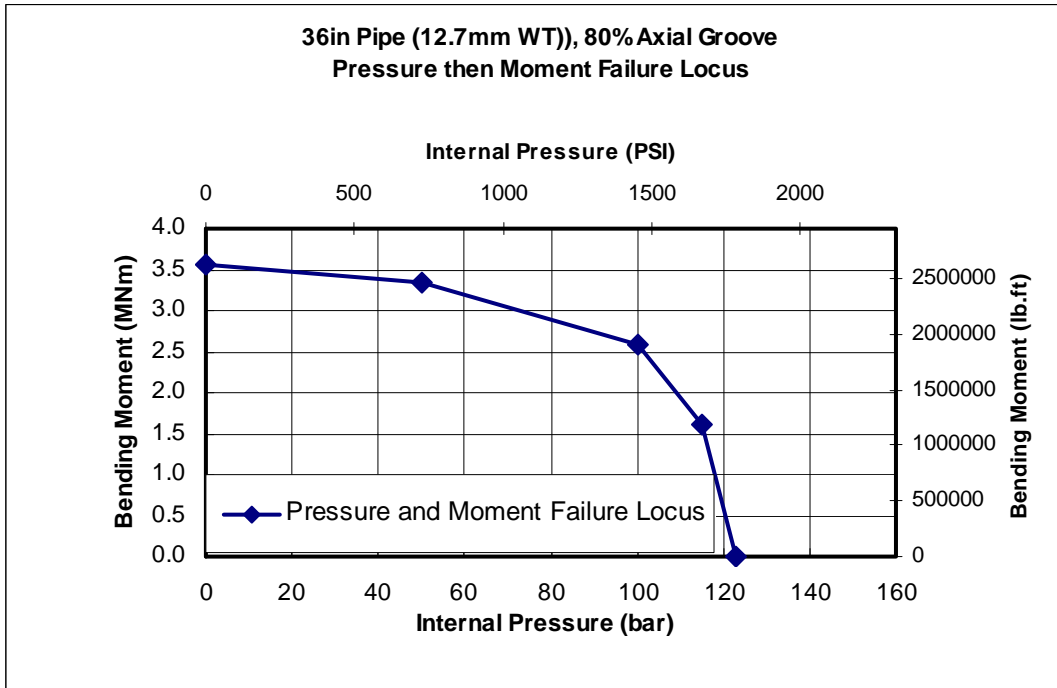
Figure D1. 914.4mm (36-inch) Diameter Grade X65 Pipe. 80% Deep Axial Groove. Moment-Pressure Failure Locus
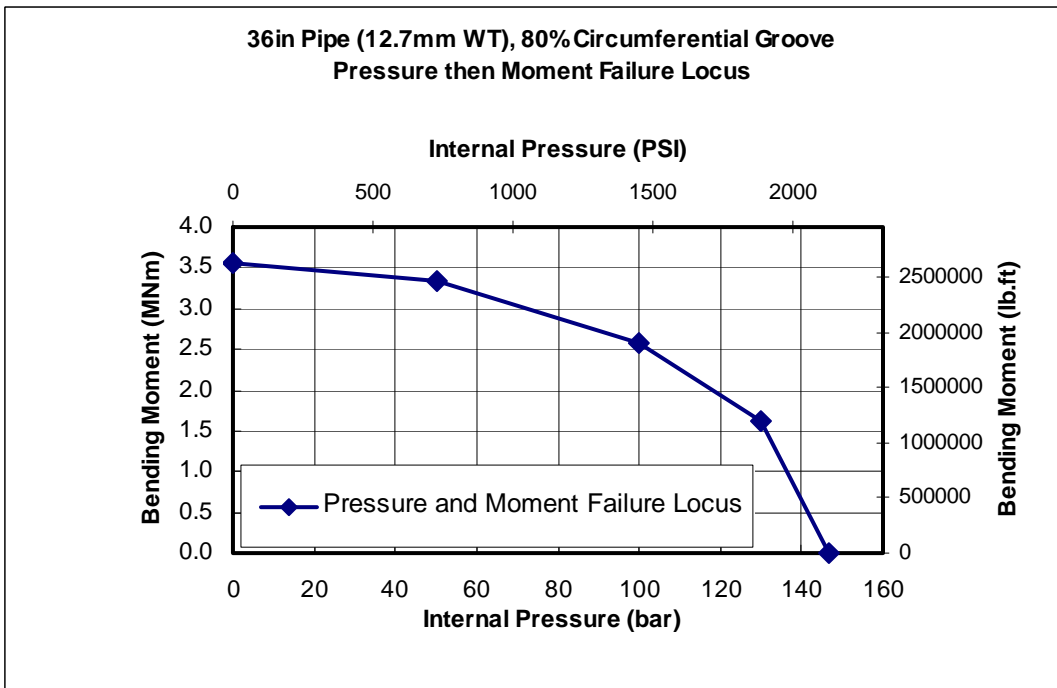
Figure D2. 914.4mm (36-inch) Diameter Grade X65 Pipe. 80% Deep Circumferential Groove. Moment-Pressure Failure Locus
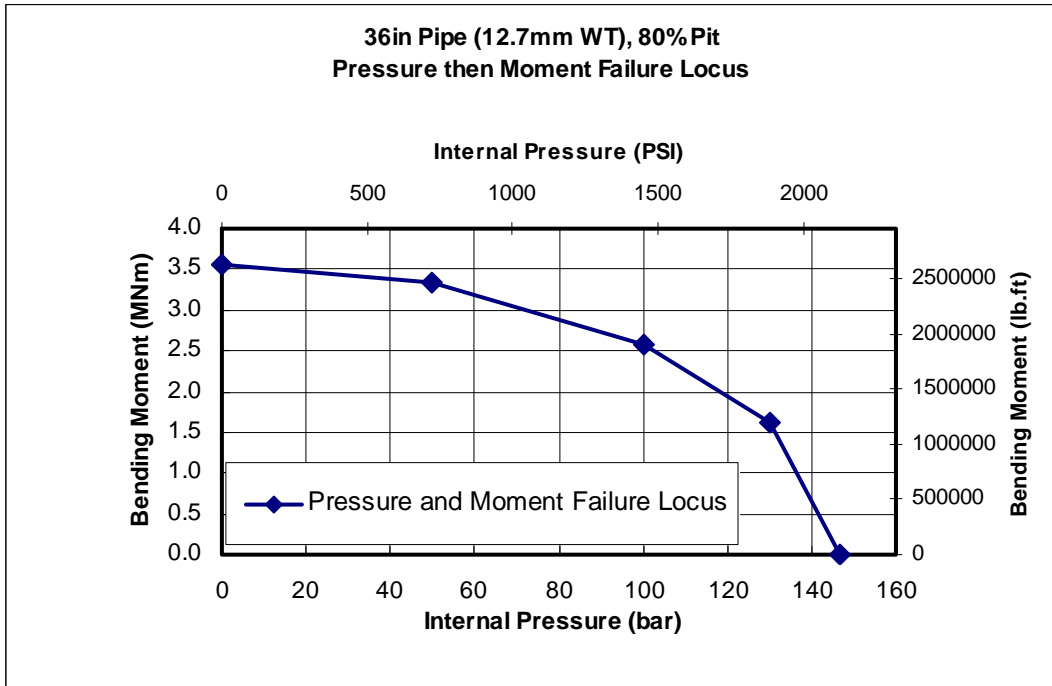
Figure D3. 914.4mm (36-inch) Diameter Grade X65 Pipe. 80% Deep Pit. Moment-Pressure Failure Locus
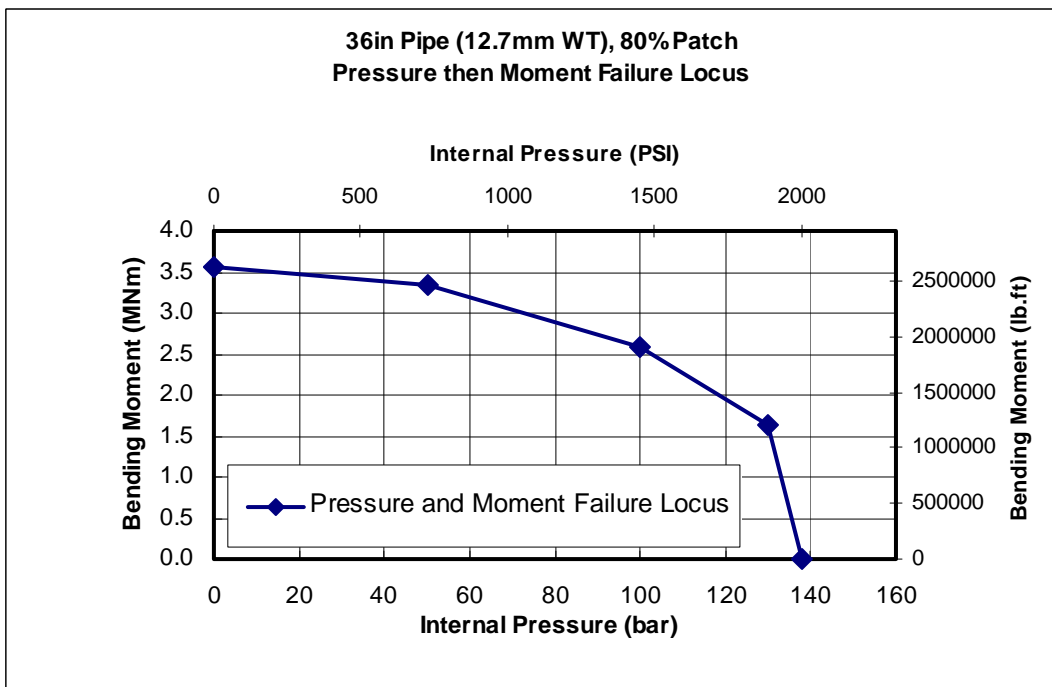

Figure D4. 914.4mm (36-inch) Diameter Grade X65 Pipe. 80% Deep Patch. Moment-Pressure Failure Locus
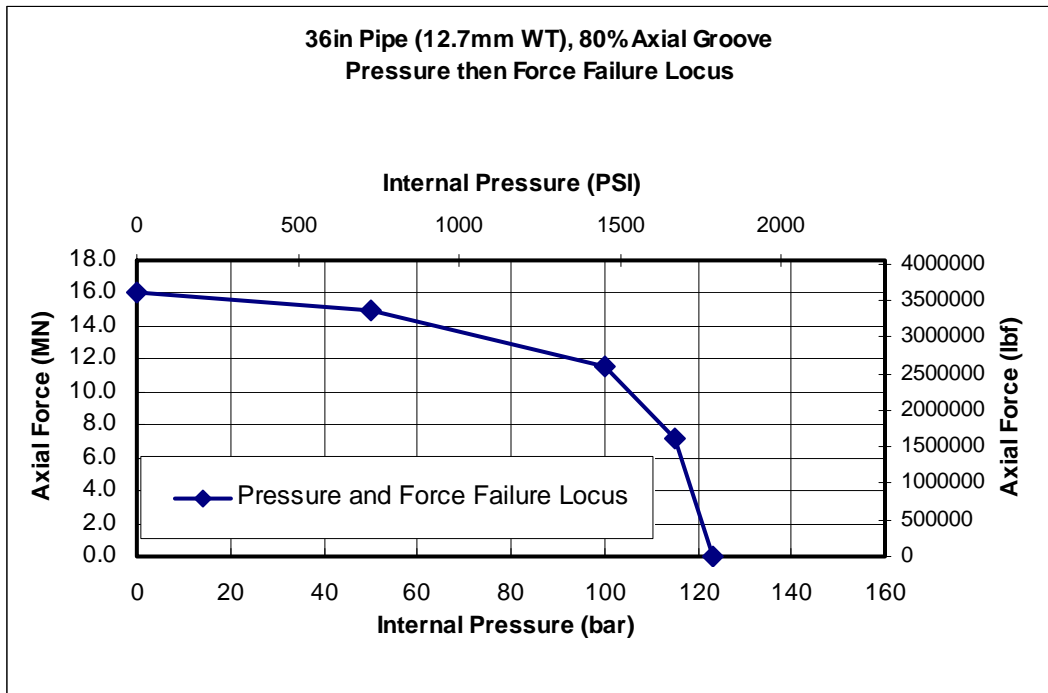
Figure D5. 914.4mm (36-inch) Diameter Grade X65 Pipe. 80% Deep Axial Groove. Compressive Force-Pressure Failure Locus
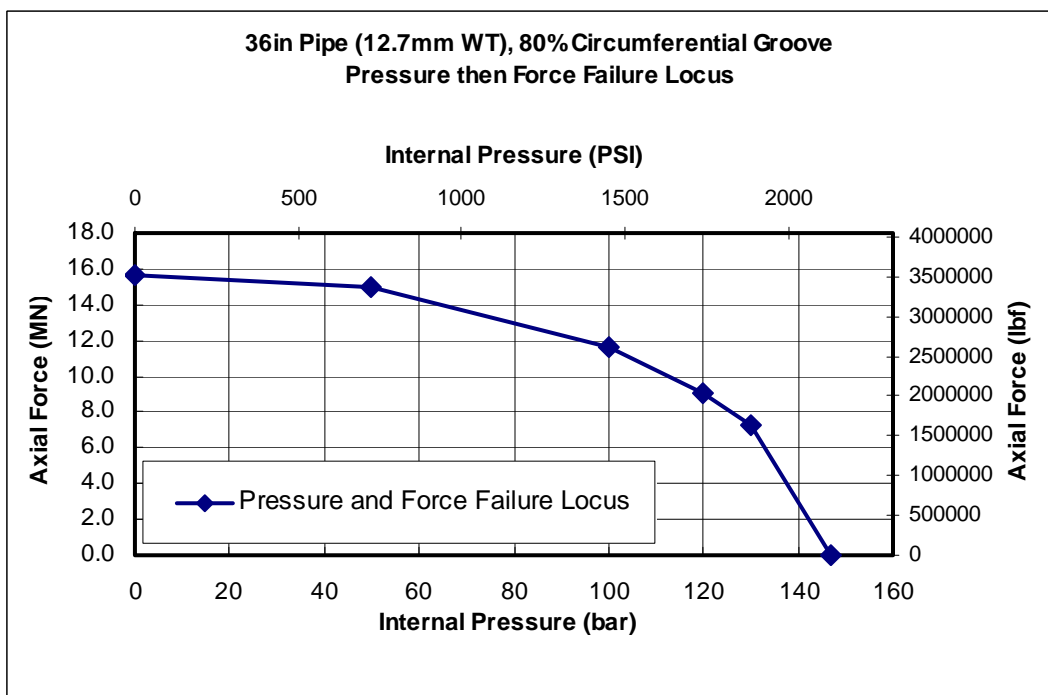

Figure D6. 914.4mm (36-inch) Diameter Grade X65 Pipe. 80% Deep Circumferential Groove. Compressive Force-Pressure Failure Locus
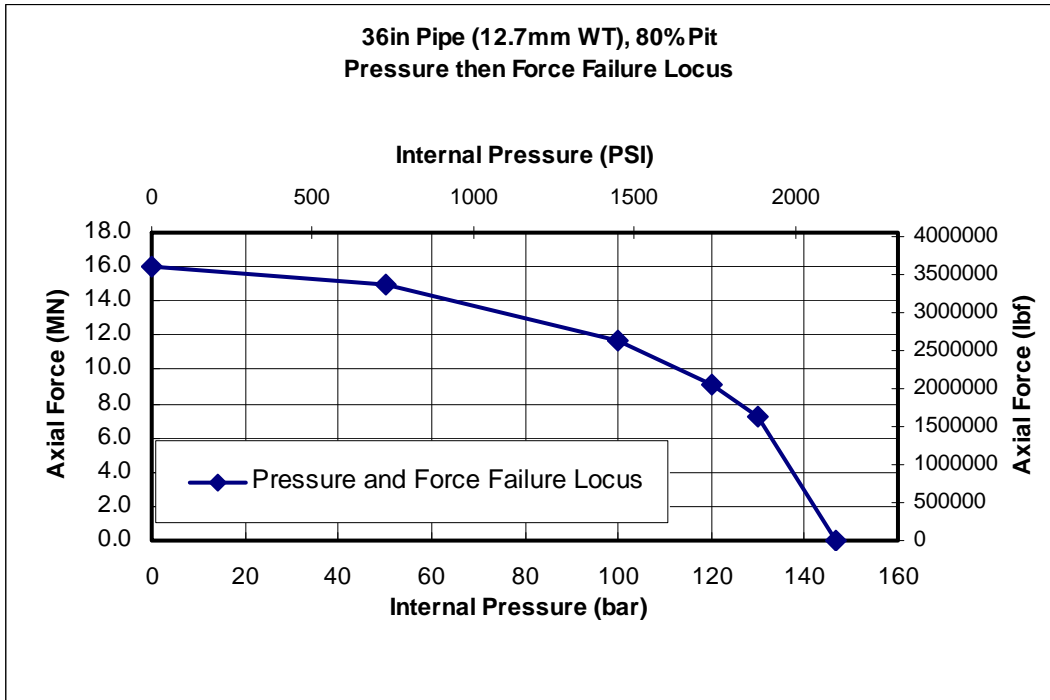
Figure D7. 914.4mm (36-inch) Diameter Grade X65 Pipe. 80% Deep Pit. Compressive Force-Pressure Failure Locus
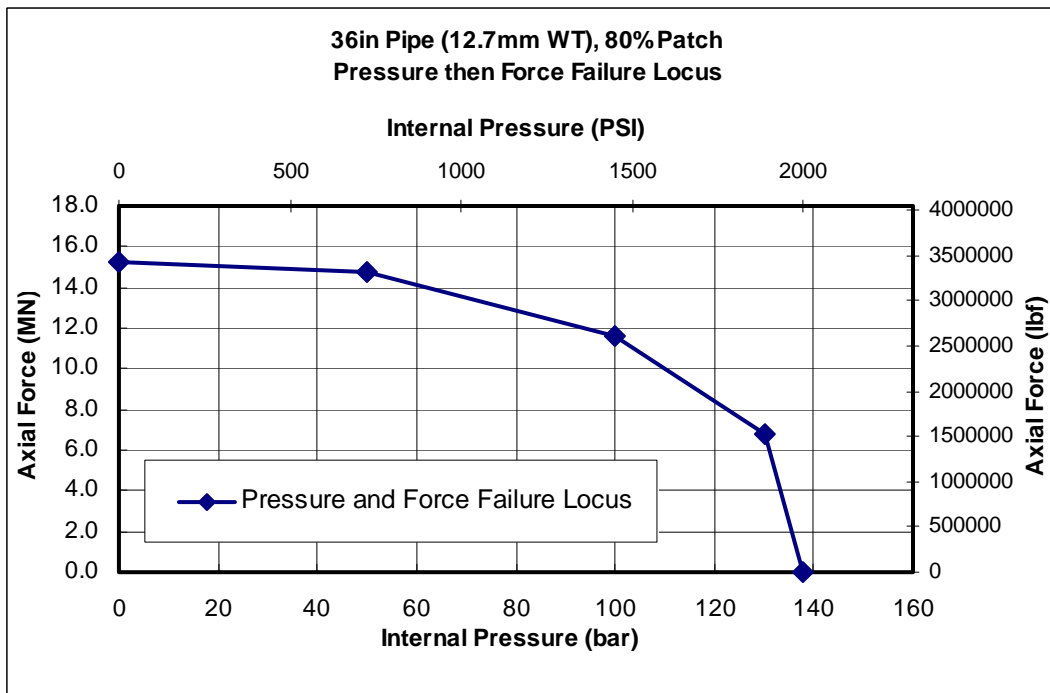

Figure D8. 914.4mm (36-inch) Diameter Grade X65 Pipe. 80% Deep Patch. Compressive Force-Pressure Failure Locus
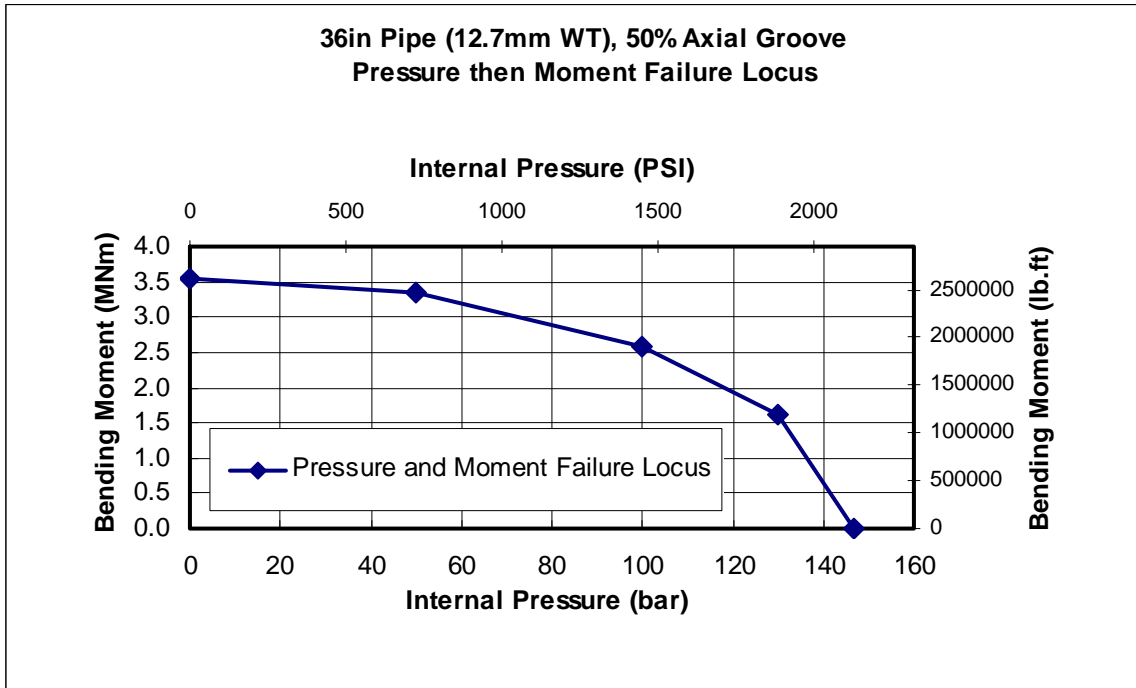
Figure D9. 914.4mm (36-inch) Diameter Grade X65 Pipe. 20%/50% Deep Axial Groove. Moment-Pressure Failure Locus
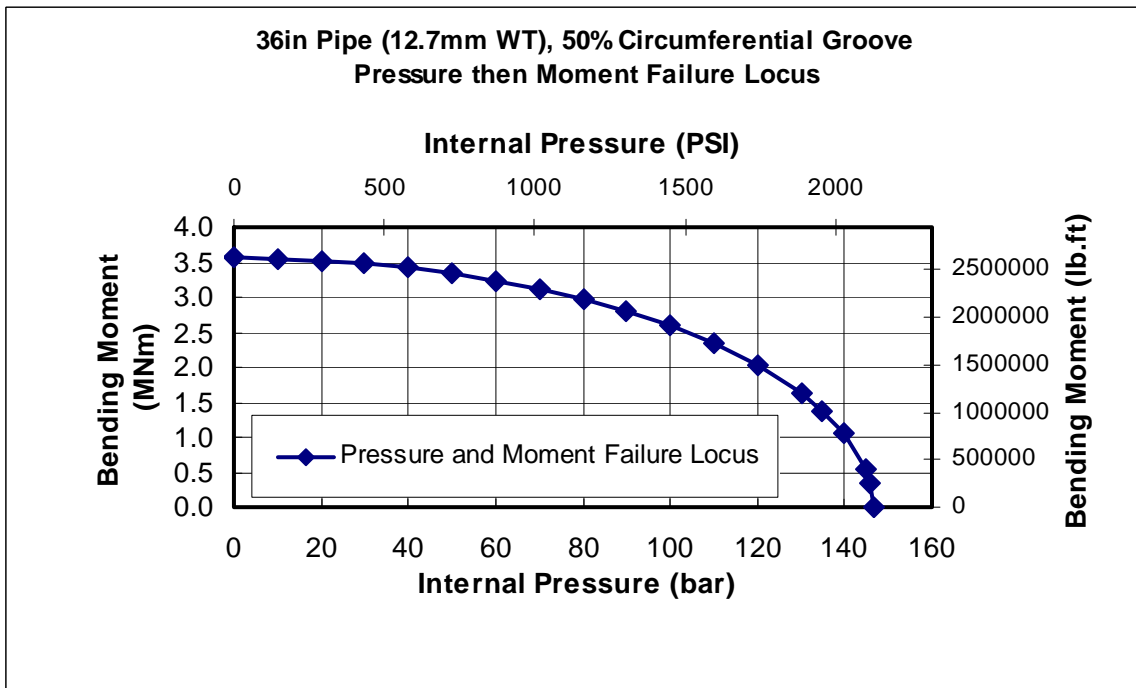
Figure D10. 914.4mm (36-inch) Diameter Grade X65 Pipe. 20%/50% Deep Circumferential Groove. Moment-Pressure Failure Locus

36in Pipe (12.7mm WT), 50% Patch
Pressure then Moment Failure Locus
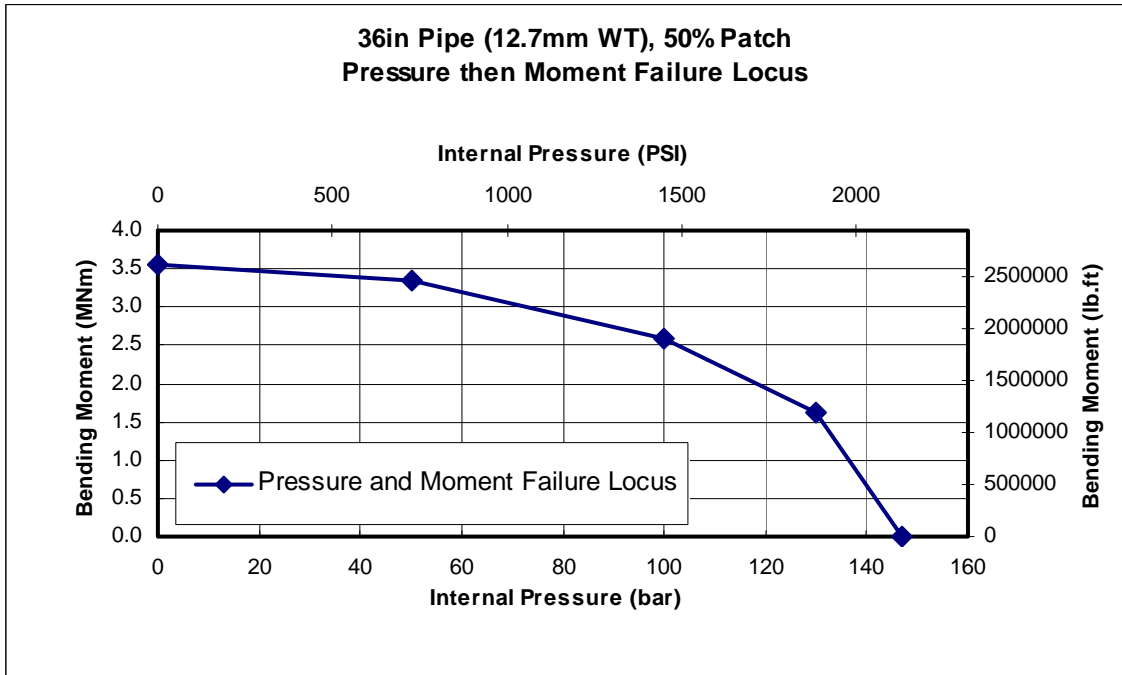
Figure D11. 914.4mm (36-inch) Diameter Grade X65 Pipe. 20%/50% Deep Patch. Moment-Pressure Failure Locus

36in Pipe (12.7mm WT), 50% Axial Groove
Pressure then Force Failure Locus
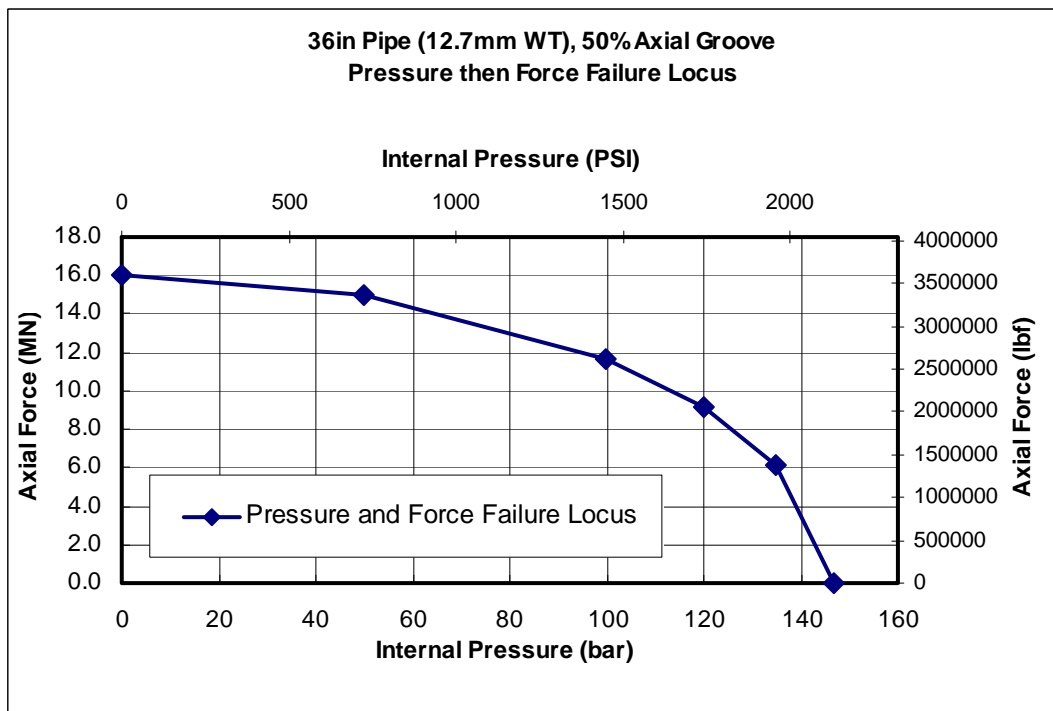
Figure D12. 914.4mm (36-inch) Diameter Grade X65 Pipe. 20%/50% Deep Axial Groove. Compressive Force-Pressure Failure Locus
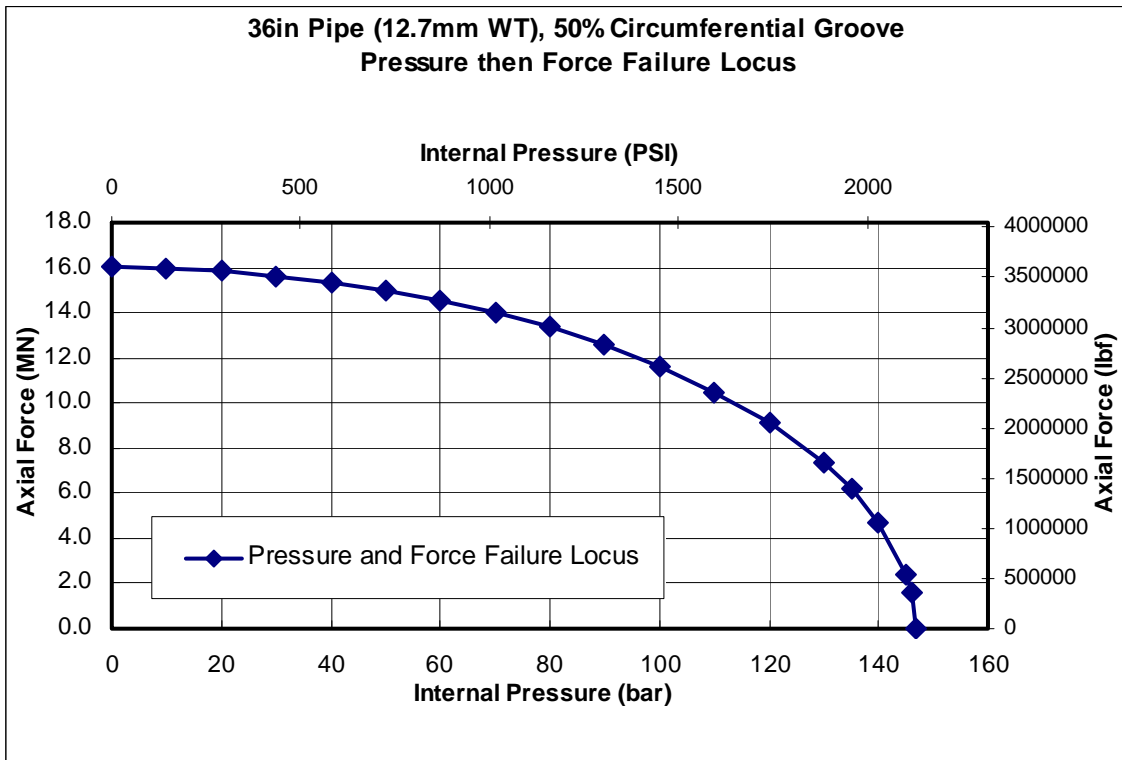
Figure D13. 914.4mm (36-inch) Diameter Grade X65 Pipe. 20%/50% Deep Circumferential Groove. Compressive Force-Pressure Failure Locus
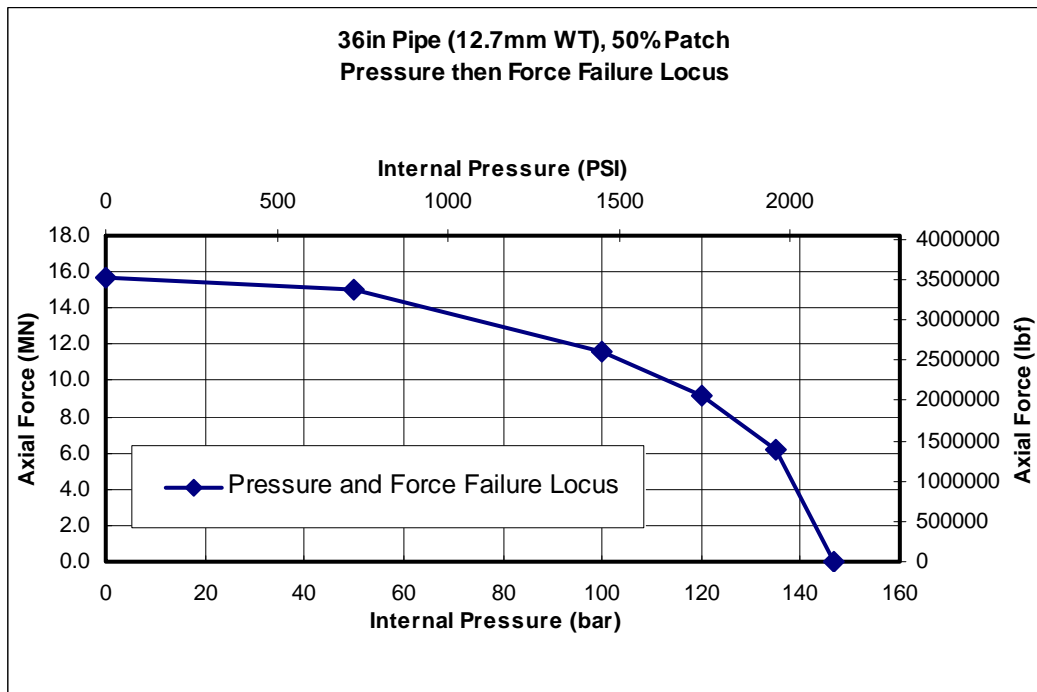

Figure D14. 914.4mm (36-inch) Diameter Grade X65 Pipe. 20%/50% Deep Patch. Compressive Force-Pressure Failure Locus

Appendix E   4 Point Bend Load Rig
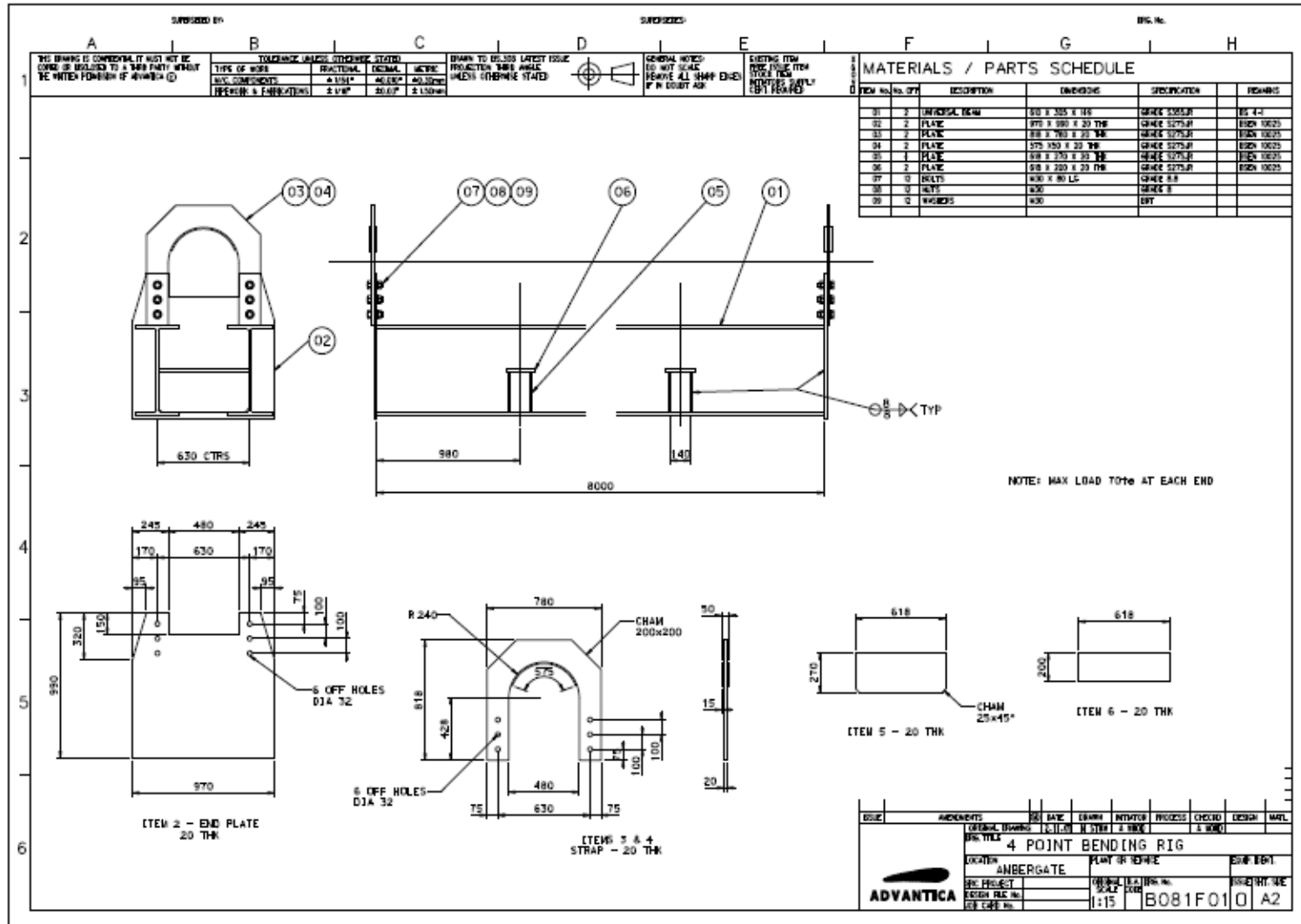
Figure E1. 4 Point Bending Rig Design - General Arrangement
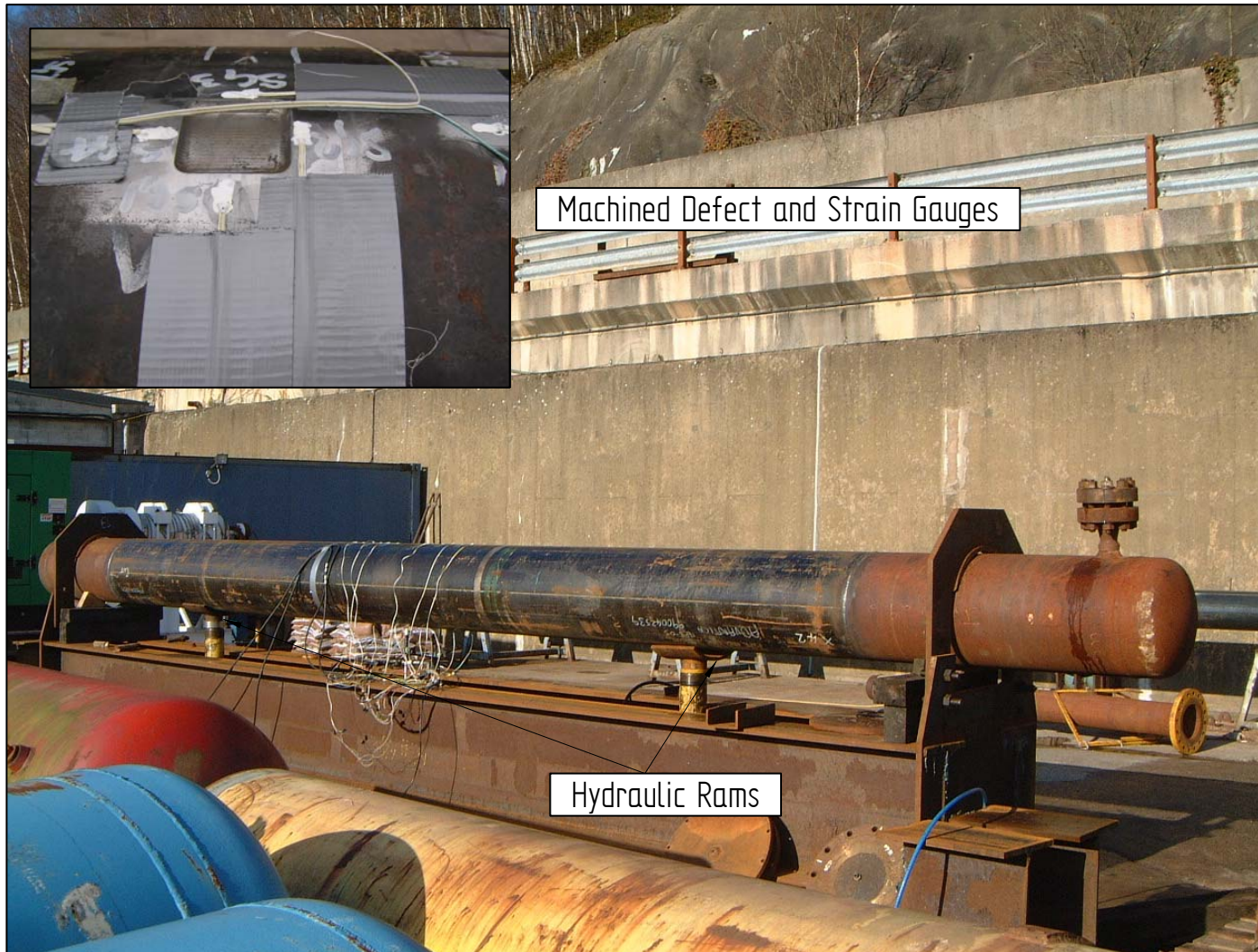
Figure E2.4 Point Bending Rig with a Fully Instrumented 457.2mm (18-inch) Diameter Grade B/X42 Pipe

GL

Appendix F   Metrology Report for Test Vessels

Appendix F   Metrology Report for Test Vessels

PMC NO. 4010823

PMC AMBERGATE

GENERAL INSPECTION REPORT

PROJECT CLIENT ADVANTICA	DATE 4-11-05
LOCATION Pmc AmberGate	INSPECTOR (CAPITALS): R. Elliott

INSPECTION TECHNIQUE

VESSEL 1

Pipe make - Corus
Pipe I.D - HLC
Pipe size - 18" x 5.6mm (nom)

A   B   C

DEPTH   WIDTH

D   E   F

LENGTH

DETAILS

DEFECT LENGTH - 44.88mm
DEFECT WIDTH - 11.61mm
DEFECT DEPTH - 4.23mm

WALL THICKNESS

A 5.3mm
B 5.3mm
C 5.3mm
D 5.3mm
E 5.3mm
F 5.3mm

$$\frac{DEFECT\ DEPTH}{MINIMUM\ W.T.} = \frac{4.23mm}{5.3mm} = 79.81\% \text{ WALL LOSS.}$$

SIGNATURE
APPROVAL & No. BGAS S1 2513
DATE 4-11-05

CIRCULATION

Document No: NDT-004	Issue 3 Dated 3.4.00

PMC AMBERGATE	PMC NO. 4010 823 GENERAL INSPECTION REPORT
PROJECT CLIENT ADVANTICA	DATE 3/2/06
LOCATION. PMC AMBERGATE	INSPECTOR (CAPITALS): R. ELLIOTT
INSPECTION TECHNIQUE VISUAL & MEASUREMENT	

Vessel № 2.

Pipe Manf. Corus
Pipe I.D. HLB
Pipe Size 18" x 5.6mm Low

Pipe Wall Thks (M.M.)

A 5.1
B 5.1
C 5.1
D 5.1

$\rightarrow |12.03| \leftarrow$

'A'

'A'   'B' LL.86

'C'

MAXIMUM DEPTH OF DEFECT $\underline{4.31}$ = 84.50 % WALL THICKNESS LOSS
MINIMUM WALL THICKNESS   5.1

SIGNATURE
APPROVAL & No. BGAS SWI 2513
DATE   3-2-06
CIRCULATION

Document No: NDT-004	Issue 3 Dated 3.4.00

PMC
AMBERGATE

PMC NO. 4910823

GENERAL INSPECTION
REPORT

| PROJECT CLIENT Advantica | DATE 16-12-05 |
| LOCATION. PMC Ambergate | INSPECTOR (CAPITALS): PP Melody |

INSPECTION TECHNIQUE Visual & Measurement

Vessel No 3

Pipe Manf. Mannesman
Pipe I.D. HLA
Pipe Size 18" x 5.6mm 304

→| 11.85 |←

'A'

Pipe Wall Thick (M.M.)

A 5.3
B 5.3
C 5.3
D 5.3

'D'   'B'

45.22mm

'C'

Max Defect Depth   4.11mm
Min Wall Thick   ──────── = 77.54% Wall Thickness Loss
                   5.3 mm

SIGNATURE PP Melody
APPROVAL & No. BGAS SPI-2 5517
DATE 16-01-2006
CIRCULATION

| Document No: NDT-004 | Issue 3 Dated 3.4.00 |

PMC NO. 7010.823

PMC AMBERGATE

GENERAL INSPECTION REPORT

PROJECT CLIENT ADVANTICA	DATE 16-01-2006
LOCATION PMC AMBERGATE	INSPECTOR (CAPITALS): PPM2004

INSPECTION TECHNIQUE VISUAL & MENSURMENT

<u>VESSEL N° 4</u>

PIPE MANF. MANESMAN
PIPE I.D. HLD
PIPE SIZE 18" x 5.6mm SCH

→|11.82|←

PIPE WALL THKS (M.M.)

A 5.4
B 5.4
C 5.4
D 54

'A'

'A'   'B'   45.14

'C'

MAX DEPTH OF DEFECT $\dfrac{4.155}{5.4}$ = 76.94 % WALL THKS LOSS
MIN WALL THKS

SIGNATURE PPMilody
APPROVAL & No. BGAS SPI-2 SS17
DATE 17-01-2006

CIRCULATION

Document No: NDT-004	Issue 3 Dated 3.4.00

PMC NO. 40.10823

PMC
AMBERGATE

GENERAL INSPECTION
REPORT

PROJECT CLIENT ADVANTICA	DATE 29-11-2005
LOCATION. PMC AMBERGATE	INSPECTOR (CAPITALS): PJ MELODY

INSPECTION TECHNIQUE Visual & Measurement

Vessel N° 5

Pipe Manf. Corus
Pipe I.D. HLC
Pipe Size 18" x 5.6 mm

Pipe Wall Thks (M.M.)

A   5.3
B   5.3
C   5.2
D   5.2

|← 44.71 →|
A

44.24

B

C

Remaining Wall Thks →

4.0 - 5.0 mm (Approx)

Wall Thickness

Profile of the edge of the Machined Patch 'Defect'

3 N° Lines of Measurements were taken Axially through the 'Defect'

Max Defect Depth   4.31 mm
Min Wall Thks   5.20 mm   = 82.8% W.T. Loss

SIGNATURE	*PJ Melody*	
APPROVAL & No. BGAS	SP12 55M	
DATE	29-11-2005	
CIRCULATION		

Document No: NDT-004	Issue 3 Dated 3.4.00

PMC
AMBERGATE

PMC NO. 4010823

GENERAL INSPECTION REPORT

PROJECT CLIENT ADVANTICA	DATE 5-1-06
LOCATION PMC AMBERGATE	INSPECTOR (CAPITALS)

INSPECTION TECHNIQUE   VISUAL & MEASUREMENT

Vessel N° 6

Pipe Manf. CORUS
Pipe I.D. HLB
Pipe size 18" x 5.6mm Nom

Pipe Wall Thks

A 5.1
B 5.1
C 5.1
D 5.1

|← 45.08 →|
A

↑
4.36
D
4.21 4.16 4.22   B
45.22
↓
4.21
C

40-5.0mm (APPROX)

REMAINING → WALL THKS

WALL THICKNESS
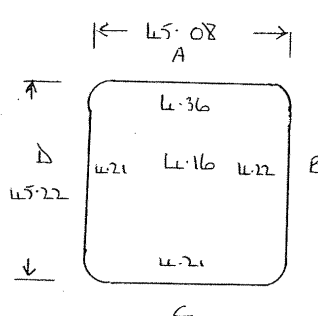
5 AREAS TAKEN IN THE DEFECT – AVERAGE WALL LOSS IS 4.232

MAX DEFECT DEPTH IS 4.36mm
AVERAGE   "   "   " 4.232mm

MAXIMUM WALL LOSS IS $\frac{4.36}{5.1}$ = 85.490 %

AVERAGE WALL LOSS IS $\frac{4.232}{5.1}$ = 82.980 %
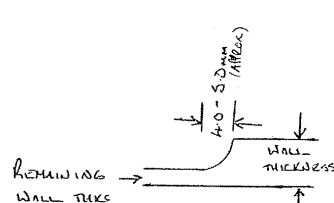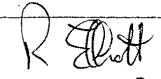
SIGNATURE   R Eliott
APPROVAL & No. BGAS Su1 2513
DATE   5-1-06

CIRCULATION

Document No: NDT-004	Issue 3 Dated 3.4.00